RTI No. 43U-954 NASA CR-132609

AN INVESTIGATION OF ERRORS AND DATA PROCESSING TECHNIQUES FOR AN RF MULTILATERATION SYSTEM

By Charles L. Britt, Jr.

Prepared under Contract NAS1-12910 by

Research Triangle Institute
Engineering Division
Research Triangle Park, North Carolina 27709

for

National Aeronautics and Space Administration
Langley Research Center
Hampton, Virginia 23665

February 1975

ACKNOWLEDGEMENT

This report was prepared by the Systems Engineering Department, Research Triangle Institute, Research Triangle Park, North Carolina, under Contract NAS1-12910. The work is being administered by the Flight Instrumentation Division, NASA Langley Research Center. Mr. Chase P. Hearn is the Langley Technical Representative for the contract.

For the studies described in this report, work has been closely coordinated and discussed with personnel at Langley Research Center. Messrs. C. Hearn, J. Schrader, R. Couch and L. Wilson have contributed heavily to the studies and analyses described herein.

RTI staff members participating in the study were:

Dr. C. L. Britt, Jr., Project Manager

Dr. J. R. Duffett, Senior Statistician

Ms. C. M. Davis, Systems Analyst

Ms. S. L. Wheelock, Mathematician.

Dr. R. W. Stroh of the North Carolina State University faculty acted as Consultant on the computational aspects of the program.

TABLE OF CONTENTS

LIST OF ILLUSTRATIONS

LIST OF ILLUSTRATIONS
(Continued)

LIST OF ILLUSTRATIONS
(Continued)

LIST OF ILLUSTRATIONS
(Continued)

LIST OF ILLUSTRATIONS
(Continued)

LIST OF TABLES

1.0 INTRODUCTION

To provide a capability of highly accurate position and velocity measurements during the approach and landing phase of VTOL aircraft, NASA personnel at Langley Research Center are developing an RF Multilateration System. The system uses an angle-modulated ranging signal to provide both range and range rate measurements between an aircraft transponder and multiple ground stations. Range and range rate measurements are converted to coordinate measurements and the coordinate and coordinate rate information is transmitted via an integral data link to the aircraft.

The objective of the work described in this report has been to conduct error analyses of the planned multilateration system and to determine and recommend data processing techniques that will provide highly accurate position and velocity measurements within the constraints imposed by computational speed and capacity. The initial studies have been concerned with the investigation of various proposed processing techniques and an investigation of errors associated with each of the techniques studied. In developing the processing techniques, it was necessary to continuously keep in mind the limitations of the ground computer. Cost and portability requirements limited the complexity of the computations and consequently also limited the computational scheme to be used.

The following sections of the report provide a brief system description, describe investigations of various data processing techniques that have been studied, and point out advantages and disadvantages of each. For the techniques considered, error calculations are provided that permit a comparison between the various techniques. A recommended data processing technique is developed and error characteristics of this technique are discussed in detail.

Finally, a ground-based mini-computer system is recommended which has both the capability of performing the recommended computations and the flexibility of performing additional computations (such as Kalman filtering) if future requirements make such computations desirable.

"Page missing from available version"

Page 2

2.0 SYSTEM DESCRIPTION

The planned multilateration system configuration is as shown generally in Figure 2-1. A single transmitter transmits a ranging signal to an aircraft transponder where the signal is offset in frequency and retransmitted to four or more ground receivers. The ground receivers contain digital processors which provide digital outputs proportional to the slant range between the receiver and the transponder and the rate of change of slant range. The digital receiver outputs then go to a central ground data processor which transforms the slant range measurements to X, Y, Z position and rate data. In the operational system, the position and rate data are then transmitted to the aircraft over a data link at the same rf frequency as the ranging signal and are available at the aircraft for use in navigation and guidance equipment.

The location of the ground receivers is chosen to provide high accuracy throughout the touchdown area. For situations in which it is desirable to have accuracy over a 360° azimuth range, a configuration such as that shown in Figure 2-2A appears desirable. The central receiver is at the touchdown point. For situations in which there is a preferred direction of approach, a configuration such as the one shown in Figure 2-2B may be more desirable. To provide higher accuracy over certain segments of the approach trajectory, additional receivers may be used.

The functional operation of the system may be understood by referring to Figure 2-3. The transmitter generates a ranging carrier, a phase modulated tone for ranging, a reference carrier, and a data subcarrier. At the aircraft transponder, the incoming signals are translated in frequency coherently using the modulation on the reference carrier. The ranging carrier and associated tone ranging modulations are then retransmitted to the ground receivers. At the ground receivers, the Doppler shifted carrier and ranging modulation are processed to derive digital signals proportional to the two-way time delay (range) and the rate of change of time delay (range-rate). These digital measurements are then transmitted to the coordinate

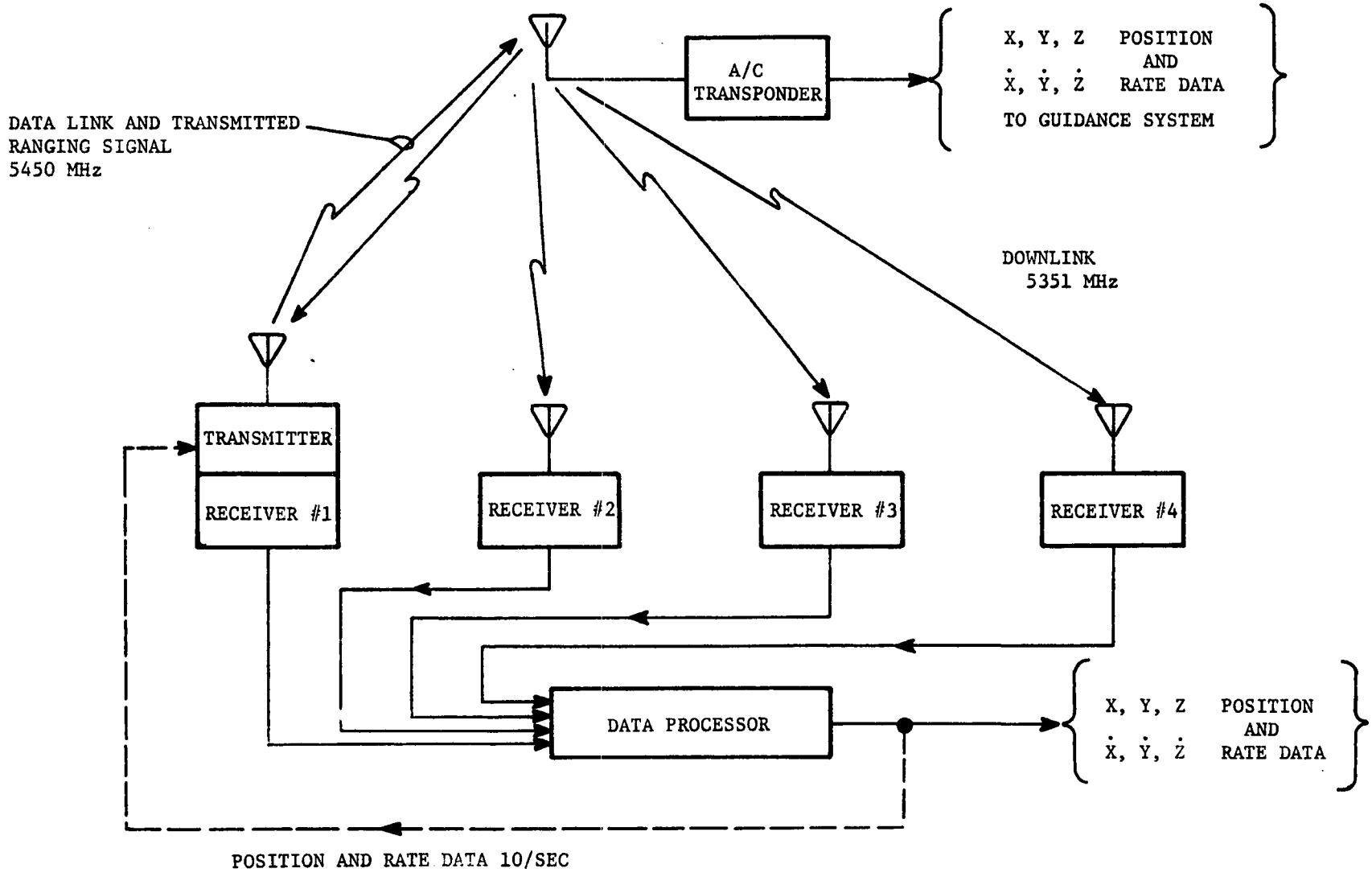

Figure 2-1. General system configuration.

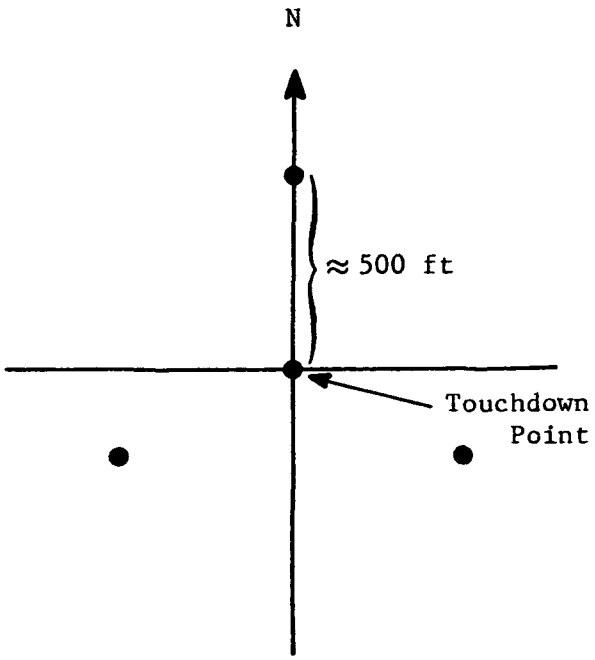

(A) Approach from 360°

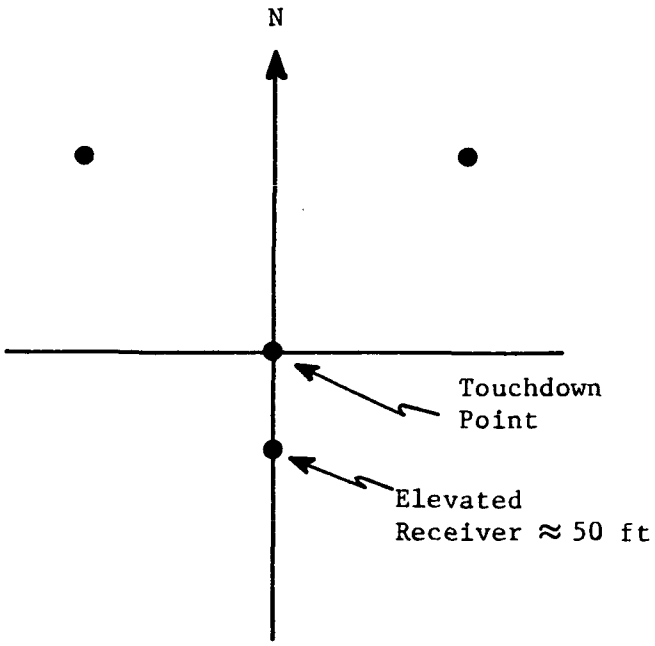

(B) Approach from North only

Figure 2-2. Plan view of possible ground receiver locations for four ground receivers.

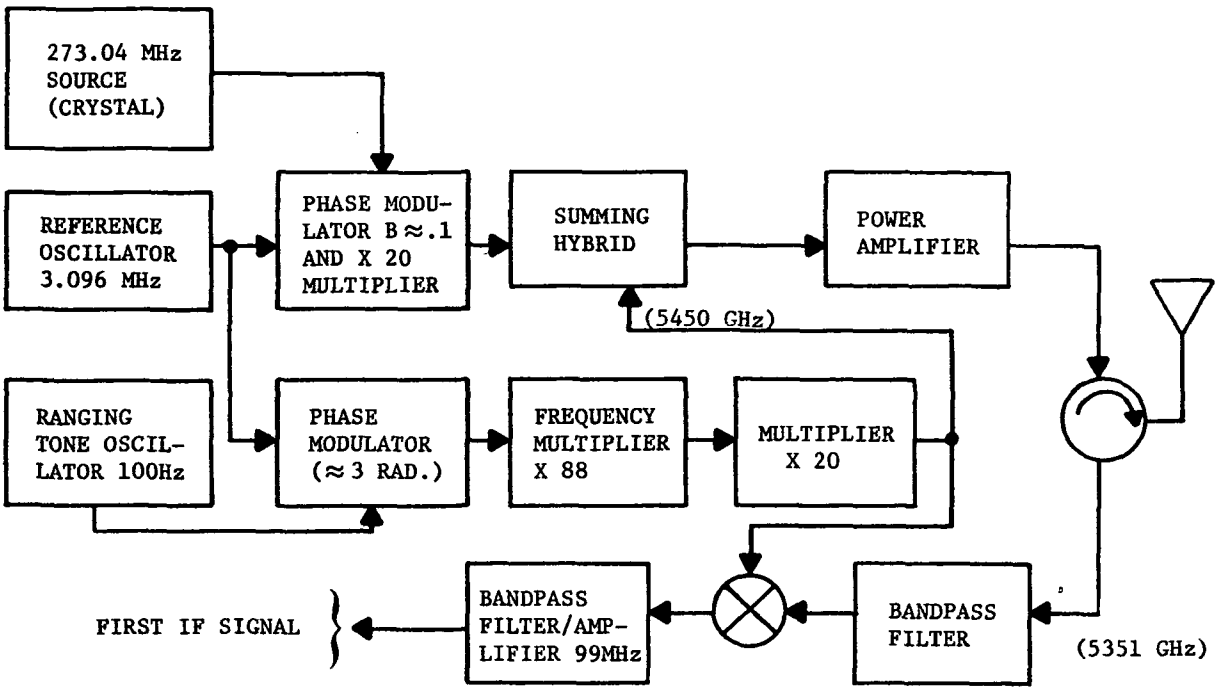

(A) Transmitter and Receiver

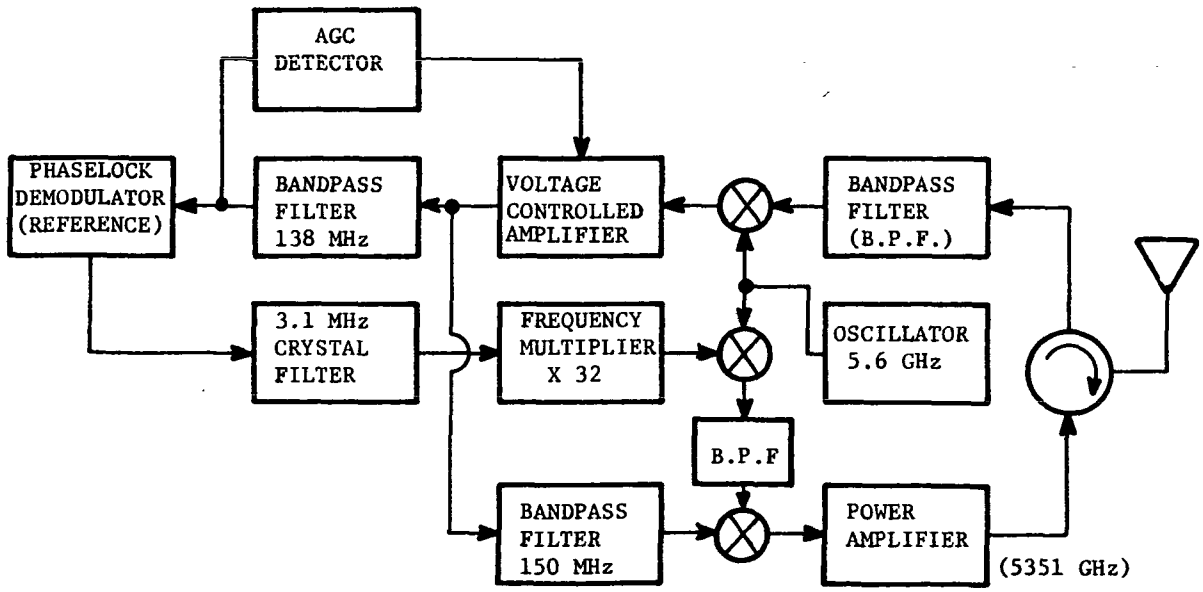

(B) Aircraft Transponder

Figure 2-3. Simplified functional block diagram.

computer for derivation of coordinate position and coordinate rates.

The theoretical operation of the system may be seen by examining the mathematical expressions for the signals throughout the system. The transmitted signal may be written as

$$v_t = V_{t1}\sin[N_1\omega_o t + \beta\sin\alpha t] + V_{t2}\sin[N_2\omega_o t + \gamma\sin\omega_o t] \qquad (2\text{-}1)$$

where

N_1 = multiplication factor (1760)

N_2 = multiplication factor (1764)

ω_o = reference oscillator frequency (3.1 MHz)

α = ranging tone frequency (100 Hz)

β = ranging tone phase deviation (5280 rad.)

γ = reference carrier phase deviation .

At the transponder in the aircraft, the signal received is similar to equation (2-1) but is delayed by a time delay τ_1. At the transponder, the signal is shifted in frequency using the reference signal, and is retransmitted and received at a ground receiver after an additional delay τ_2 as

$$v_R = V_R \sin[N_x\omega_o(t - \tau_1 - \tau_2) + \beta\sin\alpha(t - \tau_1 - \tau_2)] \qquad (2\text{-}2)$$

where

τ_1 = uplink delay

τ_2 = downlink delay

$N_x = N_1 - 32$

and the other nomenclature is defined above.

At the receiver, the incoming signal is mixed with a local reference:

$$v_{REF} = V_{REF} \sin[N_1\omega_o t + \beta \sin \alpha t] \tag{2-3}$$

and the resulting first IF signal is given by

$$v_{IF1} = V_{IF1}[(N_1 - N_x)\ \omega_o t + N_x\omega_o(\tau_1 + \tau_2) - \beta(\sin \alpha t - \sin \alpha(t - (\tau_1 + \tau_2))] \ . \tag{2-4}$$

An additional mixing operation takes place with a multiplied version of the reference oscillator signal to provide a second IF signal given by

$$v_{IF2} = V_{IF2} \sin[\omega_o t + N_x\omega_o(\tau_1 + \tau_2) + 2\beta(\sin \frac{\alpha(\tau_1 + \tau_2)}{2} \cos \alpha\ (t - \frac{(\tau_1 + \tau_2)}{2}))] \tag{2-5}$$

where the form of the last term has been modified using a trigonometric identity for the difference between two sinusoidal signals.

The instantaneous frequency of the IF signal may be determined by differentiating the argument of the sine function above and is given by

$$\omega_{IF} = \omega_o + N_x\omega_o(\dot{\tau}_1 + \dot{\tau}_2) + 2\beta\alpha[\sin \alpha(t - \frac{(\tau_1 + \tau_2)}{2}) \cdot \sin \frac{\alpha(\tau_1 + \tau_2)}{2}] + \beta\alpha\dot{\tau} \cos \alpha(t - \tau_1 - \tau_2) \tag{2-6}$$

where $\dot{\tau}$ is the rate of change of the propagation delay. The last term in equation (2-6) is an error term and system parameters are chosen to make this term small in comparison to the desired terms in the expression. Thus, the IF frequency is given approximately by

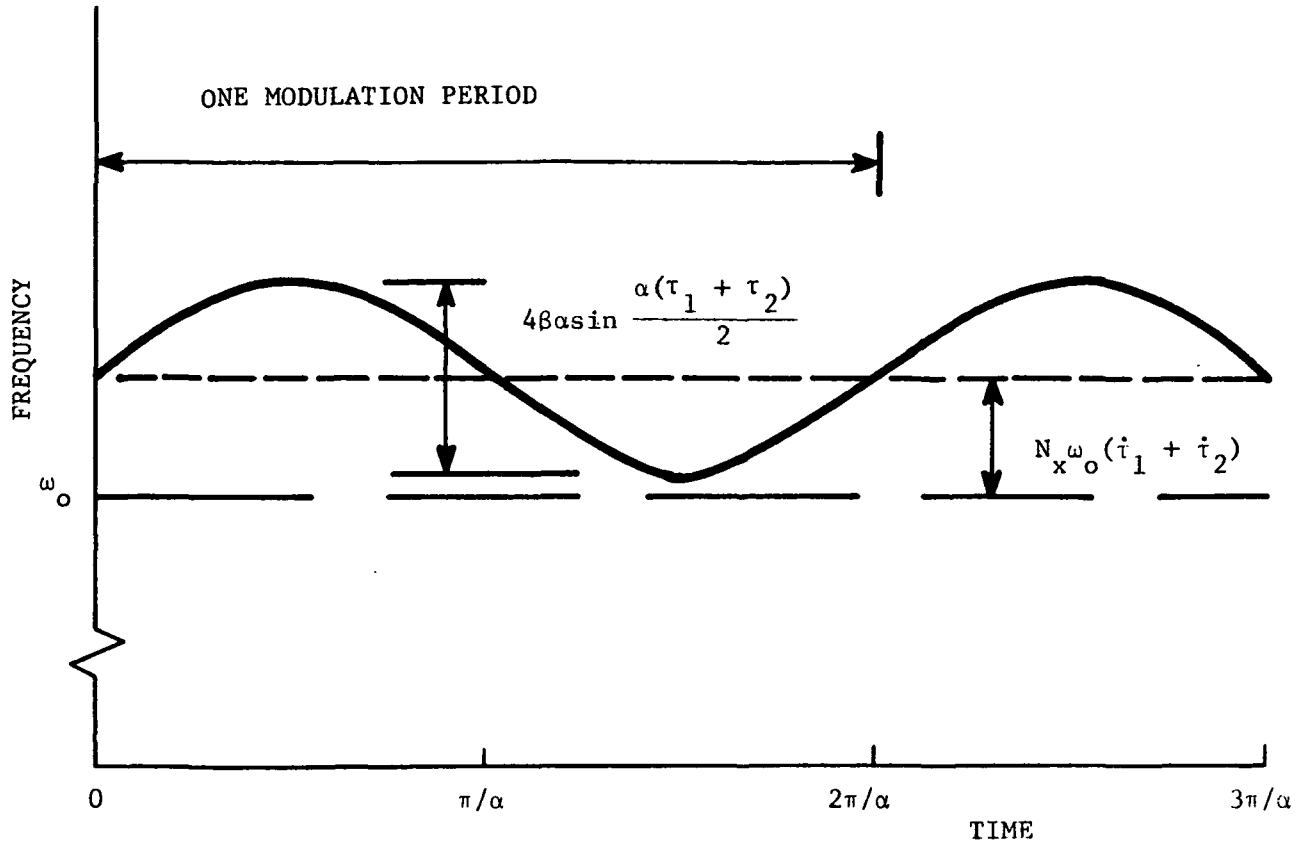

Figure 2-4. Sketch of IF frequency showing range and range rate (Doppler) terms.

$$\omega_{IF} = \omega_o + N_x\omega_o(\dot{\tau}_1 + \dot{\tau}_2) + 2\beta\alpha \sin\left(\frac{\alpha(\tau_1 + \tau_2)}{2}\right) \sin \alpha(t - \frac{\tau_1 + \tau_2}{2}) \quad . \quad (2\text{-}7)$$

A sketch of this equation is shown in Figure 2-4. As shown on the sketch, the deviation of the IF frequency over a modulation cycle is proportional to the total time delay or two-way range, and the average IF frequency is equal to the reference oscillator frequency plus a Doppler offset proportional to the two-way rate of change of delay, or range rate.

A technique of cycle counting is used to obtain measures of two-way range and range rate. Three gated counters are used to count the IF frequency over the first and second halves of the modulation cycle and the reference frequency over a full modulation cycle. The sum of the counts over the first and second halves of the modulation cycle is proportional to the average frequency and the difference in these counts is proportional to

the frequency deviation. The reference frequency counter is used to obtain the difference between the average received frequency and the transmitted frequency.

The number of counts over the first half cycle is given by

$$C_1 = \frac{1}{2\pi}\int_{\tau/2}^{\pi/\alpha + \tau/2} \omega_{IF}\, dt - e_1 \tag{2-8}$$

where e_1 is a fractional number $0 \leq e_1 < 1$ selected to make the number of counts, C, be an integer value. In the integration, $\tau = \tau_1 + \tau_2$ is assumed constant over the duration of the modulation cycle. Over the second half cycle,

$$C_2 = \frac{1}{2\pi}\int_{\pi/\alpha + \tau/2}^{2\pi/\alpha + \tau/2} \omega_{IF}\, dt - e_2 \tag{2-9}$$

where $0 \leq e_2 < 1$. The reference counter gives

$$C_r = \frac{1}{2\pi}\int_{0}^{2\pi/\alpha} \omega_o\, dt - e_3 \tag{2-10}$$

where $0 \leq e_3 < 1$.

Evaluation of the integrals using equation (2-7) and summing and differencing the counters gives, for the range rate count,

$$C_R^{\cdot} = C_1 + C_2 - C_r = \frac{\omega_o N_x}{\alpha}(\dot{\tau}_1 + \dot{\tau}_2) - e_1 - e_2 + e_3 \tag{2-11}$$

and for the range count

$$C_R = C_1 - C_2 = \frac{4\beta}{\pi}\sin\alpha\left(\frac{\tau_1 + \tau_2}{2}\right) - e_1 + e_2 \quad . \tag{2-12}$$

Since $\tau_i = R_i/c$ and $\dot{\tau}_i = \dot{R}_i/c$, where c is the propagation velocity and R_i is the distance corresponding to the delay τ_i, there is obtained,

$$C_{\dot{R}} = C_1 + C_2 - C_r = \frac{\omega_o N_x}{c\alpha} (\dot{R}_1 + \dot{R}_2) + e_{\dot{R}} \tag{2-13}$$

and

$$C_R = C_1 - C_2 = \frac{4\beta}{\pi} \sin \frac{\alpha}{2c} (R_1 + R_2) + e_R \tag{2-14}$$

where $(-2 < e_{\dot{R}} < 1)$ and $(-1 < e_R < 1)$.

Thus, the counters provide digital outputs proportional to the two-way range and range rate. These digital outputs are then used to calculate the one-way ranges and range rates and the coordinate position and velocity components of the aircraft. Conversion of the range and range rate measurements to coordinate position and velocity is accomplished in the ground computer.

Page Intentionally Left Blank

3.0 SOLUTION TECHNIQUES

3.1 General Discussion

As seen in the previous section, the basic system measurements are the range and rate between the ground stations and the airborne transponder. These basic measurements will contain random and bias errors due to system characteristics, quantization errors, and calibration errors. It has not been within the scope of the present work to investigate the sources of these errors in detail, but to consider only the effect of the basic measurement errors on the solution for coordinate velocities and position. The central data processor in the system has the function of converting the basic measurements to coordinate rates ($\dot{x}$, $\dot{y}$, $\dot{z}$) and coordinate position (x, y, z). These coordinate positions and rates are then transmitted to the aircraft for use in the navigation and guidance system. The basic measurements will be taken at a data rate of approximately ten per second.

The overall accuracy achievable with the multilateration system will depend strongly on the data processing techniques used. For example, with four or more ground stations, a redundant measurement is available which may be combined with other measurements to improve the system accuracy. It is also possible to provide in-flight calibration so that a sequence of measurements is used to correct for bias in the system during the initial stages of an approach path. In general, it is desirable to use all of the basic measurement information available to provide the most precise position and velocity estimation possible.

Since a fast-time response is desired in the system, it is preferable if possible to use point estimation techniques; that is, to calculate coordinate position and velocities each sample instant based on the measured data. While the accuracy can be substantially improved by using the time history of the measurements in a filtering technique (e.g., Kalman filtering), these techniques have not been considered in this study. They will, however, be considered in future work.

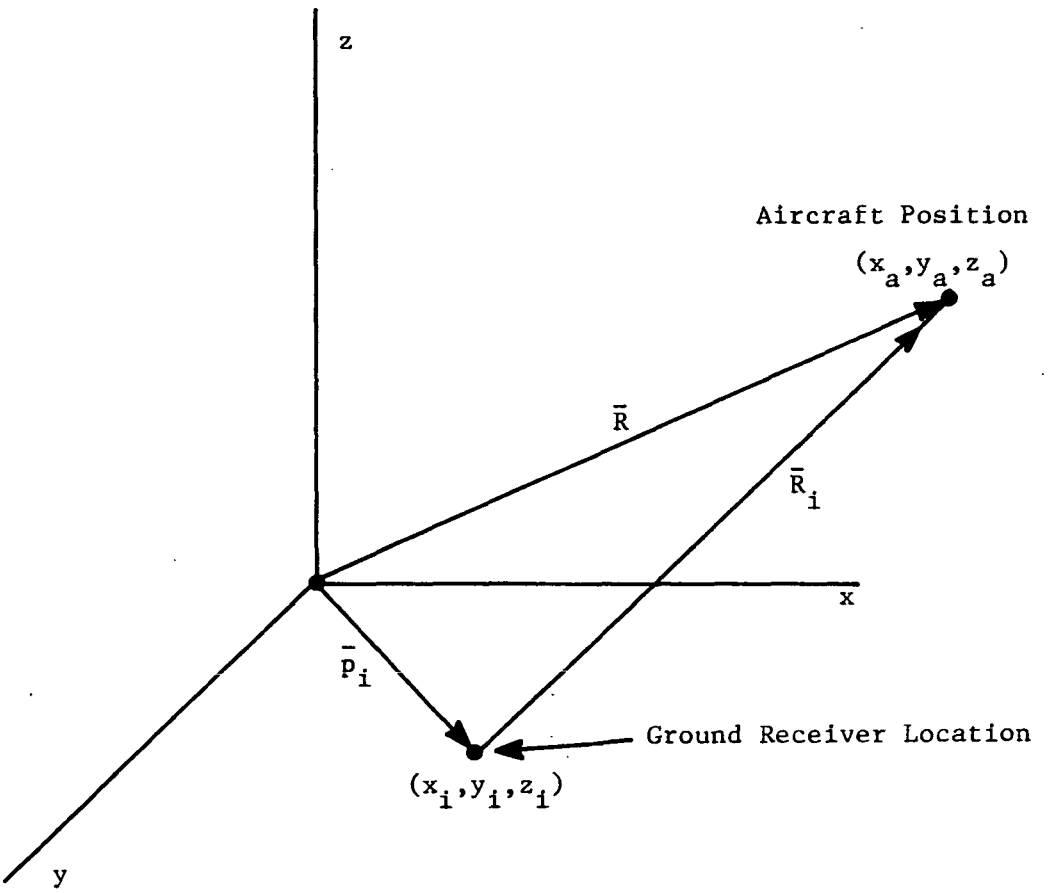

Fig. 3-1. Definition of vectors.

The equations necessary for conversion of range measurements to coordinate positions are non-linear, hence the determination of the best solution technique is not a straightforward problem. In this report, several solution techniques have been developed and the advantages and disadvantages of each technique have been determined. For convenience, the solution techniques developed have been broken down as follows:

A. Solutions for position coordinates.
   1. Explicit solutions for three ground stations.
   2. Linearized minimum variance solution.
   3. Iterative minimum variance solution.
   4. Explicit minimum variance solution for N ground stations.

B. Solution for coordinate rates.
   1. Explicit minimum variance solution for N ground stations.

C. Bias (system time delay) removal techniques.

Solutions combining rate estimation with position estimation have not been considered because of the computational complexity involved.

The following sections discuss the above solution techniques and outline the considerations that lead to the determination of the recommended solution technique discussed in Section 6.0.

3.2 Explicit Solutions for Aircraft Position Coordinates with Three Ground Stations

In vector terminology, the range vector from a receiver i to the aircraft transponder may be written as

$$\bar{R}_i = \bar{R} - \bar{p}_i \tag{3-1}$$

where the vectors are defined in Figure 3-1. The magnitude squared of the vector $\bar{R}_i$ is

$$R_i^2 = R^2 + p_i^2 - 2\bar{R} \cdot \bar{p}_i^2 \quad . \tag{3-2}$$

Thus, one equation of the above form will be obtained for each ground receiver in the system. A minimum of three stations is required to solve for the three unknown position coordinates of the aircraft (x_a, y_a, z_a) where z_a is assumed positive in all cases and the station locations are known.

For three stations, the coordinate system can always be chosen so that one station defines the origin of coordinates, one station defines the X axis, and the third station defines the XY plane. Therefore, let the station locations be as follows.

Station	Coordinates
1	(0, 0, 0)
2	(0, y_2, 0)
3	(x_3, y_3, 0)

With this choice of coordinate system, the following equations apply:

$$R_1^2 = x_a^2 + y_a^2 + z_a^2 \tag{3-3}$$

$$R_2^2 = x_a^2 + y_a^2 + z_a^2 + y_2^2 - 2\, y_a y_2 \tag{3-4}$$

$$R_3^2 = x_a^2 + y_a^2 + z_a^2 + x_3^2 + y_3^2 - 2\, x_a x_3 - 2\, y_a y_3 \quad ; \tag{3-5}$$

and the solution for x_a, y_a, z_a is straightforward. First solve for y_a,

$$y_a = \frac{1}{2y_2} (R_1^2 - R_2^2 + y_2^2) \tag{3-6}$$

then solve for x_a,

$$x_a = \frac{1}{2x_3} (R_1^2 - R_3^2 + x_3^2 + y_3^2 - 2\, y_a y_3) \tag{3-7}$$

and finally, solve for z_a

$$z_a = + (R_1^2 - x_a^2 - y_a^2)^{1/2} \quad . \tag{3-8}$$

This solution in the coordinates x, y, z can then be obtained in another coordinate system X, Y, Z by using a linear transformation

$$\bar{X} = [K]\,\bar{x} \tag{3-9}$$

where

$$x = \begin{Bmatrix} x \\ y \\ z \end{Bmatrix} \qquad \bar{X} = \begin{Bmatrix} X \\ Y \\ Z \end{Bmatrix}$$

and [K] is a 3 x 3 matrix for the linear coordinate transformation.

A completely general explicit solution for the three station case in an arbitrary coordinate system is derived in Appendix A. A technique for error analysis of this type of solution is given in Appendix B.

3.3 Linearized Minimum Variance Solution for N Ground Stations

3.3.1 The weighted least squares technique.— With more than three ground receivers, redundant information is available which may be used to improve the accuracy of the aircraft position estimate. For example, with four ground receivers, four estimates of aircraft position may be obtained using all combinations of three of the equations relating the measurements to the position coordinates. To combine the measurements in some optimal manner, the technique of weighted least squares estimation is used. This technique provides a means of linearly combining solutions so that the resultant estimate has minimum variance.

To demonstrate this technique, consider for example two measurements, y_1 and y_2, of a parameter y and of uncertainty implied by their respective known standard deviations σ_1 and σ_2. To determine an estimate of the parameter y given the measurements, we form a linear weighted average,

$$\hat{y} = w_1 y_1 + w_2 y_2 \tag{3-10}$$

where w_1 and w_2 are weighting factors and $w_1 + w_2 = 1$.

The variance of errors associated with the estimate $\hat{y}$ is calculated from the above equation as

$$\sigma_{\hat{y}}^2 = w_1^2 \sigma_1^2 + w_2^2 \sigma_2^2 \tag{3-11}$$

where, for simplicity, y_1 and y_2 are assumed independent with zero correlation. To determine the w_i that minimizes the variance $\sigma_{\hat{y}}^2$, differentiate eq. (3-11) with respect to w_1 and set the result equal to zero.

$$\sigma_{\hat{y}}^2 = w_1^2 \sigma_1^2 + (1 - w_1)^2 \sigma_2^2 \tag{3-12}$$

$$\frac{\partial(\sigma_{\hat{y}}^2)}{\partial w_1} = 2 w_1 \sigma_1^2 + 2(1 - w_1)(-1) \sigma_2^2 = 0 \ . \tag{3-13}$$

Therefore the weighting factors are

$$w_1 = \frac{\sigma_2^2}{\sigma_1^2 + \sigma_2^2} \ , \qquad w_2 = \frac{\sigma_1^2}{\sigma_1^2 + \sigma_2^2} \ ,$$

and

$$\hat{y}\Big|_{\text{min variance}} = \left(\frac{\sigma_2^2}{\sigma_1^2 + \sigma_2^2}\right) y_1 + \left(\frac{\sigma_1^2}{\sigma_1^2 + \sigma_2^2}\right) y_2 \ . \tag{3-14}$$

The variance of $\hat{y}$ is minimized and is given by

$$\sigma_{\hat{y}}^2\Big|_{\text{min}} = \frac{\sigma_1^2 \sigma_2^2}{\sigma_1^2 + \sigma_2^2} \ . \tag{3-15}$$

The above result can also be obtained by selecting $\hat{y}$ to minimize the weighted mean square error risk function R, where

$$R = \left(\frac{y_1 - \hat{y}}{\sigma_1}\right)^2 + \left(\frac{y_2 - \hat{y}}{\sigma_2}\right)^2 \quad . \tag{3-16}$$

Minimizing with respect to $\hat{y}$ gives

$$\frac{\partial R}{\partial \hat{y}} = (y_1 - \hat{y}) \ \frac{1}{\sigma_1^2} + (y_2 - \hat{y}) \ \frac{1}{\sigma_2^2} = 0 \tag{3-17}$$

$$\hat{y}\Big|_{\substack{\text{min mean} \\ \text{square error}}} = \left(\frac{\sigma_2^2}{\sigma_1^2 + \sigma_2^2}\right) \ y_1 + \left(\frac{\sigma_1^2}{\sigma_1^2 + \sigma_2^2}\right) \ y_2 \quad . \tag{3-18}$$

The matrix formulation of the weighted least squares or minimum variance technique provides results as shown above in a very compact notation. In ref. 1 it is shown that if the measurement vector $\bar{y}$ is related to the estimator vector b by an equation

$$\bar{y} = [A] \ b + \bar{v} \tag{3-19}$$

where $\bar{v}$ is the (zero mean) measurement noise vector, then the estimate vector which minimizes a weighted least squares risk function is

$$\hat{b} = (A^T \ \psi^{-1} \ A)^{-1} \ A^T \ \psi^{-1} \ \bar{y} \tag{3-20}$$

where ψ is the weighting matrix. For minimum covariance, the weighting function ψ must be the covariance matrix of the measurement errors ($\psi_{\Delta \bar{y}}$). If this is the case, the covariance matrix of the estimate error is

$$\psi_{\Delta \hat{b}} = (A^T \ \psi_{\Delta \bar{y}}^{-1} \ A)^{-1} \quad . \tag{3-21}$$

The matrix technique can be demonstrated by applying it to the example previously discussed. For the two measurements y_1 and y_2 we have

$$y_1 = \hat{y} + v_1 \qquad \text{Var } \Delta y_1 = \text{Var } v_1 = \sigma_1^2 \tag{3-22}$$

$$y_2 = \hat{y} + v_2 \qquad \text{Var } \Delta y_2 = \text{Var } v_2 = \sigma_2^2 \tag{3-23}$$

$$\text{Cov } \Delta y_1, \Delta y_2 = \text{Cov } v_1 v_2 = 0 \quad .$$

Thus in this case

$$A = \begin{Bmatrix} 1 \\ 1 \end{Bmatrix} \qquad \psi = \begin{bmatrix} \sigma_1^2 & 0 \\ 0 & \sigma_2^2 \end{bmatrix} \tag{3-24}$$

and the answer follows directly from eq. (3-20). The various calculations in obtaining the solution are as follows:

$$\psi^{-1} = \begin{bmatrix} \frac{1}{\sigma_1^2} & 0 \\ 0 & \frac{1}{\sigma_2^2} \end{bmatrix} \tag{3-25}$$

$$A^T \psi^{-1} = \begin{Bmatrix} \frac{1}{\sigma_1^2} & \frac{1}{\sigma_2^2} \end{Bmatrix} \tag{3-26}$$

$$A^T \psi^{-1} A = \frac{1}{\sigma_1^2} + \frac{1}{\sigma_2^2} \tag{3-27}$$

$$(A^T \psi^{-1} A)^{-1} = \frac{\sigma_1^2 \sigma_2^2}{\sigma_1^2 + \sigma_2^2} = \sigma^2_{\Delta\hat{b}} \tag{3-28}$$

$$\hat{b} = (A^T \psi^{-1} A)^{-1} A^T \psi^{-1} \underline{y} = \left(\frac{\sigma_2^2}{\sigma_1^2 + \sigma_2^2} \right) y_1 + \left(\frac{\sigma_1^2}{\sigma_1^2 + \sigma_2^2} \right) y_2 \tag{3-29}$$

which is the same equation obtained previously.

The advantages of the matrix notation in dealing with four or more equations and correlated measurement errors should be evident.

3.3.2 Linearized solution for the special case of all ground stations in a plane. — For all ground receivers in a plane, the range equations (see Figure 3-1 for definition of vectors),

$$R_i^2 = R^2 + p_i^2 - 2\bar{R} \cdot \bar{p}_i \qquad i = 1, n \quad , \tag{3-30}$$

can be linearized by treating R^2 as an independent variable. Letting $u = R^2/2$ and

$$q_i = \frac{R_i^2 - p_i^2}{2} = -x_i x - y_i y + u \tag{3-31}$$

gives the equation

$$\bar{Q} = [P]\bar{x} \tag{3-32}$$

where, for n = 4,

$$\bar{Q} = \begin{Bmatrix} q_1 \\ q_2 \\ q_3 \\ q_4 \end{Bmatrix} \qquad \bar{x} = \begin{Bmatrix} x \\ y \\ u \end{Bmatrix}$$

$$[P] = -\begin{bmatrix} x_1 & y_1 & -1 \\ x_2 & y_2 & -1 \\ x_3 & y_3 & -1 \\ x_4 & y_4 & -1 \end{bmatrix} .$$

The solution is given by

$$\bar{x} = (P^T \Psi_{\Delta Q}^{-1} P)^{-1} P^T \Psi_{\Delta Q}^{-1} \bar{Q} \tag{3-33}$$

where $\Psi_{\Delta Q}$ is the covariance matrix of errors in the q_i. Since

$$\Delta q_i \approx R_i \Delta R_i \quad \text{and} \quad \Delta\bar{Q} = [\bar{T}]\,\overline{\Delta R} \tag{3-34}$$

we have

$$\Psi_{\Delta Q} = E\{\Delta\bar{Q}\ \Delta\bar{Q}^T\} = T\ \Psi_{\Delta\bar{R}}\ T^T \tag{3-35}$$

where $\Psi_{\Delta R}$ is the covariance matrix of the slant range measurements (derived in Appendix C) and

$$T = \begin{bmatrix} R_1 & 0 & 0 & 0 \\ 0 & R_2 & 0 & 0 \\ 0 & 0 & R_3 & 0 \\ 0 & 0 & 0 & R_4 \end{bmatrix} .$$

After calculation of $\hat{x}$, $\hat{y}$, and $\hat{u}$ the z estimate is found as

$$\hat{z} = (2\hat{u} - \hat{x}^2 - \hat{y}^2)^{1/2} . \tag{3-36}$$

An error analysis of this solution technique is given in Appendix D.

3.3.3 Linearized solution for the special case of all ground stations not in a plane. — For four or more ground stations not in a plane, a linear solution can be found using range difference equations. Using the same nomenclature as before, define

$$q_i = \frac{R_i^2 - R_n^2 + p_n^2 - p_i^2}{2} . \tag{3-37}$$

By subtracting the nth range equation from the remaining equations, we obtain

$$q_i = -\bar{R} \cdot (\bar{p}_i - \bar{p}_n) \tag{3-38}$$

or in matrix form

$$Q = [P]\bar{x} \tag{3-39}$$

where

$$\bar{Q} = \begin{Bmatrix} q_1 \\ q_2 \\ \vdots \\ q_n \end{Bmatrix} \qquad [P] = \begin{bmatrix} x_1-x_n & y_1-y_n & z_1-z_n \\ x_2-x_n & y_2-y_n & z_2-z_n \\ \vdots & \vdots & \vdots \\ x_{n-1}-x_n & y_{n-1}-y_n & z_{n-1}-z_n \end{bmatrix}$$

$$\bar{x} = \begin{Bmatrix} x \\ y \\ z \end{Bmatrix} \quad .$$

For four ground stations not in a plane, the solution is unique and is given by

$$\bar{x} = (P^T P)^{-1} P^T \bar{Q} \quad . \tag{3-40}$$

Note that if the stations lie in a plane, the inverse $(P^T P)^{-1}$ does not exist.

For more than four ground stations not in a plane, the weighted least squares solution may be used. This solution is

$$\bar{x} = (P^T \gamma_{\Delta\bar{Q}}^{-1} P)^{-1} P^T \gamma_{\Delta\bar{Q}}^{-1} \bar{Q} \tag{3-41}$$

where $\gamma_{\Delta\bar{Q}}$ is the covariance matrix of the errors in the vector $\bar{Q}$ (see Sec. 3.3.2). An error analysis of this solution is given in Appendix E.

3.4 Iterative Minimum Variance Solution

The derivation of an iterative minimum variance solution is given in Appendix F. The technique is summarized as follows.

The two-way range measurements $(R_1 + R_i)$ are related to the coordinate positions as follows:

$$A_i = [(x - x_1)^2 + (y - y_1)^2 + (z - z_1)^2]^{1/2} + [(x - x_i)^2 + (y - y_i)^2 + (z - z_i)^2]^{1/2} \qquad i = 1, n \quad , \tag{3-42}$$

or $A_i = f_i(x, y, z)$.

The above equations are expanded in a Taylor's series around an initial estimate of the solution to obtain

$$f_i(x,y,z)\Big]_0 + \frac{\partial f_i}{\partial x}\Big]_0 \Delta x + \frac{\partial f_i}{\partial y}\Big]_0 \Delta y + \frac{\partial f_i}{\partial z}\Big]_0 \Delta z = A_i \quad . \tag{3-43}$$

Thus,

$$\Delta A_i = A_i - f_i(x,y,z)\Big]_0 = \frac{\partial f_i}{\partial x}\Big]_0 \Delta x + \frac{\partial f_i}{\partial y}\Big]_0 \Delta y + \frac{\partial f_i}{\partial z}\Big]_0 \Delta z \quad . \tag{3-44}$$

The set of equations above can be written in matrix form as

$$\overline{\Delta A} = [D]\,\overline{\Delta x} \tag{3-45}$$

where

$$\overline{\Delta A} = \begin{Bmatrix} \Delta A_1 \\ \Delta A_2 \\ \vdots \\ \Delta A_n \end{Bmatrix} , \qquad \overline{\Delta x} = \begin{Bmatrix} \Delta x \\ \Delta y \\ \Delta z \end{Bmatrix} ,$$

and [D] is a n x 3 matrix of partial derivatives of the f_i.

Solving for $\overline{\Delta x}$ from eq. (3-45) gives the least squares form,

$$\overline{\Delta x} = (D^T D)^{-1} D^T \overline{\Delta A} \tag{3-46}$$

and an improved estimate of $\bar{x}$ is obtained over the initial estimate where

$$\bar{x}_{k+1} = \bar{x}_k + \overline{\Delta x}_k \quad . \tag{3-47}$$

This improved estimate is then used as the initial solution and the process is repeated.

Thus, the iterative solution procedure is :

1. Determine initial solution by some means.
2. Calculate D matrix.

3. Calculate $\overline{\Delta A}$.
4. Calculate $\overline{\Delta x}$.
5. Calculate improved estimate of $\bar{x}$.
6. Go to step 2. and repeat calculations until $|\overline{\Delta x}|$ is smaller than some predetermined value. This indicates the solution has converged to the value for $\bar{x}$ within the limit preselected.

The covariance matrix for the estimation errors is, from eq. (3-46),

$$\underset{\Delta x}{\psi} = E\{\overline{\Delta x}\ \overline{\Delta x}^T\} = (D^T D)^{-1} D^T \underset{\Delta A}{\psi} D(D^T D)^{-1} \quad . \tag{3-48}$$

3.5 An Explicit Minimum Variance Solution for n Ground Stations in an Arbitrary Coordinate System

For n ground stations, n equations of the form

$$R_i^2 = R^2 + p_i^2 - 2\bar{R} \cdot \bar{p}_i \qquad i = 1, 2, \ldots, n \tag{3-49}$$

are obtained where R_i is the measured slant range and $\bar{p}_i$ is the vector from the origin of coordinates to station i. $\bar{R}$ is the slant range vector from the origin to the aircraft.

Now, subtracting the n^{th} equation from the other n-1 equations gives

$$\frac{R_i^2 - R_n^2 - p_i^2 + p_n^2}{2} = \bar{R} \cdot (\bar{p}_n - p_i) \qquad i = 1, 2, \ldots, (1-n) \tag{3-50}$$

or

$$q_i = \bar{R} \cdot (\bar{p}_n - p_i) \tag{3-51}$$

where q_i equals the term on the left-hand side of equation (3-50).

The set of equations (3-51) can be expressed in matrix form by

$$\bar{Q} = [P]\bar{x} \tag{3-52}$$

where

$$Q = \begin{Bmatrix} q_1 \\ q_2 \\ \vdots \\ q_{n-1} \end{Bmatrix} \qquad \bar{x} = \begin{Bmatrix} x \\ y \\ z \end{Bmatrix}$$

$$P = -\begin{bmatrix} x_1 - x_n & y_1 - y_n & z_1 - z_n \\ x_2 - x_n & y_2 - y_n & z_2 - z_n \\ \vdots & \vdots & \vdots \\ x_{n-1} - x_n & y_{n-1} - y_n & z_{n-1} - z_n \end{bmatrix}_{(n-1) \times 3} .$$

Now partition [P] and $\bar{x}$ as follows:

$$\bar{Q} = [A \; B] \begin{Bmatrix} \bar{\rho} \\ z \end{Bmatrix} \tag{3-53}$$

where $\bar{\rho} = \begin{Bmatrix} x \\ y \end{Bmatrix}$, $\qquad B = -\begin{bmatrix} z_1 - z_n \\ \vdots \\ z_{n-1} - z_n \end{bmatrix}_{(n-1) \times 1}$

and $$A = -\begin{bmatrix} x_1 - x_n & y_1 - y_n \\ x_2 - x_n & y_2 - y_n \\ \vdots & \vdots \\ x_{n-1} - x_n & y_{n-1} - y_n \end{bmatrix}_{(n-1) \times 2} .$$

With this partitioning, we have

$$\bar{Q} = A\bar{\rho} + Bz \quad . \tag{3-54}$$

To obtain a least squares estimate of $\bar{\rho}$, we assume that $\bar{Q} - Bz$ is the observed data. Under this assumption,

$$\hat{\bar{\rho}}_{\ell.s.} = C\bar{Q} - CBz \tag{3-55}$$

where $$C = (A^T \psi_{QB}^{-1} A)^{-1} A^T \psi_{QB}^{-1} \quad . \tag{3-56}$$

The expression ψ_{QB} is the covariance matrix of errors in $(\bar{Q} - Bz)$. (Note: For all ground stations in a plane, B = 0 and equation (3-44) is considerably simplified. In this case, the covariance matrix ψ_{QB} becomes the covariance of errors in $\bar{Q}$ only.)

The original equations (3-49) may be written in terms of $\bar{\rho}$ as follows:

$$R_i^2 = (\bar{\rho} - \bar{\rho}_i)^T (\bar{\rho} - \bar{\rho}_i) + z^2 - 2z_i z + z_i^2 \quad i = 1, 2, \ldots, n \tag{3-57}$$

where $$\bar{\rho}_i = \begin{Bmatrix} x_i \\ y_i \end{Bmatrix} \quad .$$

Any of the n equations may be used to solve for $\hat{z}$ by substitution of the estimate for $\bar{\rho}$, equation (3-55), into equation (3-57). When this is done, the resulting equation can be solved for z to yield:

$$z(i) = \frac{-b_i \pm \sqrt{b_i^2 - 4ac_i}}{2a} \qquad i = 1, n \tag{3-58}$$

where $$a = 1 + B^T C^T CB$$

$$b_i = -2z_i - 2\bar{Q}^T C^T CB + 2\bar{\rho}_i^T CB$$

$$c_i = -R_i^2 + \bar{\rho}_i^T \bar{\rho}_i - 2\bar{\rho}_i^T C\bar{Q} + \bar{Q}^T C^T C\bar{Q} + z_i^2 \quad .$$

The z estimate $\hat{z}$ can be obtained as a weighted average of the n z(i) values obtained above. Thus, we have for $\hat{z}$

$$\hat{z} = (U^T \psi_{\Delta z}^{-1} U)^{-1} U^T \psi_{\Delta z}^{-1} \bar{z} \tag{3-59}$$

where $U = \begin{Bmatrix} 1 \\ 1 \\ 1 \\ \cdot \\ \cdot \end{Bmatrix}_{n \times 1}$, $\bar{z} = \begin{Bmatrix} z(1) \\ z(2) \\ \cdot \\ \cdot \\ z(n) \end{Bmatrix}_{n \times 1}$,

and $\psi_{\Delta z}$ is the covariance matrix of the errors in z(i). This matrix is derived in Appendix G. The standard deviation of the z estimation error is

$$\sigma_{\Delta \hat{z}}^2 = (U^T \psi_{\Delta z}^{-1} U)^{-1} \quad . \tag{3-60}$$

The x and y estimates now determined from eq. (3-55) are

$$\hat{\rho} = \begin{Bmatrix} \hat{x} \\ \hat{y} \end{Bmatrix} = C\bar{Q} - CB\hat{z} \quad . \tag{3-61}$$

Error covariances associated with this solution technique are derived in Appendix G.

3.6 Minimum Variance Solution for Coordinate Rates in an Arbitrary Coordinate System

For the velocity components, the measurements made by the receivers are (for four receivers)

$$\dot{M}_i = \dot{R}_1 + \dot{R}_i \qquad i = 1, 2, 3, 4 \tag{3-62}$$

where $\dot{R}_i$ is the range rate between the transponder and receiver i. In vector terminology, the magnitude of the range rate is given by

$$\dot{R}_i = \frac{\bar{R}_i \cdot \dot{\bar{x}}}{|\bar{R}_i|} \tag{3-63}$$

where $\dot{\bar{x}} = 1_x \dot{x} + 1_y \dot{y} + 1_z \dot{z}$ and $\bar{R}_i$ is the range vector from receiver i to the transponder. Since the estimate of $\bar{R}_i$ can be calculated first, the velocity estimate can be obtained from

$$\dot{A}_i = \frac{\hat{\bar{R}}_i \cdot \dot{\bar{x}}}{|\hat{\bar{R}}_i|} \qquad i = 1, 2, 3, 4 \quad . \tag{3-64}$$

where

$$\dot{A}_i = \dot{M}_i - \dot{M}_1/2 \qquad i = 1, 2, 3, 4 \quad .$$

In matrix form,

$$\dot{\bar{A}} = [S]\, \dot{\bar{x}} \tag{3-65}$$

where

$$\dot{\bar{A}} = \begin{Bmatrix} \dot{A}_1 \\ \dot{A}_2 \\ \dot{A}_3 \\ \dot{A}_4 \end{Bmatrix}_{4 \times 1} \qquad \dot{\bar{x}} = \begin{Bmatrix} \dot{x} \\ \dot{y} \\ \dot{z} \end{Bmatrix}_{3 \times 1}$$

$$[S] = \begin{bmatrix} \frac{\hat{x} - x_1}{|\hat{R}_1|} & \frac{\hat{y} - y_1}{|\hat{R}_1|} & \frac{\hat{z} - z_1}{|\hat{R}_1|} \\ \frac{\hat{x} - x_2}{|\hat{R}_2|} & \frac{\hat{y} - y_2}{|\hat{R}_2|} & \frac{\hat{z} - z_2}{|\hat{R}_2|} \\ \frac{\hat{x} - x_3}{|\hat{R}_3|} & \frac{\hat{y} - y_3}{|\hat{R}_3|} & \frac{\hat{z} - z_3}{|\hat{R}_3|} \\ \frac{\hat{x} - x_4}{|\hat{R}_4|} & \frac{\hat{y} - y_4}{|\hat{R}_4|} & \frac{\hat{z} - z_4}{|\hat{R}_4|} \end{bmatrix}_{4 \times 3}$$

and the solution is given by

$$\dot{\bar{x}} = (S^T \psi_{\Delta\dot{A}}^{-1} S)^{-1} S^T \psi_{\Delta\dot{A}}^{-1} \dot{\bar{A}} \quad , \tag{3-66}$$

where $\psi_{\Delta\dot{A}}$ is the covariance matrix of the range rate measurement errors. The explicit form of this matrix is derived in Appendix C and, for the case of equal error variance in each two-way measurement, is given by (for four ground stations):

$$\psi_{\Delta\dot{A}} = \frac{\sigma^2_{\Delta\dot{M}}}{4} \begin{bmatrix} 1 & -1 & -1 & -1 \\ -1 & 5 & 1 & 1 \\ -1 & 1 & 5 & 1 \\ -1 & 1 & 1 & 5 \end{bmatrix} \tag{3-67}$$

where $\sigma^2_{\Delta\dot{M}}$ is the variance of the two-way range rate measurement error. The error covariance matrix for coordinate rates is derived in Appendix H.

3.7 Time Delay Bias Removal Techniques

3.7.1 General technique.— The measured ranges from the ground receivers to the aircraft transponders will contain bias due to unknown time delays in the transmitter, transponder, and receivers. For the four-station case, measurements (M_i) made by the four receivers are

$$M_i = R_1 + R_i + \varepsilon_i \qquad i = 1, 4 \tag{3-68}$$

where ε_i is an error corresponding to an uncompensated delay in the R_1, R_i path.

A suggested technique for removal of the uncompensated bias errors involves the estimation of the error from the equation

$$\varepsilon_i = M_i - \hat{M}_i \quad , \tag{3-69}$$

where $\hat{M}_i = \hat{R}_1 + \hat{R}_i$ is the calculated estimate of the two-way slant range. The estimate is then smoothed by using a long time constant low-pass digital filter such as

$$\hat{\varepsilon}_i^{\,k+1} = \hat{\varepsilon}_i^{\,k} + \frac{\Delta t}{\tau} (\varepsilon_i^{\,k} - \hat{\varepsilon}_i^{\,k}) \quad , \tag{3-70}$$

where τ is the filter time constant and Δt is the calculation increment.

A flow chart of this calculation technique is shown in Figure 3-2.

3.7.2 Variance of errors in time delay bias estimation.— The variance of errors associated with this estimation technique can be determined as follows. A small change in the estimate is written

$$\Delta\varepsilon_i = \Delta M_i - \Delta\hat{M}_i \quad . \tag{3-71}$$

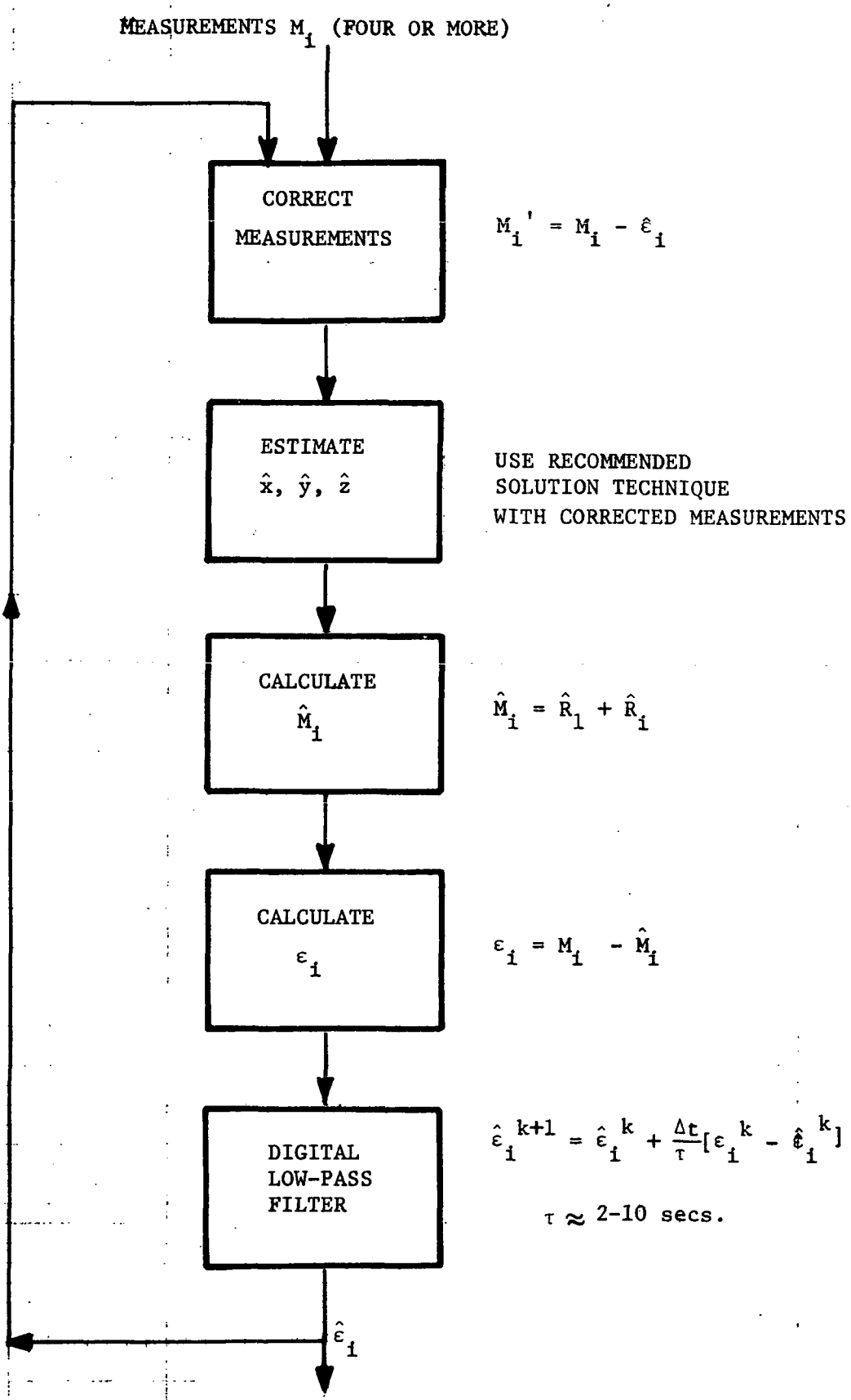

Fig. 3-2. Removal of uncompensated delay bias with four or more ground stations.

Also, a small error in $\hat{M}_i = [(\hat{x} - x_i)^2 + (\hat{y} - y_i)^2 + (\hat{z} - z_i)^2]^{1/2} + \hat{R}_1$ may be written in terms of errors in $\hat{x}$, $\hat{y}$, $\hat{z}$

$$\Delta\hat{M}_i = \frac{\partial\hat{M}_i}{\partial\hat{x}}\Delta\hat{x} + \frac{\partial\hat{M}_i}{\partial\hat{y}}\Delta\hat{y} + \frac{\partial\hat{M}_i}{\partial\hat{z}}\Delta\hat{z} \tag{3-72}$$

or in matrix form

$$\Delta\hat{M}_i = [E_i]\,\overline{\Delta x} \tag{3-73}$$

where

$$E_i = \left\{ \frac{\partial\hat{M}_i}{\partial\hat{x}}, \frac{\partial\hat{M}_i}{\partial\hat{y}}, \frac{\partial\hat{M}_i}{\partial\hat{z}} \right\}$$

and

$$\overline{\Delta x} = \begin{Bmatrix} \Delta\hat{x} \\ \Delta\hat{y} \\ \Delta\hat{z} \end{Bmatrix} .$$

Thus,

$$\Delta\varepsilon_i = \Delta M_i - E_i\overline{\Delta x} \ . \tag{3-74}$$

An <u>upper bound</u> on the bias estimation error can be determined by assuming unity correlation between errors in an individual measurement M and errors in the estimated value of the measurement $\hat{M}$. This upper bound is given by

$$\sigma^2_{\Delta\varepsilon_i} \leq \left[\sigma_{\Delta M_i} + \left\{ E_i \, \psi_{\overline{\Delta x}} \, E_i^T \right\}^{1/2} \right]^2 \tag{3-75}$$

where $\sigma^2_{\Delta M_i}$ is the variance of the two-way range measurement and $\psi_{\overline{\Delta x}}$ is the covariance matrix of the estimation error. The expression $\psi_{\overline{\Delta x}}$ is derived in the appendices for the various solutions considered.

A more exact estimate of the bias error estimation can be obtained if the relationship between the two-way measurement errors $\overline{\Delta M}$ and the $\overline{\Delta x}$ is known. This relationship depends on the solution technique used; for example, for the iterative method described in Appendix F, we have

$$\overline{\Delta x} = G^{-1} D^T \overline{\Delta M} \tag{3-76}$$

where $\overline{\Delta M}$ in the above equation corresponds to $\underset{\sim}{\Delta A}$ in the nomenclature used in the appendix. Using eqs. (3-74) and (3-76) we have

$$\Delta\varepsilon_i = \Delta M_i - E_i G^{-1} D^T \overline{\Delta M} \tag{3-77}$$

or in another form

$$\Delta\varepsilon_i = \beta_i \overline{\Delta M} - E_i G^{-1} D^T \overline{\Delta M} \tag{3-78}$$

where

$$\beta_1 = \{1, 0, 0, 0\} , \quad \beta_2 = \{0, 1, 0, 0\} , \text{ etc.}$$

Thus, the variance of a single measurement of a time delay bias is given by

$$\sigma^2_{\Delta\varepsilon_i} = [\beta_i - E_i G^{-1} D^T] \psi_{\overline{\Delta M}} [\beta_i - E_i G^{-1} D^T]^T \tag{3-79}$$

where $\psi_{\overline{\Delta M}}$ is the measurement error covariance matrix. This variance can be considerably reduced by filtering as is shown in the following section.

3.7.3 Reduction of time delay bias estimation errors by filtering.— Using the digital low-pass filter given by eq. (3-70), the variance of errors in the smoothed estimate $\hat{\varepsilon}_i^{k+1}$ is given by

$$\text{Var } \hat{\varepsilon}_i^{k+1} = (1-\alpha)^2 \text{ Var } \hat{\varepsilon}_i^{k} + \alpha^2 \text{ Var } \varepsilon_i^{k} \quad , \tag{3-80}$$

where $\alpha = \Delta t/\tau$. For times $t >> \tau$ the smoothed variances will not change with time so that for $t << \tau$

$$\text{Var } \hat{\varepsilon}_i^{k+1} \approx \text{Var } \hat{\varepsilon}_i^{k} \tag{3-81}$$

and the variance of the filtered output may be written in terms of the variance of the unsmoothed estimate of ε_i,

$$\text{Var } \hat{\varepsilon}_i = \frac{\alpha}{2 - \alpha} \text{ Var } \varepsilon_i \; ; \; t >> \tau \tag{3-82}$$

or approximately, $\text{Var } \hat{\varepsilon}_i \approx \frac{\Delta t}{2\tau} \text{ Var } \varepsilon_i \; ; \; t >> \tau >> \Delta t$. Thus, for a calculation increment of .1 second and a filter constant τ of 2 seconds, the variance of the smoothed estimate is 2.5% of the unsmoothed estimate. Longer filter time constants provide correspondingly better variance reductions.

It should be noted that instead of a conventional low-pass filter, a minimum variance (i.e., optimal) filter could be used. For this type of filter, the parameter α in the filter equation is recalculated for each time increment, starting with an initial value of unity. The recursive relationship for minimum variance is derived as

$$\alpha^{k+1} = \frac{\alpha^k}{\alpha^k + 1} \; ; \; \alpha^0 = 1. \tag{3-83}$$

In using this technique, the value of α will eventually converge to zero, corresponding to an infinite time constant filter. For this reason, it is desirable to limit the minimum value of α^k to a small number on the order of .01 (i.e., the number .01 corresponds to a low-pass filter of 10 second time constant when using a calculation increment of .1 second). The advantage of the optimal filter is that initial values of the estimate are more accurate than those from a conventional low-pass filter with its inherent transient buildup to the steady state.

Page Intentionally Left Blank

4.0 ERROR STUDIES

4.1 General Discussion

This section considers the errors associated with the various solution techniques discussed in the previous section. The error variances associated with the solution for position coordinates as a function of the slant range measurements are a function of the following system parameters:

1. Basic slant range measurement errors,
2. Station location,
3. Aircraft location,
4. Solution technique,
5. Number of ground stations.

The errors in estimation of the coordinate rates are functions of all the above parameters plus the additional parameters:

6. Aircraft velocity.
7. Range rate measurement errors.

In order to present the results of the error studies in a useful form, several techniques have been used. For the position errors, contour plots are useful for visualizing the rms errors that will be found at various geometrical locations. For presenting results on errors associated with coordinate rates, specific trajectories must be defined and used in the error calculations. In this section, several specific trajectories have been defined and the position and rate errors associated with these trajectories have been calculated. These results are shown in the following sections.

4.2 Comparison of Position Error Variances for Various Solution Techniques

To compare the efficiency of the solution techniques discussed in Section 3.0, tables have been prepared to compare the solution techniques for specific station locations and aircraft locations. The derivation of the error equations is given in the appendices.

In addition to the theoretical error variances, computer simulation techniques have been used to determine actual variances that might be encountered under experimental conditions. For these computer simulations,

the technique shown on the flow chart of Fig. 4-1 is used. A random number generator is used to calculate random perturbations on the slant range measurements and the various solution techniques are used to solve for the coordinate positions. These coordinate positions are then compared to the true coordinate positions to determine coordinate errors. Five hundred samples of this calculation are made, and the mean and variance of the coordinate errors are determined. This simulation technique gives confidence in the theoretical results in cases where the numerical values compare favorably.

Table 4-1 provides a comparison of various solution techniques for an aircraft at the position (1000 ft, 1000 ft, 100 ft) and for the station locations given in the table. In this case, the position of the aircraft is somewhat out of the operational range of the system (i.e., below 15° elevation); however, an extreme case was desired to provide large errors for comparative purposes. As may be seen, the iterative solution, explicit solution and the linearized minimum variance solution provide the same standard deviations of coordinate errors. The three-station trilateration solution is the worst of the solution techniques considered, as would be expected. Values from the computer simulation compare favorably to the theoretical values, and it should be noted that the iterative solution converges quite rapidly (i.e., only a few iterations are required).

Table 4-2 provides the same type of comparison, except that two of the ground stations are elevated by 100 ft. Notice that the standard deviations in the z coordinate are considerably improved over the values with all ground stations at z = 0. Standard deviations of x and y are also improved by elevating the ground stations. Tables 4-3 and 4-4 provide the same type of comparison, except for an aircraft position of (1000, 1000, 500). Notice that at reasonable altitudes, the standard deviation in the z coordinate improves dramatically. Tables 4-5 and 4-6 provide the same comparison for the aircraft located at (100, 100, 50). As the aircraft approaches the landing position, the benefit of elevated stations decreases. In all cases with elevated stations, the iterative solution provides the best accuracy, followed closely by the explicit minimum variance solution. For non-elevated stations, all solution techniques give the same accuracy.

All of the above calculations were made with a fixed-station configuration as given in the tables. The effect of changing station locations is considered in the following section.

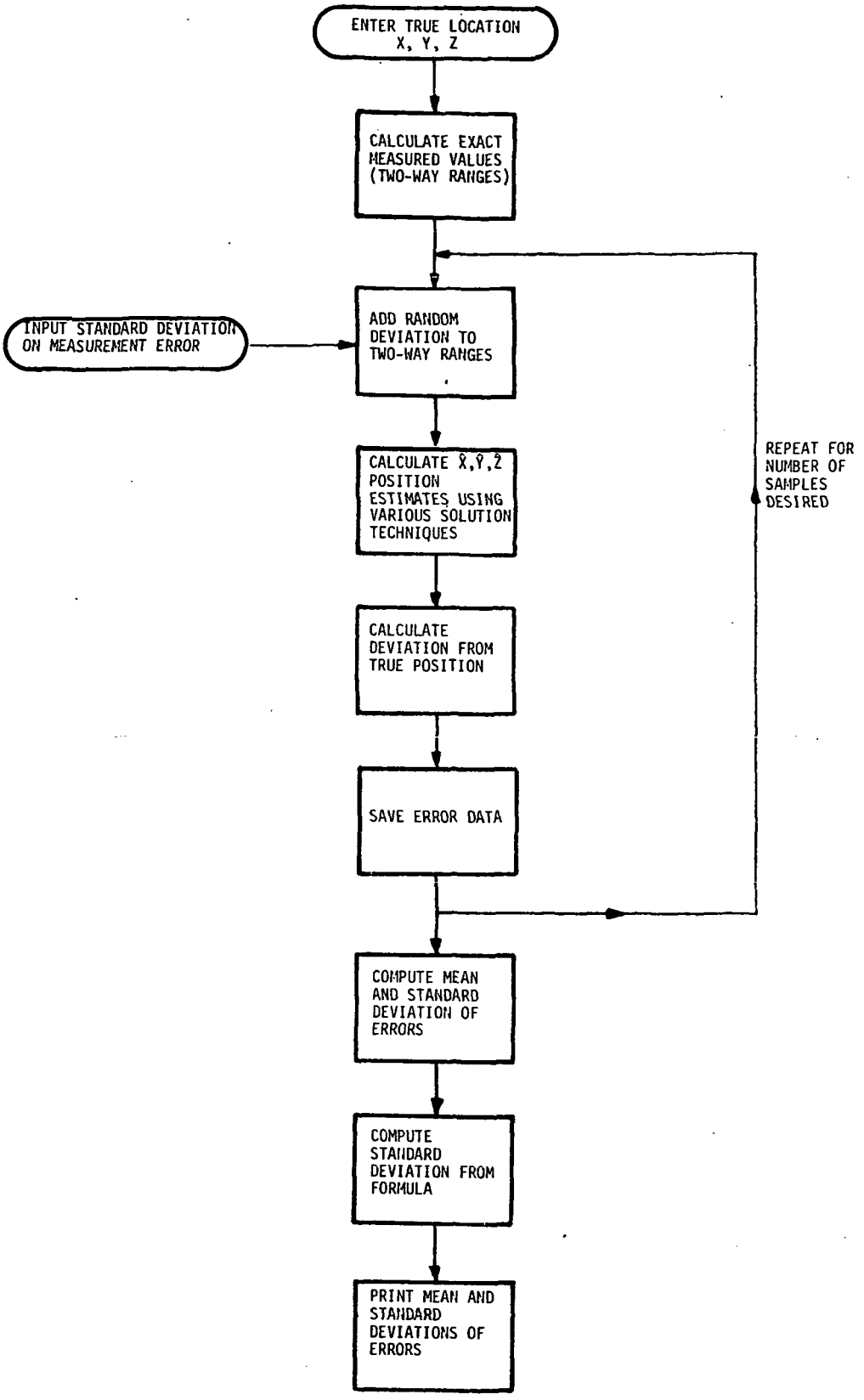

Figure 4-1. Flow Chart of Technique for Direct Computation of Mean and Standard Deviation of Coordinate Errors by Computer Simulation.

Table 4-1. Comparison of error standard deviations for various solution techniques for an aircraft at the position (1000,1000,100) and for the station locations indicated.

Solution Techniques and Station Locations	Standard Deviations of Error Assuming 2 ft rms Two-Way Range Measurement Error					
Station Locations #1 (0, 500, 0) #2 (-433, -250, 0) #3 (433, -250, 0) #4 (0, 0, 0)	Theoretical Values			Values From Computer Simulation		
	σ_x	σ_y	σ_z	σ_x	σ_y	σ_z
1. Three station (trilateration) solution (#1, #2, #3)	5.46	4.84	70.7	5.18	4.31	45.9
2. Linearized minimum variance solution	5.42	4.78	70.3	5.07	4.20	95.4
3. Explicit minimum variance solution	5.42	4.78	70.3	5.07	4.20	43.7
4. Iterative solution	5.42	4.78	70.3	4.06	3.80	41.79

Table 4-2. Comparison of error standard deviations for various solution techniques for an aircraft at the position (1000,1000,100) and for the station locations indicated. (2 Stations Elevated)

Solution Techniques and Station Locations	Standard Deviations of Error Assuming 2 ft rms Two-Way Range Measurement Error					
Station Locations (ft) #1 (0, 500, 0) #2 (-433, -250, 100) #3 (433, -250, 100) #4 (0, 0, 0)	Theoretical Values (ft)			Values From Computer Simulation (ft)		
	σ_x	σ_y	σ_z	σ_x	σ_y	σ_z
1. Three station (trilateration) solution (#1, #2, #3)	5.45	4.22	42.4	5.17	4.40	45.3
2. Linearized minimum variance solution	5.45	7.61	49.7	5.08	7.52	49.7
3. Explicit minimum variance solution	5.83	3.93	36.6	5.45	3.67	36.2
4. Iterative solution	4.69	3.88	34.0	4.62	3.61	32.6

Table 4-3. Comparison of error standard deviations for various solution techniques for an aircraft at the position (1000,1000,500) and for the station locations indicated.

Solution Techniques and Station Locations	Standard Deviations of Error Assuming 2 ft rms Two-Way Range Measurement Error					
Station Locations #1 (0, 500, 0) #2 (-433, -250, 0) #3 (433, -250, 0) #4 (0, 0, 0)	Theoretical Values			Values From Computer Simulation		
	σ_x	σ_y	σ_z	σ_x	σ_y	σ_z
1. Three station (trilateration) solution (#1, #2, #3)	5.69	5.10	14.7	5.53	4.61	15.4
2. Linearized minimum variance solution	5.65	5.06	14.7	5.71	4.41	15.3
3. Explicit minimum variance solution	5.65	5.06	14.7	5.71	4.41	15.4
4. Iterative solution	5.65	5.06	14.7	5.71	4.41	15.3

Table 4-4. Comparison of error standard deviations for various solution techniques for an aircraft at the position (1000,1000,500) and for the station locations indicated. (2 Stations Elevated)

Solution Techniques and Station Locations	Standard Deviations of Error Assuming 2 ft rms Two-Way Range Measurement Error					
Station Locations #1 (0, 500, 0) #2 (-433, -250, 100) #3 (+433, -250, 100) #4 (0, 0, 0)	Theoretical Values			Values From Computer Simulation		
	σ_x	σ_y	σ_z	σ_x	σ_y	σ_z
1. Three station (trilateration) solution (#1, #2, #3)	5.60	4.07	12.9	5.45	3.44	13.5
2. Linearized minimum variance solution	5.60	8.11	52.4	5.64	7.26	50.6
3. Explicit minimum variance solution	5.69	4.20	12.8	5.74	3.49	13.25
4. Iterative solution	5.57	4.07	12.7	5.20	3.50	12.17

Table 4-5. Comparison of error standard deviations for various solution techniques for an aircraft at the position (100,100,50) and for the station locations indicated.

Solution Techniques and Station Locations	Standard Deviations of Error Assuming 2 ft rms Two-Way Range Measurement Error					
Station Locations #1 (0, 500, 0) #2 (-433, -250, 0) #3 (+433, -250, 0) #4 (0, 0, 0)	Theoretical Values			Values From Computer Simulation		
	σ_x	σ_y	σ_z	σ_x	σ_y	σ_z
1. Three station (trilateration) solution (#1, #2, #4)	2.48	1.28	5.3	2.69	1.77	7.34
2. Linearized minimum variance solution	1.81	1.27	5.2	1.91	1.69	7.46
3. Explicit minimum variance solution	1.81	1.27	5.3	1.91	1.69	7.12
4. Iterative solution	1.81	1.27	5.2	1.91	1.69	7.46

Table 4-6. Comparison of error standard deviations for various solution techniques for an aircraft at the position (100,100,50) and for the station locations indicated. (2 Stations Elevated)

Solution Techniques and Station Locations	Standard Deviations of Error Assuming 2 ft rms Two-Way Range Measurement Error					
Station Locations #1 (0, 500, 0) #2 (-433, -250, 0) #3 (+433, -250, 0) #4 (0, 0, 0)	Theoretical Values			Values From Computer Simulation		
	σ_x	σ_y	σ_z	σ_x	σ_y	σ_z
1. Three station (trilateration) solution (#1, #2, #4)	4.21	1.28	9.9	4.33	1.77	9.9
2. Linearized minimum variance solution	1.86	1.28	9.3	1.92	1.77	10.3
3. Explicit minimum variance solution	1.98	1.31	6.2	2.12	1.65	7.95
4. Iterative solution	1.84	1.25	6.0	1.85	1.94	6.61

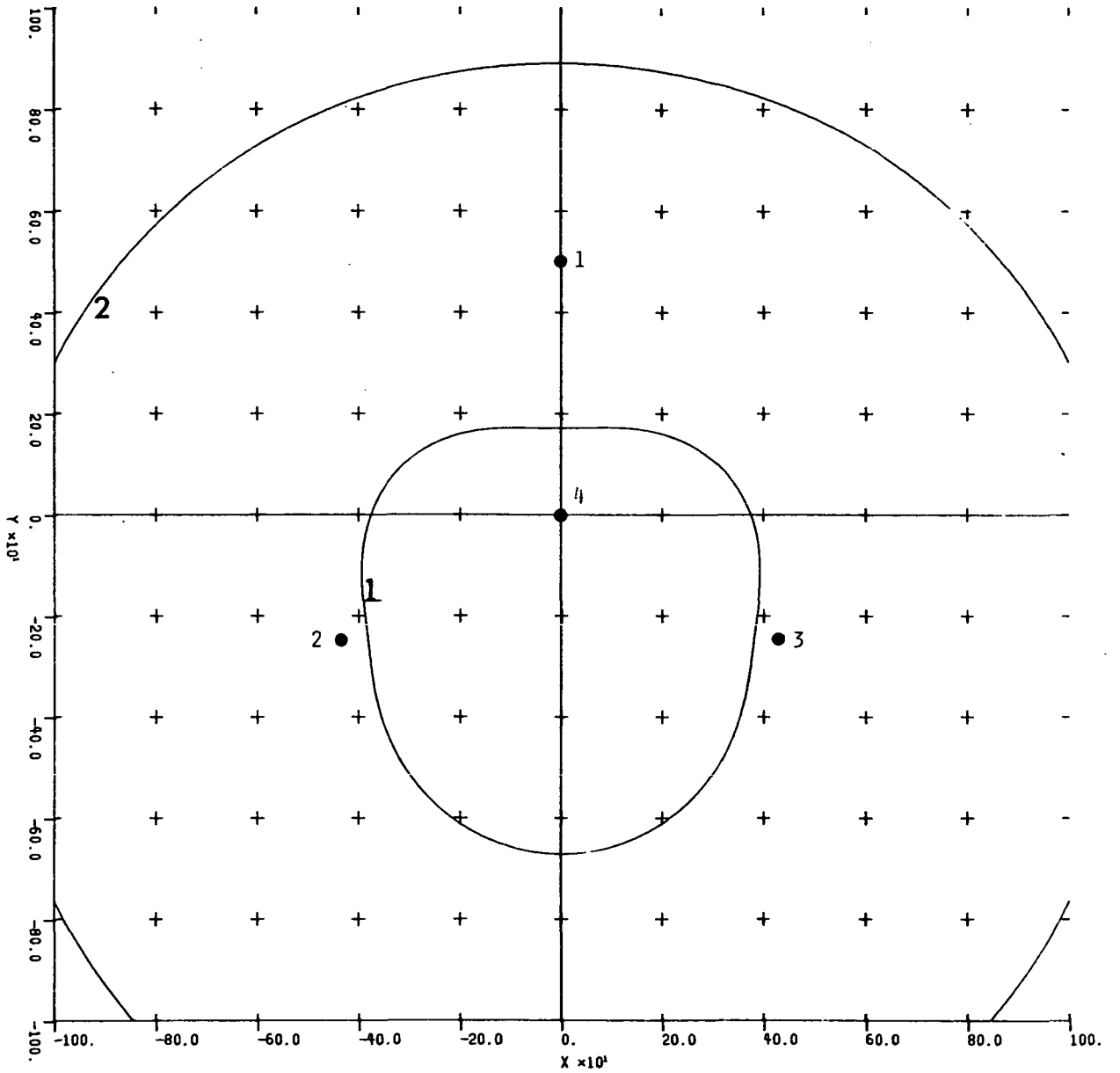

Fig. 4-2. Plot of normalized equal rms error contours in the x coordinate (σ_x/σ_R) in the plane z = 100 ft. The ground station locations are shown on the plot.

From the above comparisons it may be concluded that the iterative solution always provides the lowest value of coordinate standard deviations. This is as would be expected. However, the iterative solution causes calculation difficulties in that several iterations must be made each calculation increment. The linearized minimum variance solutions provide good values of standard deviation; however, separate solutions are required for the case where all ground stations are in the plane $z = 0$, and the case where ground stations are elevated. Standard deviations for the explicit minimum variance solution are close to that of the iterative solution, and since the solution is completely general and straightforward, the advantages may outweigh the slight disadvantage of increased error standard deviations.

4.3 Position Error Contours

Error contours have been generated for particular cases to indicate the geometrical regions where equal errors occur. These error contours have been generated from the theoretical standard deviations of the minimum variance iterative solution.

Figure 4-2 shows a contour plot of the errors in the x coordinate at a constant z plane ($z = 100$ ft). For this and all plots, it has been assumed that the two-way slant range measurements have equal random error variances, and the plot gives the ratio of the coordinate standard deviation to the two-way range measurement standard deviation. In this particular figure, contours showing error multiplication factors of unity and two are the only integer contours which appear on the plot within the region plotted (-1000 to +1000 ft in x and y).

Figure 4-3 shows a similar plot of the x coordinate error, except at an elevation of $z = 500$ ft. Figure 4-4 is similar except for an elevation of $z = 1000$ ft. Figures 4-5, 4-6 and 4-7 show similar plots for the y coordinate error. The y coordinate error appears comparable to the x coordinate error at all elevation planes.

Error contours for the z coordinate are shown in Figures 4-8, 4-9 and 4-10. The z coordinate errors, as indicated in Tables 4-1 through 4-6, are much more severe than those in x and y. At higher elevation angles, however, as indicated in the $z = 500$ ft plane, the z axis errors become considerably smaller.

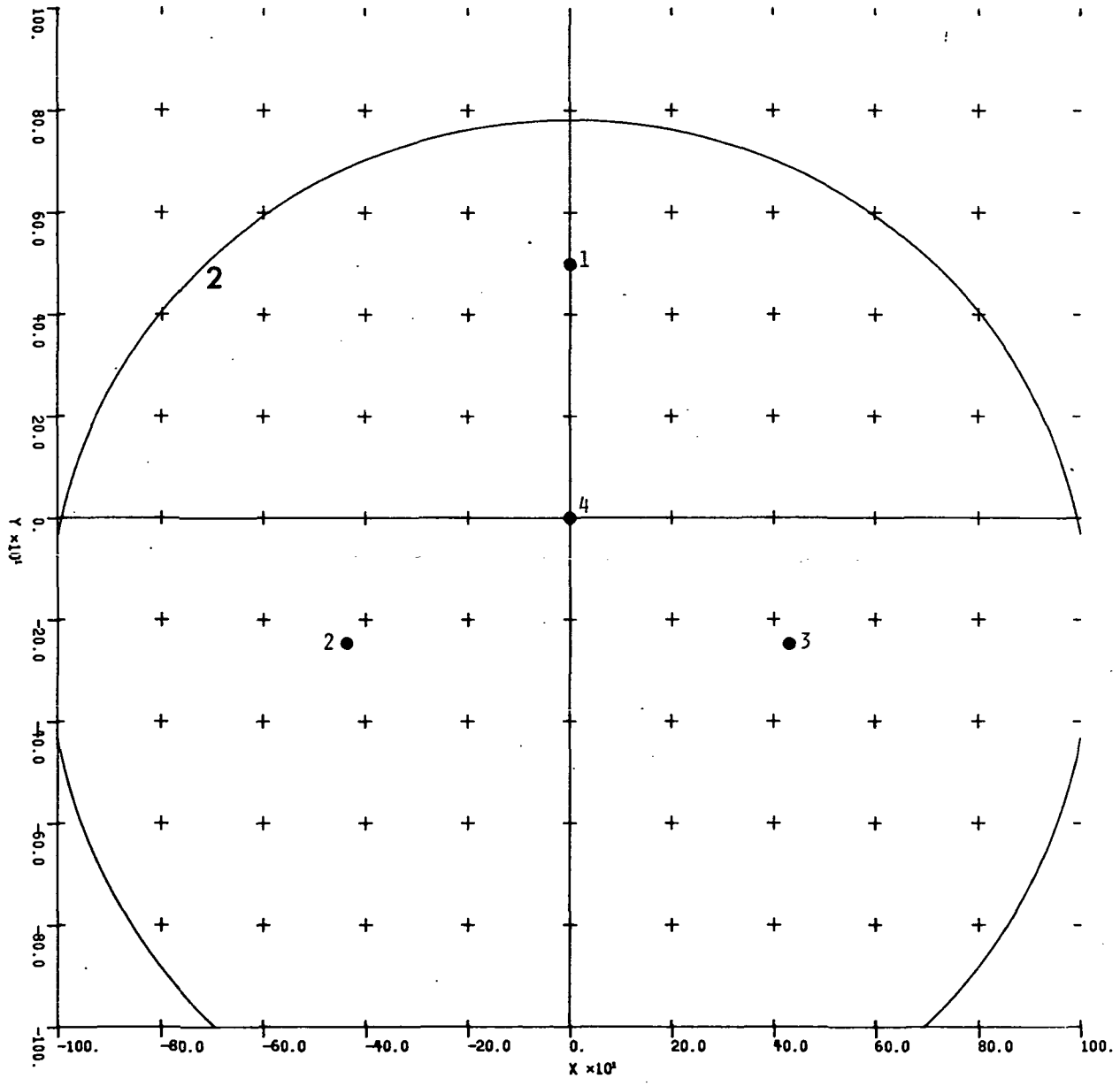

Fig. 4-3. Plot of normalized equal rms error contours in the x coordinate (σ_X/σ_R) in the plane z = 500 ft. The ground station locations are shown on the plot.

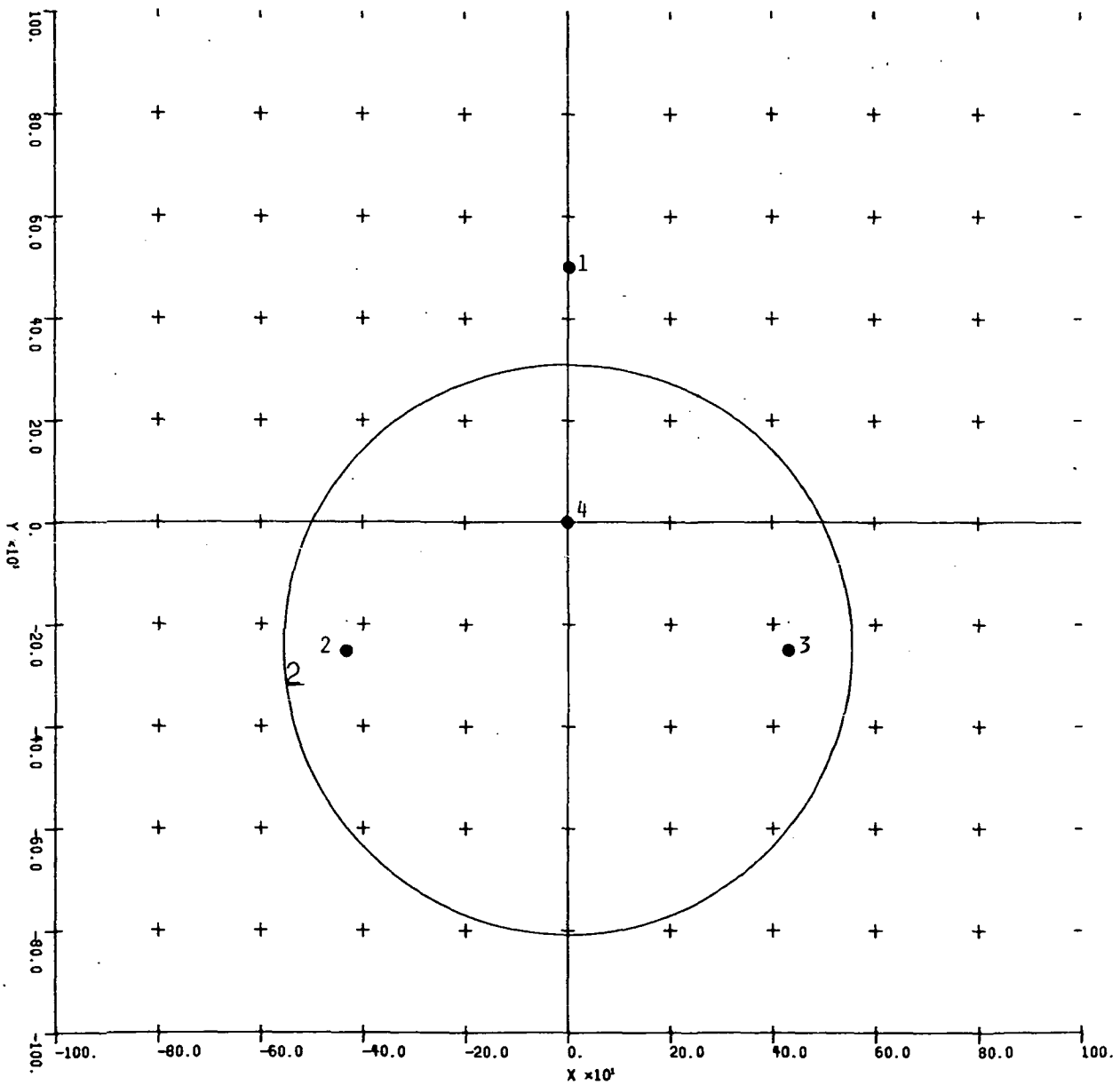

Fig. 4-4. Plot of normalized equal rms error contours in the x coordinate (σ_x/σ_R) in the plane z = 1000 ft. The ground station locations are shown on the plot.

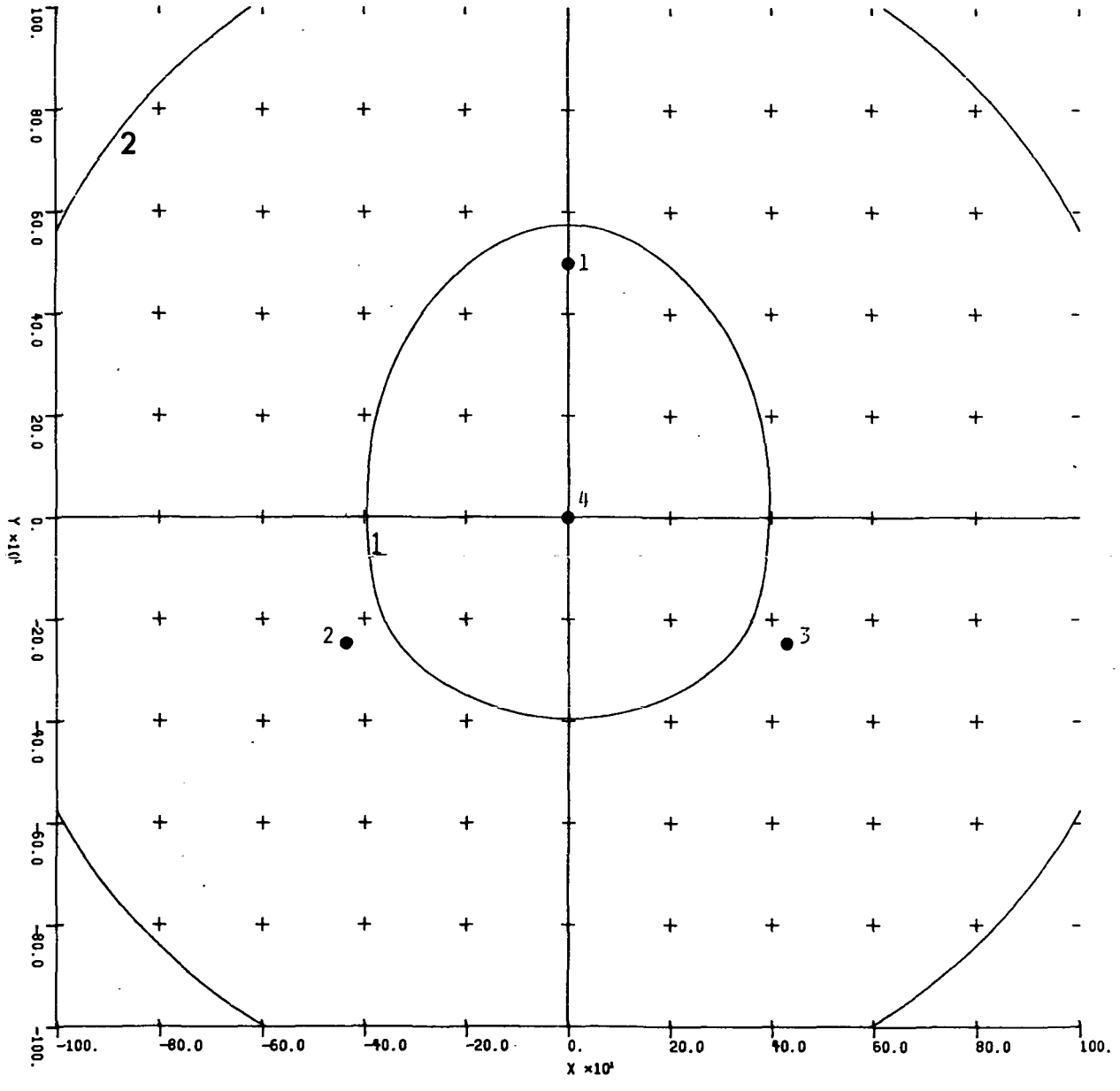

Fig. 4-5. Plot of normalized equal rms error contours in the y coordinate (σ_y/σ_R) in the plane z = 100 ft. The ground station locations are shown on the plot.

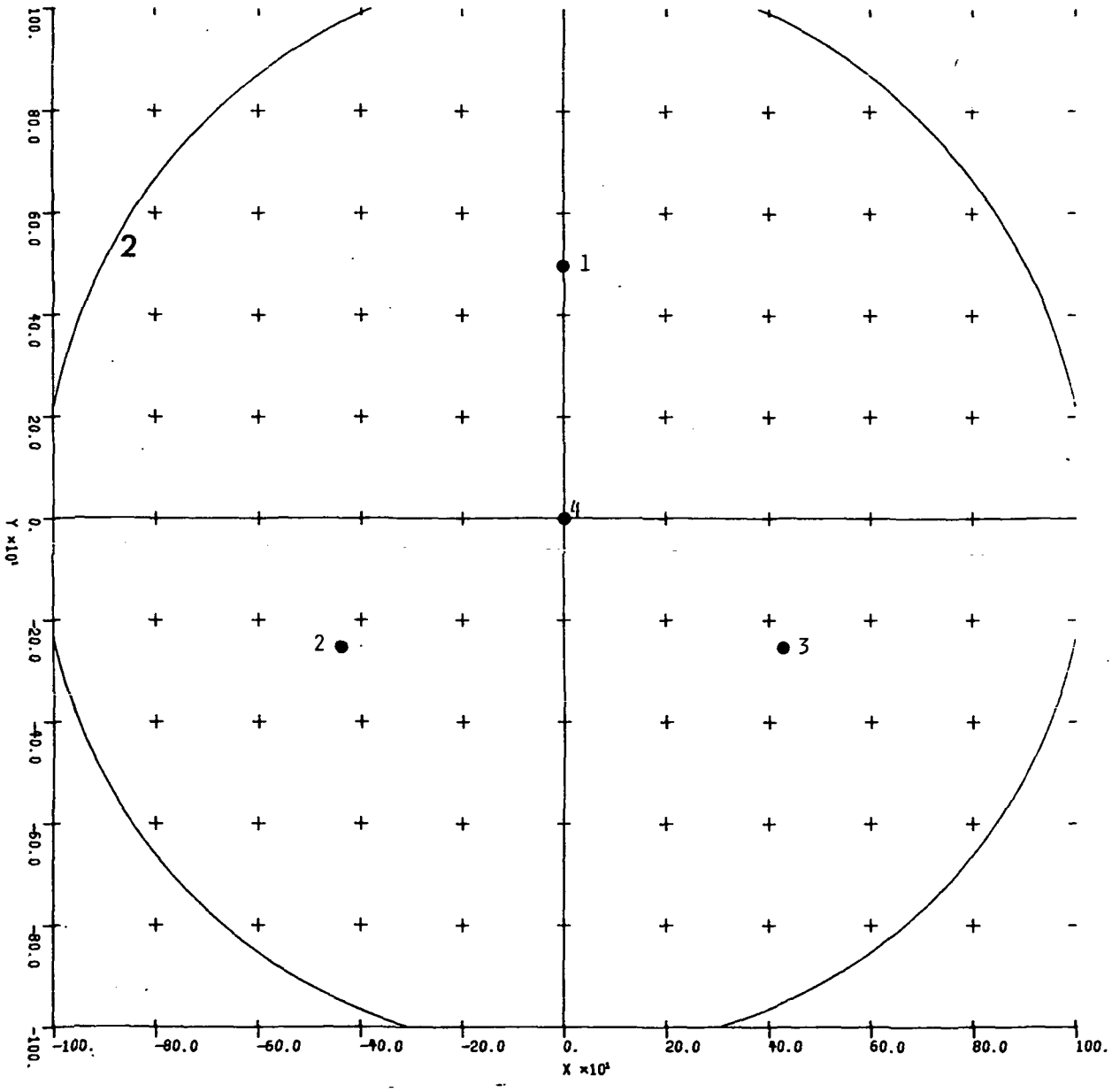

Fig. 4-6. Plot of normalized equal rms error contours in the y coordinate (σ_y/σ_R) in the plane z = 500 ft. The ground station locations are shown on the plot.

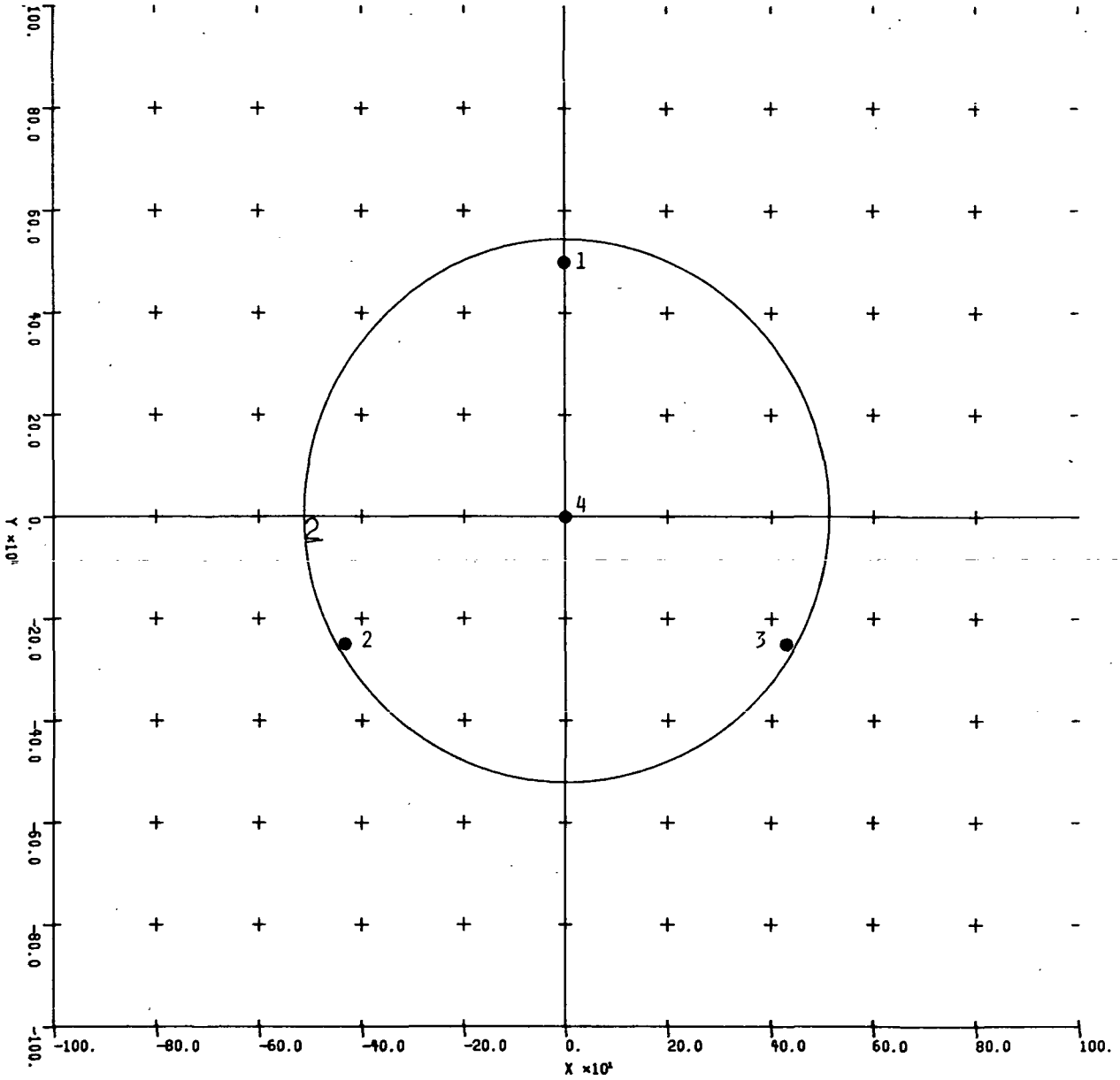

Fig. 4-7. Plot of normalized equal rms error contours in the y coordinate (σ_y/σ_R) in the plane z = 1000 ft. The ground station locations are shown on the plot.

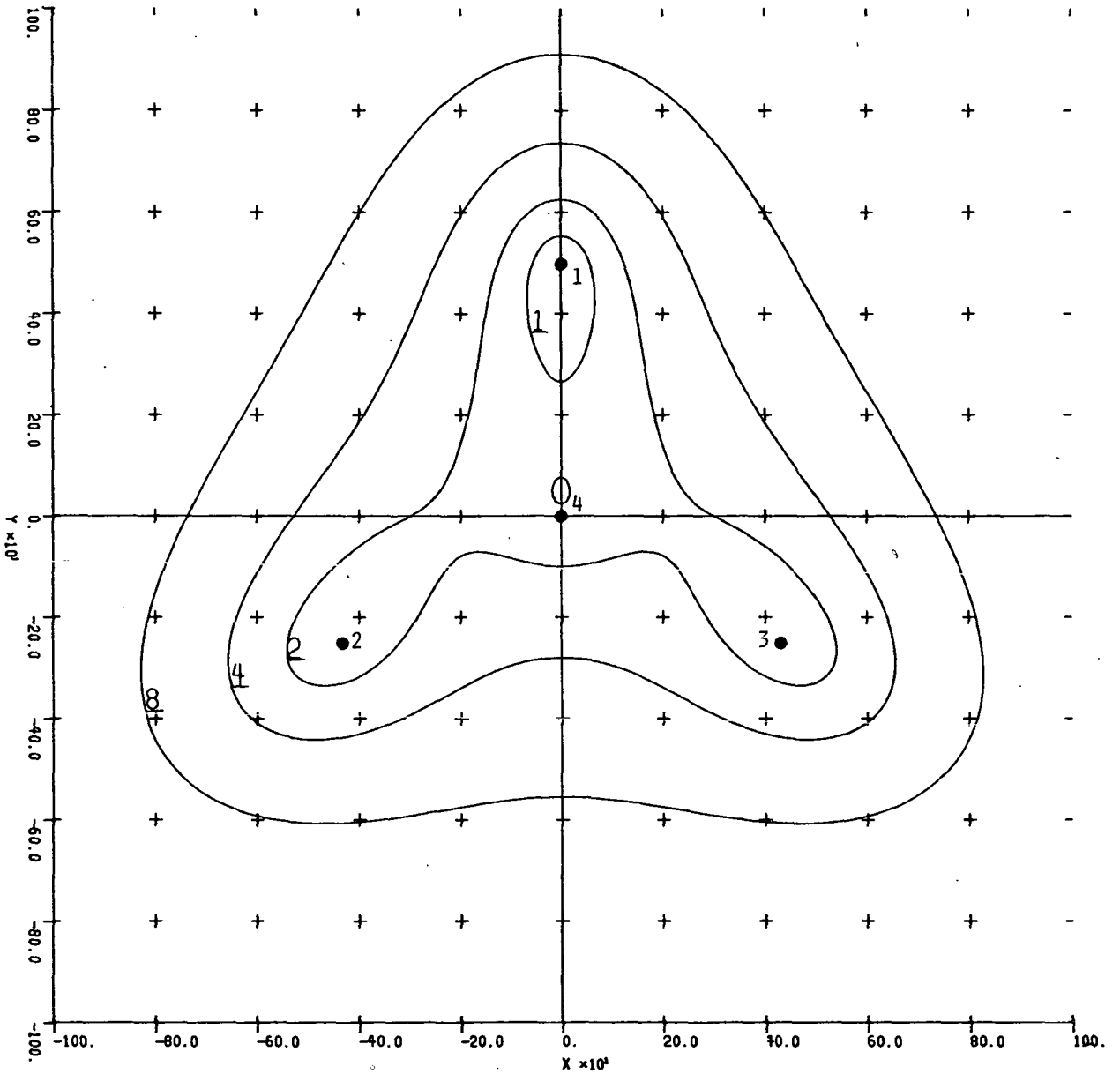

Fig. 4-8. Plot of normalized equal rms error contours in the z coordinate (σ_z/σ_R) in the plane z = 100 ft. The ground station locations are shown on the plot.

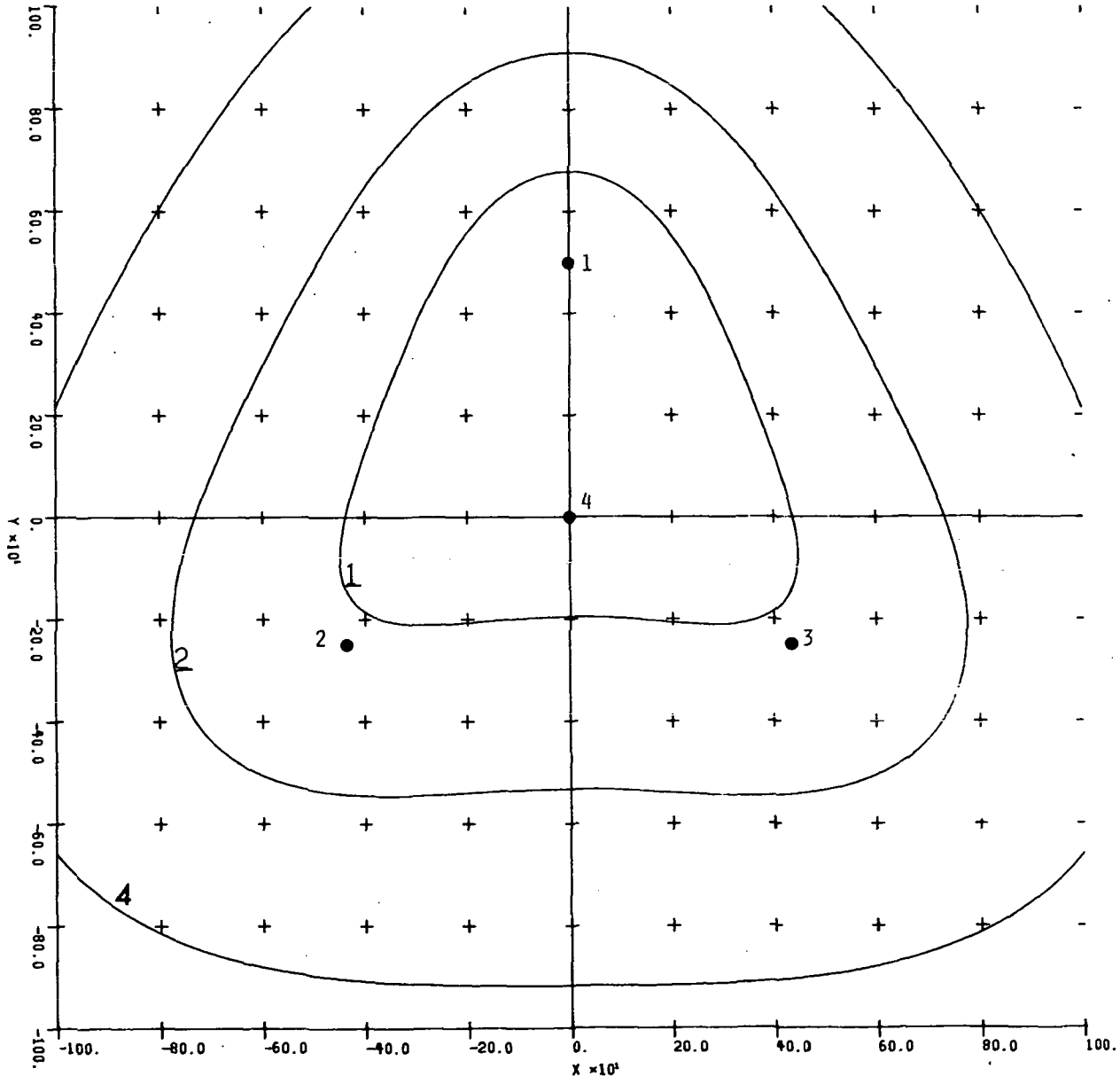

Fig. 4-9. Plot of normalized equal rms error contours in the z coordinate (σ_z/σ_R) in the plane z = 500 ft. The ground station locations are shown on the plot.

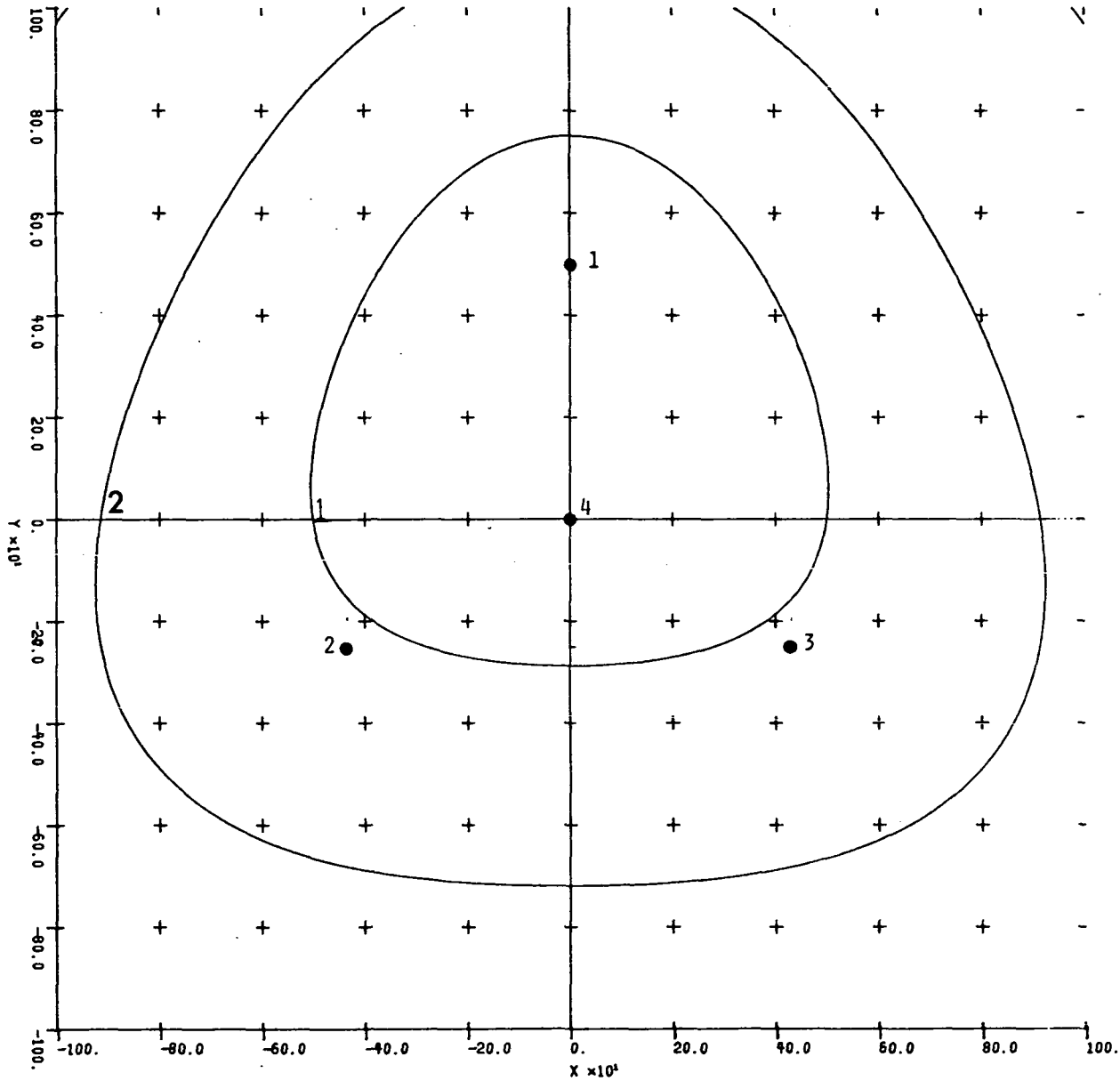

Fig. 4-10. Plot of normalized equal rms error contours in the z coordinate (σ_z/σ_R) in the plane z = 1000 ft. The ground station locations are shown on the plot.

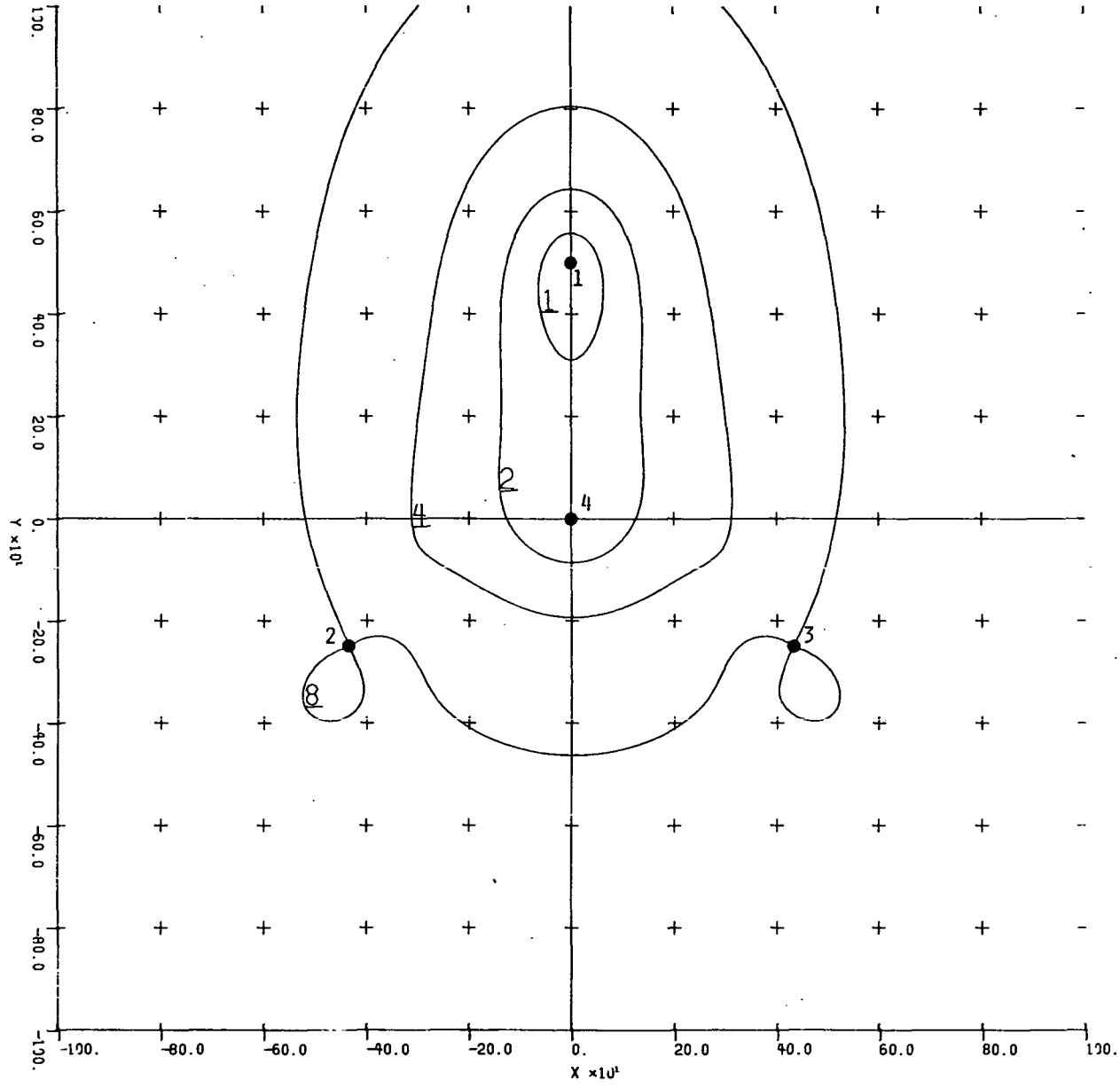

Fig. 4-11. Plot of normalized equal rms error contours in the z coordinate (σ_z/σ_R) in the plane z = 100 ft. The ground station locations are shown on the plot (stations #2 and #3 elevated 100 ft).

Figures 4-11 and 4-12 show the effect on the position error contours when two of the ground stations (#2 and #3) are elevated 100 ft. Comparing Figure 4-11 with Figure 4-8 we see significant improvement in the z axis accuracy. The improvement has a larger effect at positions distant from the ground stations. Comparison of Figures 4-12 and 4-9 leads to the same conclusion. In Figure 4-12, the area of the contours has increased from those in Figure 4-8, with the outer contours increasing more than the inner contours.

Figures 4-13 and 4-14 show the effect of changing the ground station location to a configuration that favors approaches from the positive y axis. The ground station location for this new configuration is shown on the plot. All stations are in the plane z = 0 for this configuration. Notice that the regions of good accuracy are moved out along the negative y axis, whereas the accuracy near the landing point (0,0) is not greatly affected.

These error contour plots showing the effects of elevating stations and moving the ground location of the stations indicate the flexibility of the system in tailoring the accuracy to particular approach paths. The situation is somewhat analogous to that of obtaining directivity in the proper direction with a series of antenna dipoles. If approaches will be from a preferred direction, the accuracy in that direction can be improved by tailoring the ground station locations accordingly.

4.4 Position and Rate Errors for Specific Aircraft Trajectories

4.4.1 General discussion.— As previously discussed, an analysis of the coordinate rate errors requires definition of specific trajectories because the coordinate rate errors are dependent on aircraft velocity and heading, as well as aircraft position. In order to investigate the coordinate rate errors, specific straight-in approach trajectories have been defined with glide slope angles of 1.3 and 15 degrees. The velocity and acceleration profiles of the trajectories are defined in the following section.

The trajectory with the glide slope angle of 1.3 degrees is not within the design range of the system, but was included to investigate the severity of errors at extreme low angle approaches.

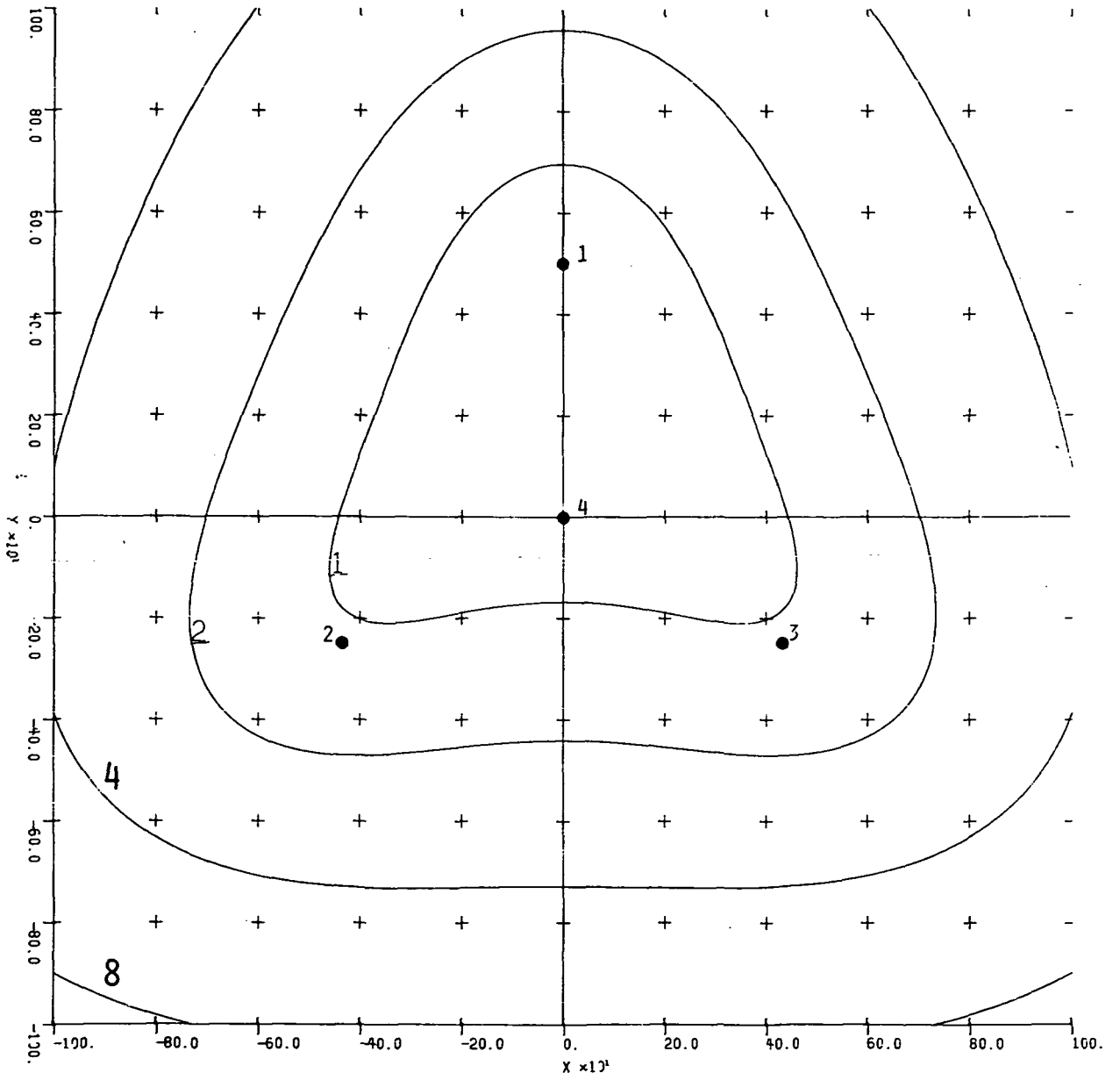

Fig. 4-12. Plot of normalized equal rms error contours in the z coordinate (σ_z/σ_R) in the plane z = 500 ft. The ground station locations are shown on the plot (stations #2 and #3 elevated 100 ft).

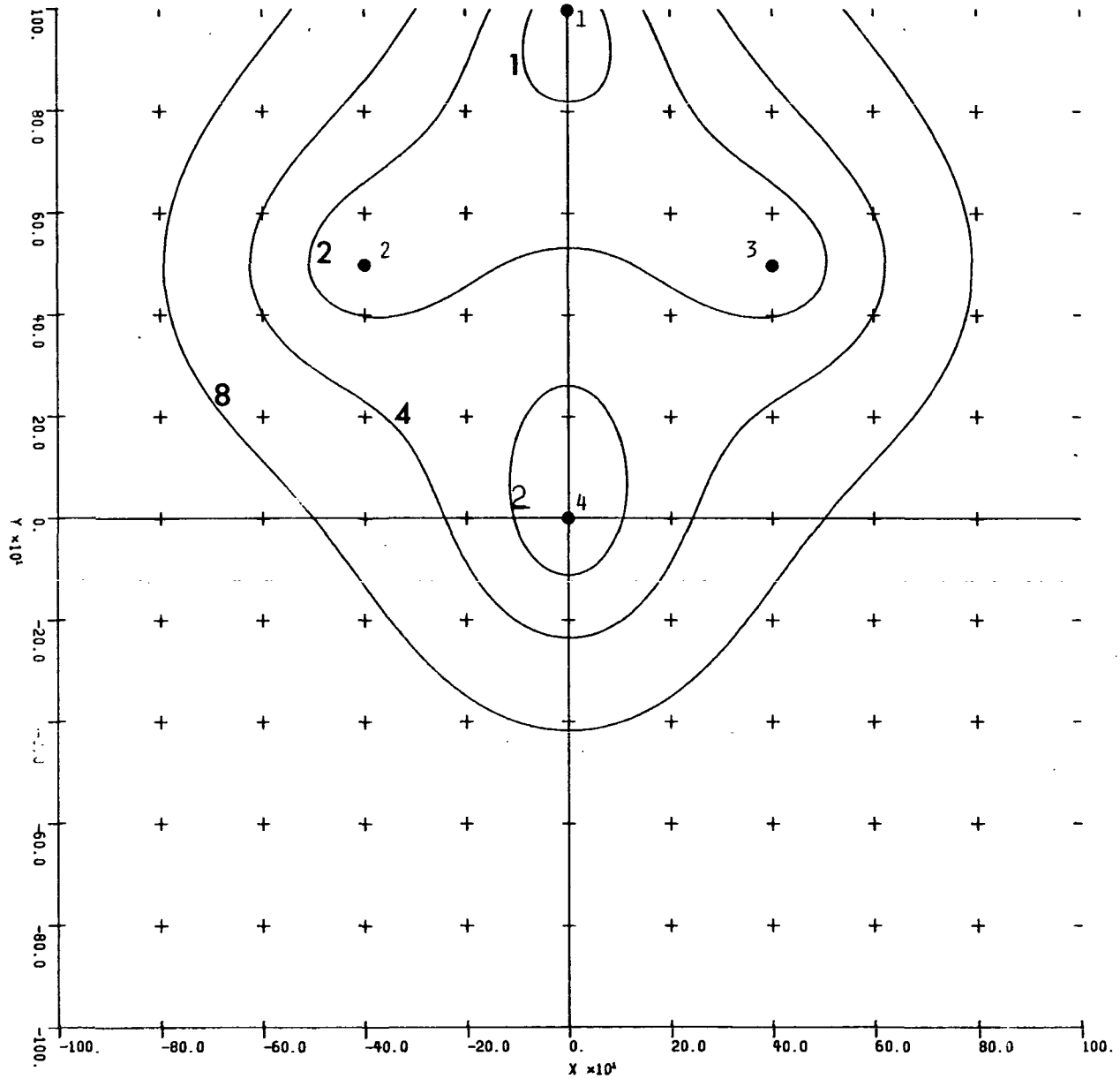

Fig. 4-13. Plot of normalized equal rms error contours in the z coordinate (σ_z/σ_R) in the plane z = 100 ft. The ground station locations are shown on the plot.

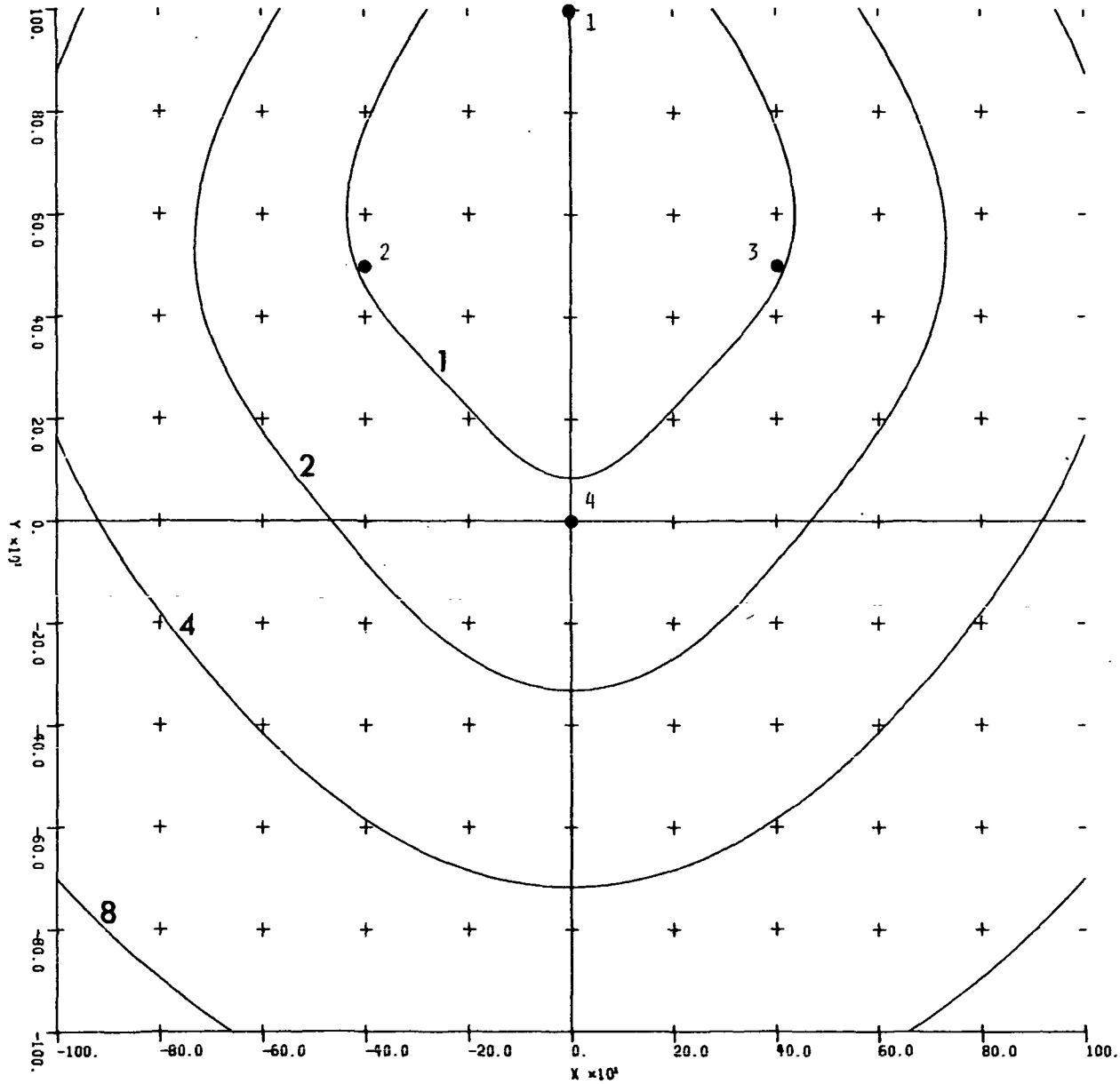

Fig. 4-14. Plot of normalized equal rms error contours in the z coordinate (σ_z/σ_R) in the plane z = 500 ft. The ground station locations are shown on the plot.

4.4.2 Measurement errors in coordinate positions and coordinate rates for a straight-in approach trajectory with glide slope angles of 1.3 and 15 degrees.— This section provides calculations of errors in coordinate positions and rates for the four-station multilateration system using a straight-in trajectory similar to the Wall St. approach discussed in ref. 2. The placement of the ground receivers was varied to determine the variation of coordinate errors as a function of ground station location.

The trajectories considered are shown in Fig. 4-15. The top curve plots the velocity profile as a function of distance along the y axis. The velocity is constant until a distance of 553 ft from the touchdown point is reached, at which point a deceleration at a constant rate of 6.15 ft/sec^2 takes place. The final velocity is 1.7 ft/sec at the touchdown point. A plot of altitude vs. distance along the y axis is shown in the bottom plot of Fig. 4-15. For comparative purposes, two glide slopes are used in the calculations: a 1.3° glide slope, which represents the Wall St. trajectory, and 15°, which is representative of a higher angle approach. The final altitude at the touchdown point is 10 ft in both cases. Note that the low-angle glide slope only reaches an altitude of approximately 50 ft at 1800 ft from the touchdown point.

Figure 4-16 provides a sketch of the receiver locations for four different cases. The first case is a symmetrical configuration with the receivers located on a 500-ft radius circle from the origin of coordinates. Case 2 is an L-shaped configuration with three stations located along the axis of the trajectory and one station offset along the y axis for a distance of 500 ft. Case 3 is a staggered situation with the four receivers offset slightly from the ground projection of the trajectory. Case 4 is a diamond-shaped configuration with one ground receiver placed 1000 ft out along the y axis. In the sketches, the location of the transmitter is located by the circled dots. In all cases, the ground projection of the trajectory lies along the y axis and the touchdown point is at the origin of the coordinates (station 4 location).

The error calculations are made in accordance with the techniques outlined in Section 3.4. In all cases, a standard deviation in range measurement of 2 ft and a standard deviation in range rate measurement of .1 ft/sec are assumed. Plots are then made of the standard deviation of the errors in the x, y, and z coordinates, and the corresponding standard deviation of errors in the $\dot{x}$, $\dot{y}$, $\dot{z}$ coordinate rates. Figures 4-17 through 4-20 show the error

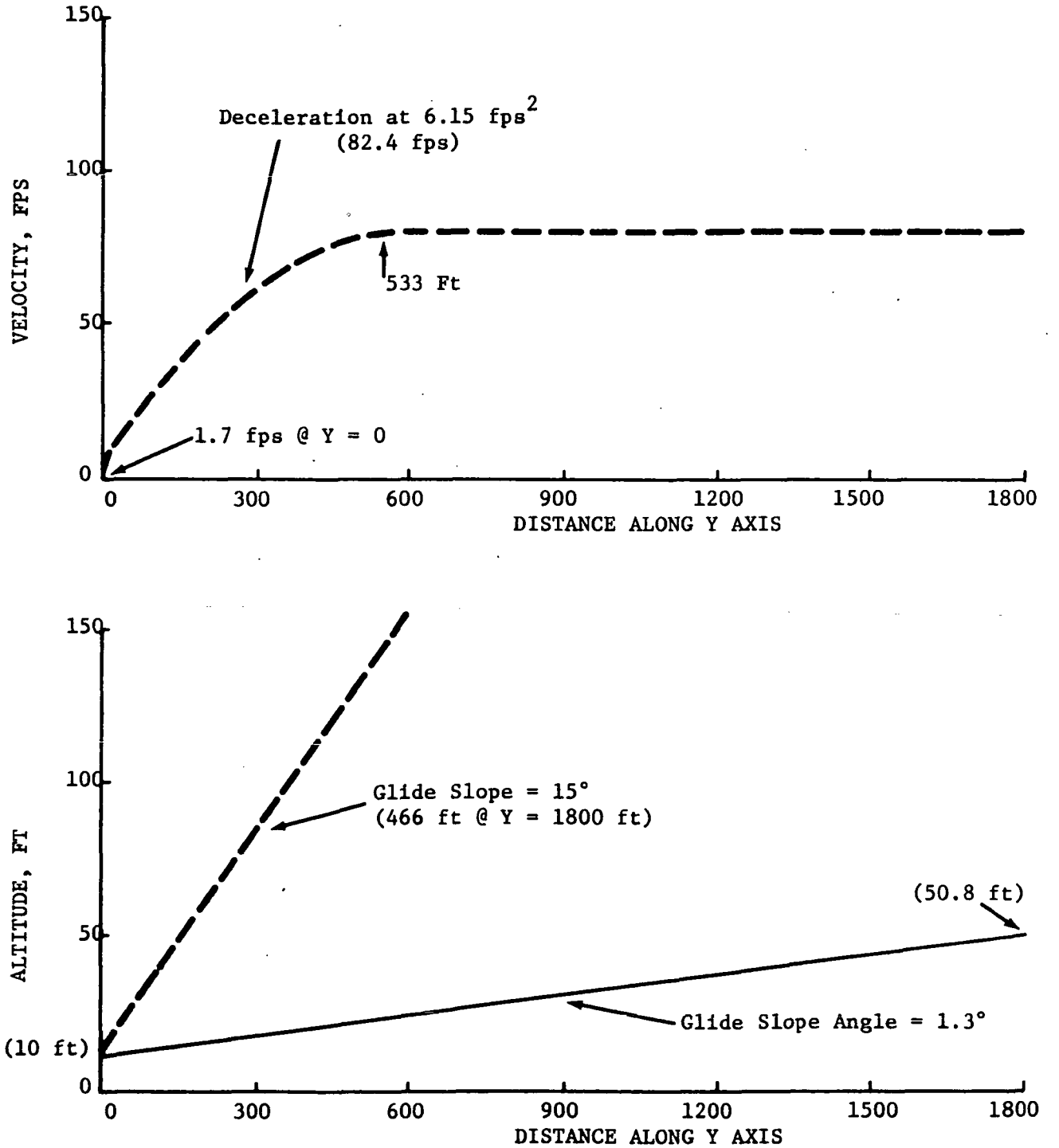

Fig. 4-15. Velocity and altitude plotted vs. distance along the y axis for assumed trajectories.

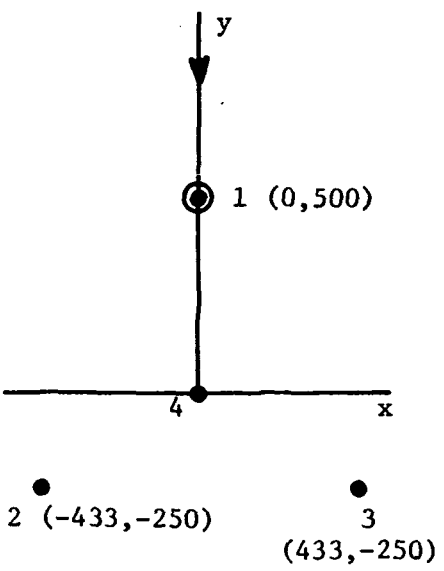

CASE 1

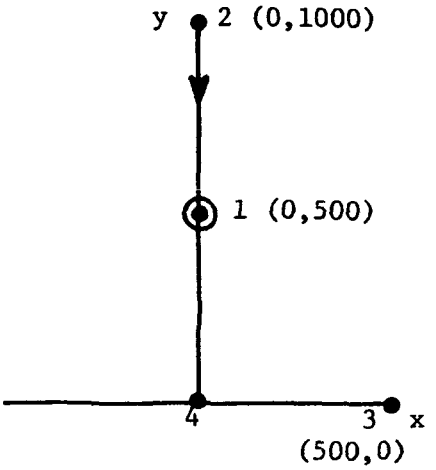

CASE 2

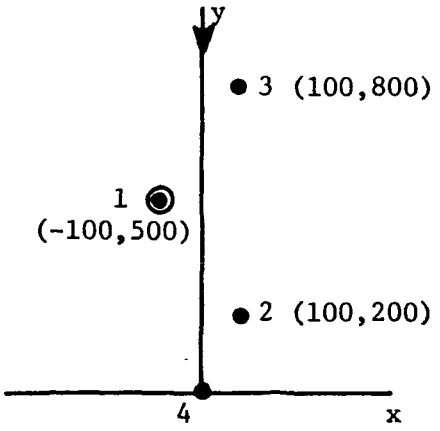

CASE 3

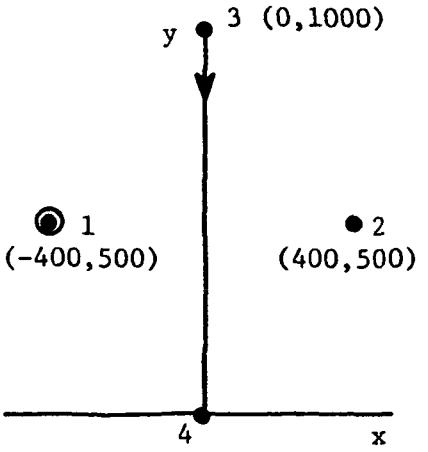

CASE 4

Fig. 4-16. Sketch of receiver locations for various cases considered. The trajectory is along the y axis. The transmitter is circled.

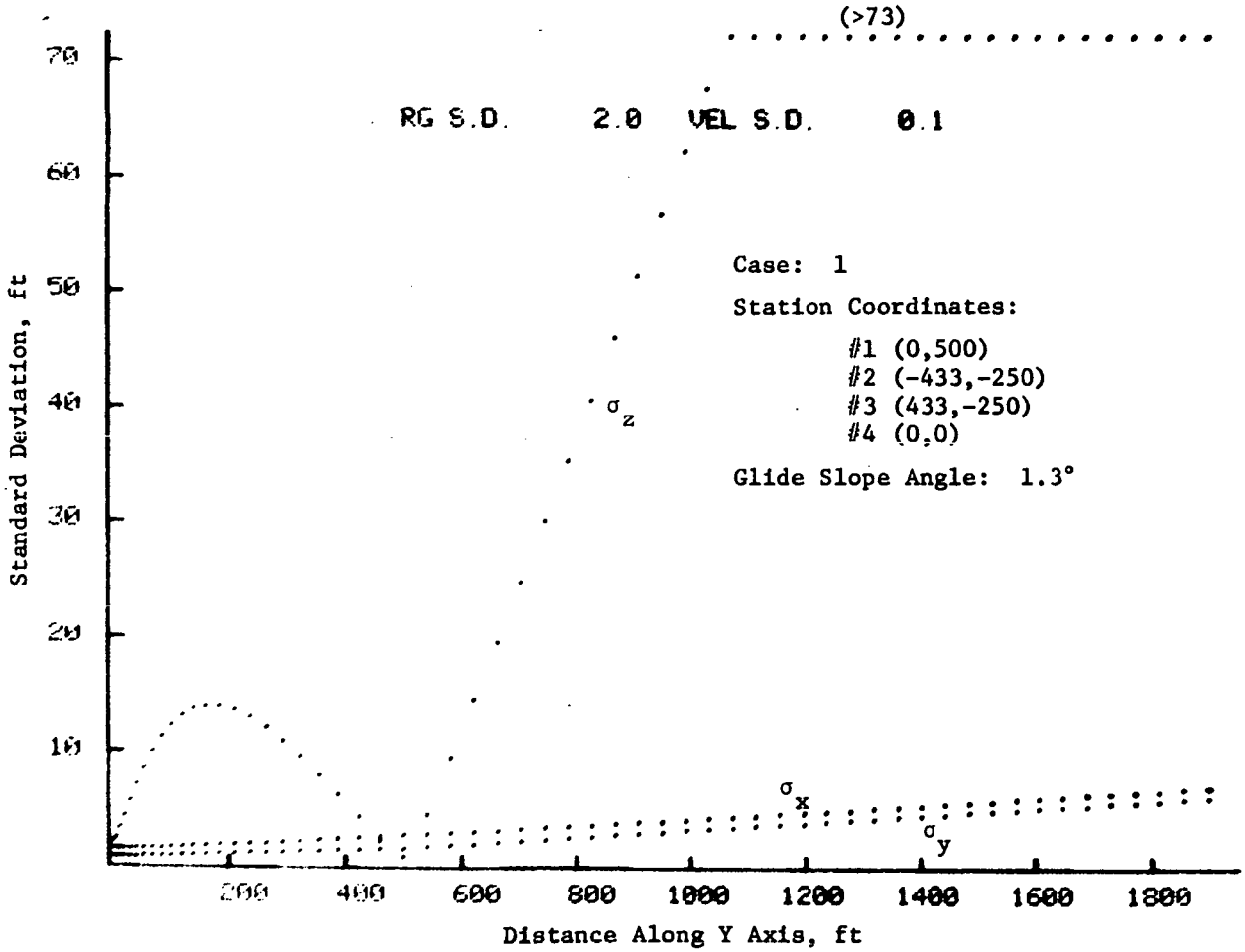

Fig. 4-17. Standard deviation of errors in coordinate positions plotted vs. ground projection of slant range for the specified trajectory. Dots are .5 sec apart. Measurement errors are 2 ft rms in range and .1 fps rms in range rate.

plots for the four cases considered for a glide slope angle of 1.3°. As may be seen, the standard deviation in the altitude coordinate (z) is larger than that for x and y, as would be expected.

Figures 4-21 through 4-24 plot the standard deviation in the coordinate rate errors as a function of distance along the y axis for the various cases considered. The standard deviation of $\dot{z}$ has a rather large variation in most cases, with several peaks and valleys. In all cases, however, the standard deviations become small at the touchdown point.

Figures 4-25 through 4-32 plot similar curves except for a glide slope angle of 15°. This glide slope angle is more consistent with the design objectives of the multilateration system. For all station locations considered, the coordinate position errors remain small (approximately 5 ft rms), and the coordinate rate errors are under 1 ft/sec for the most part. For this glide slope angle, the errors are not a strong function of receiver location; however, it is possible to attain better accuracy over certain portions of the trajectory by judicious location of the ground receivers.

4.4.3 Measurement errors in coordinate position and coordinate rates using elevated ground stations.— Figures 4-33 through 4-40 plot the standard deviation of errors in range and range rate using receiver locations similar to those shown in Fig. 4-16, except that certain stations are elevated 100 ft. The receiver locations for the various cases are specified on the figures. For all cases, a 1.3° glide slope is used and the basic measurement errors are 2 ft rms in range and .1 ft/sec rms in range rate.

Elevation of one or more of the receivers improves the position measurement accuracy significantly in the z coordinate. The major improvement is achieved at ranges outside the region of station location (greater than 1000 ft from touchdown). For example, compare Figure 4-19 with Figure 4-35. Measurements of coordinate rates are also more accurate at longer ranges with elevated receivers. However, there are locations along the trajectory at which large range rate errors occur. For example, see Figure 4-39, where the errors peak at a y axis distance of approximately 650 ft.

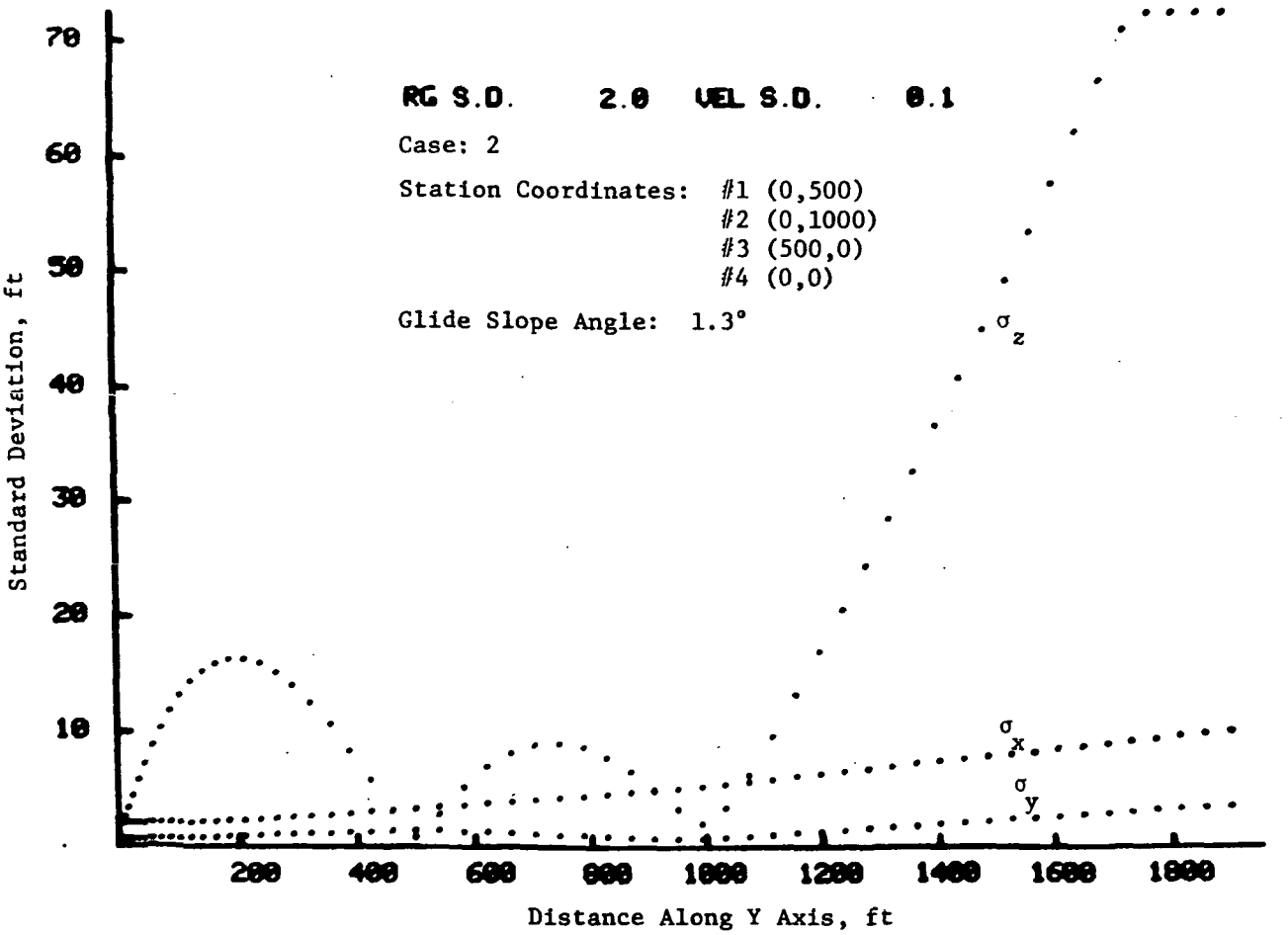

Fig. 4-18. Standard deviation of errors in coordinate positions plotted vs. ground projection of slant range for the specified trajectory. Dots are .5 sec apart. Measurement errors are 2 ft rms in range and .1 fps rms in range rate.

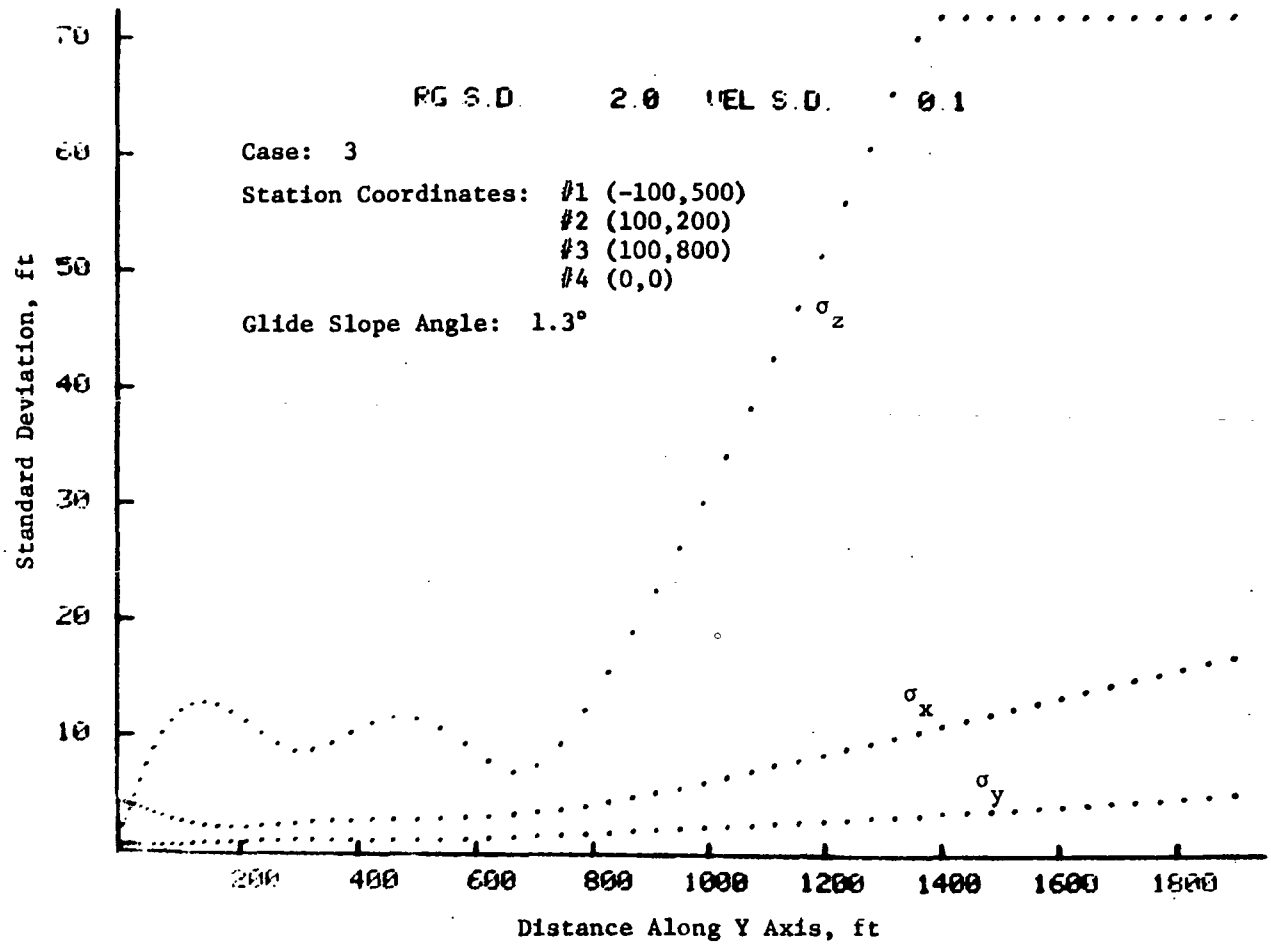

Fig. 4-19. Standard deviation of errors in coordinate positions plotted vs. ground projection of slant range for the specified trajectory. Dots are .5 sec apart. Measurement errors are 2 ft rms in range and .1 fps rms in range rate.

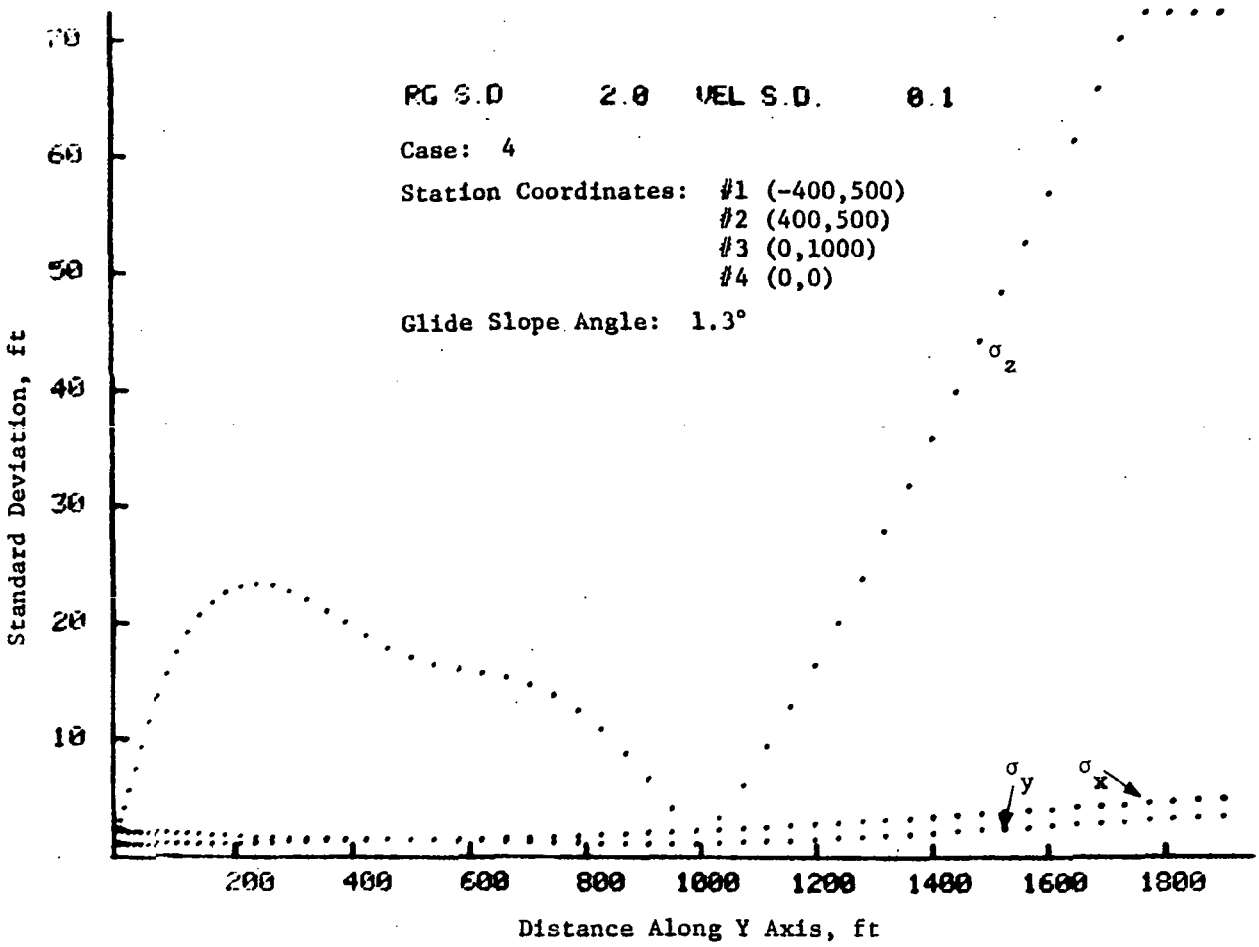

Fig. 4-20. Standard deviation of errors in coordinate positions plotted vs. ground projection of slant range for the specified trajectory. Dots are .5 sec apart. Measurement errors are 2 ft rms in range and .1 fps rms in range rate.

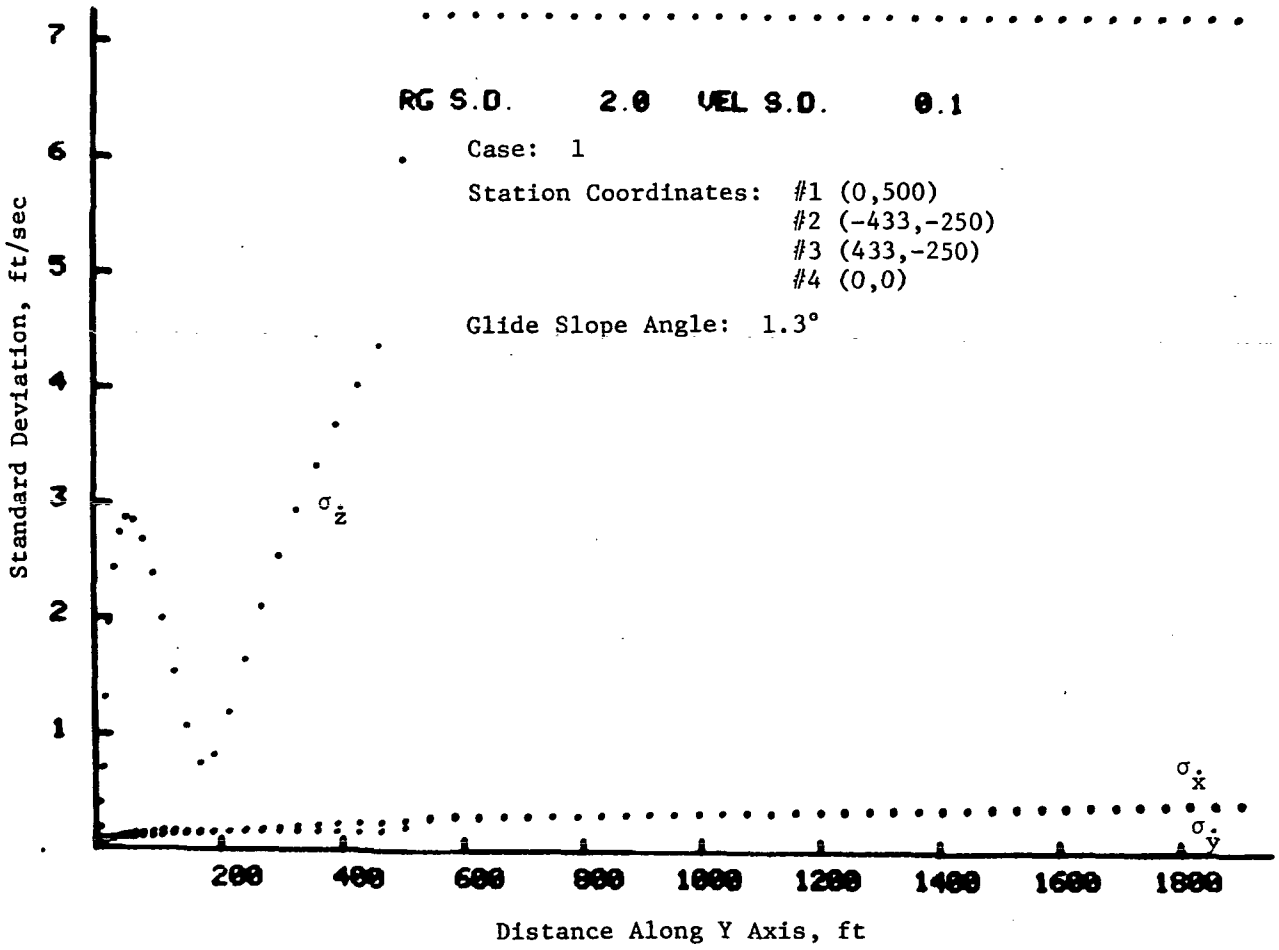

Fig. 4-21. Standard deviation of errors in coordinate rates plotted vs. ground projection of slant range for the specified trajectory. Dots are .5 sec apart. Measurement errors are 2 ft rms in range and .1 fps rms in range rate.

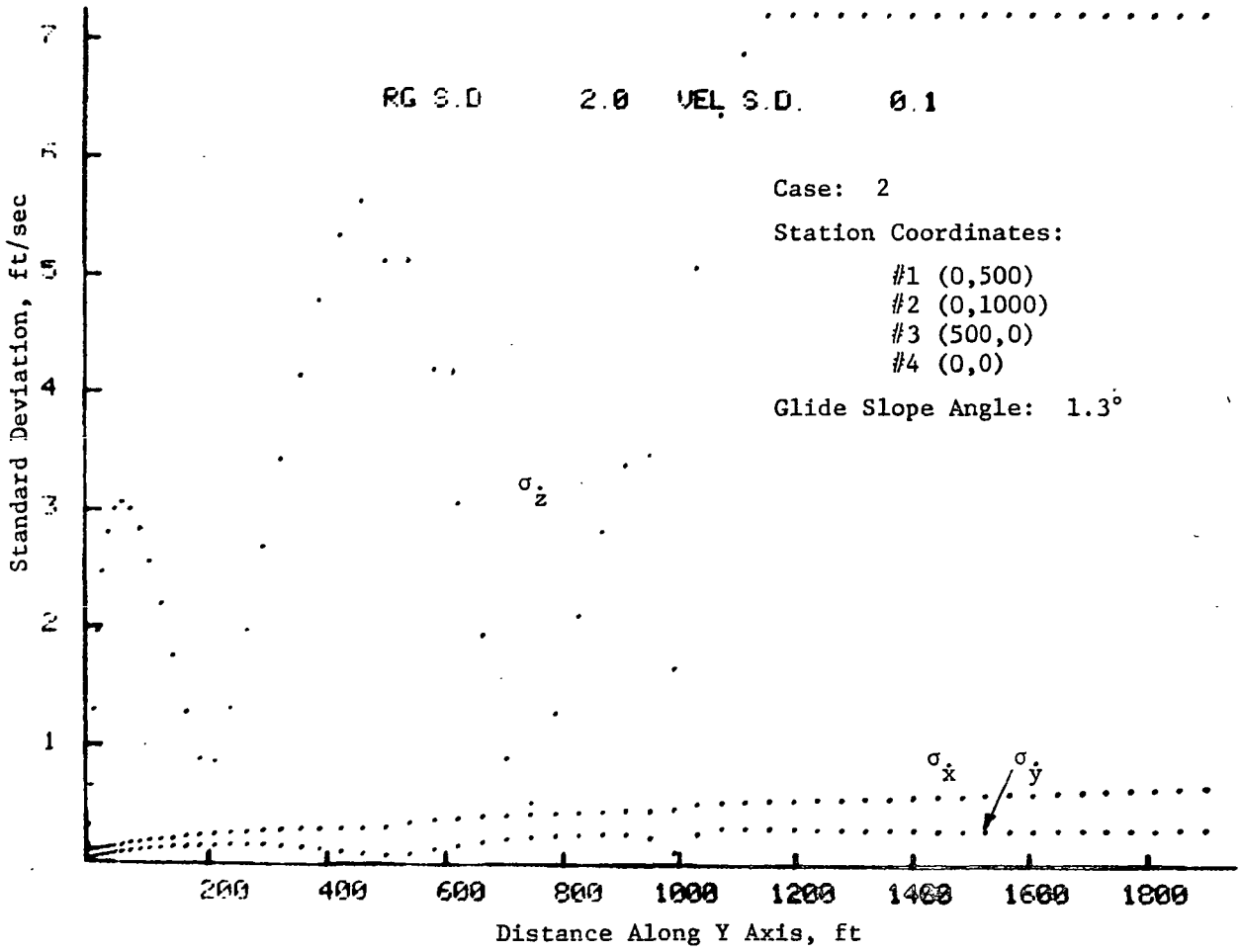

Fig. 4-22. Standard deviation of errors in coordinate rates plotted vs. ground projection of slant range for the specified trajectory. Dots are .5 sec apart. Measurement errors are 2 ft rms in range and .1 fps rms in range rate.

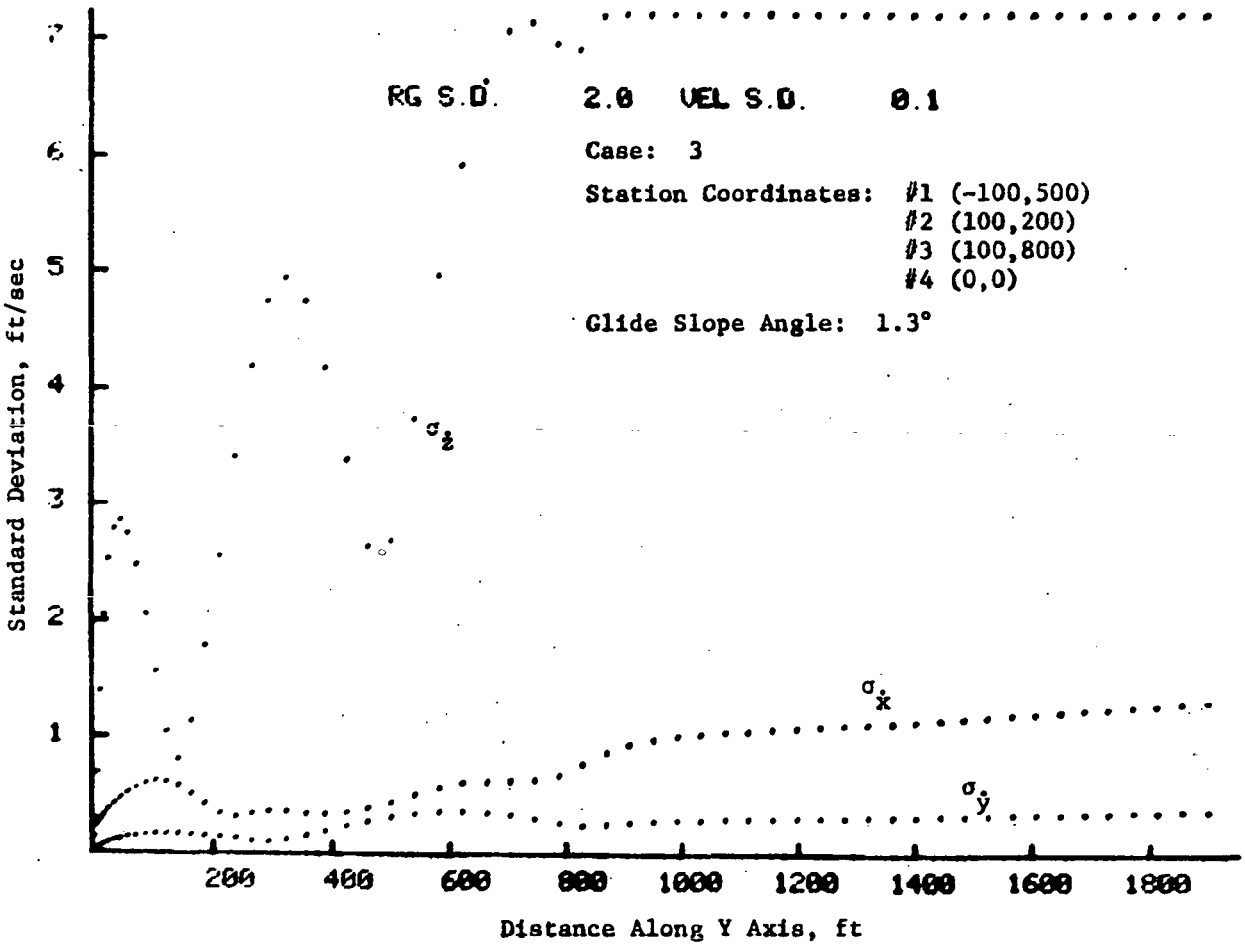

Fig. 4-23. Standard deviation of errors in coordinate rates plotted vs. ground projection of slant range for the specified trajectory. Dots are .5 sec apart. Measurement errors are 2 ft rms in range and .1 fps rms in range rate.

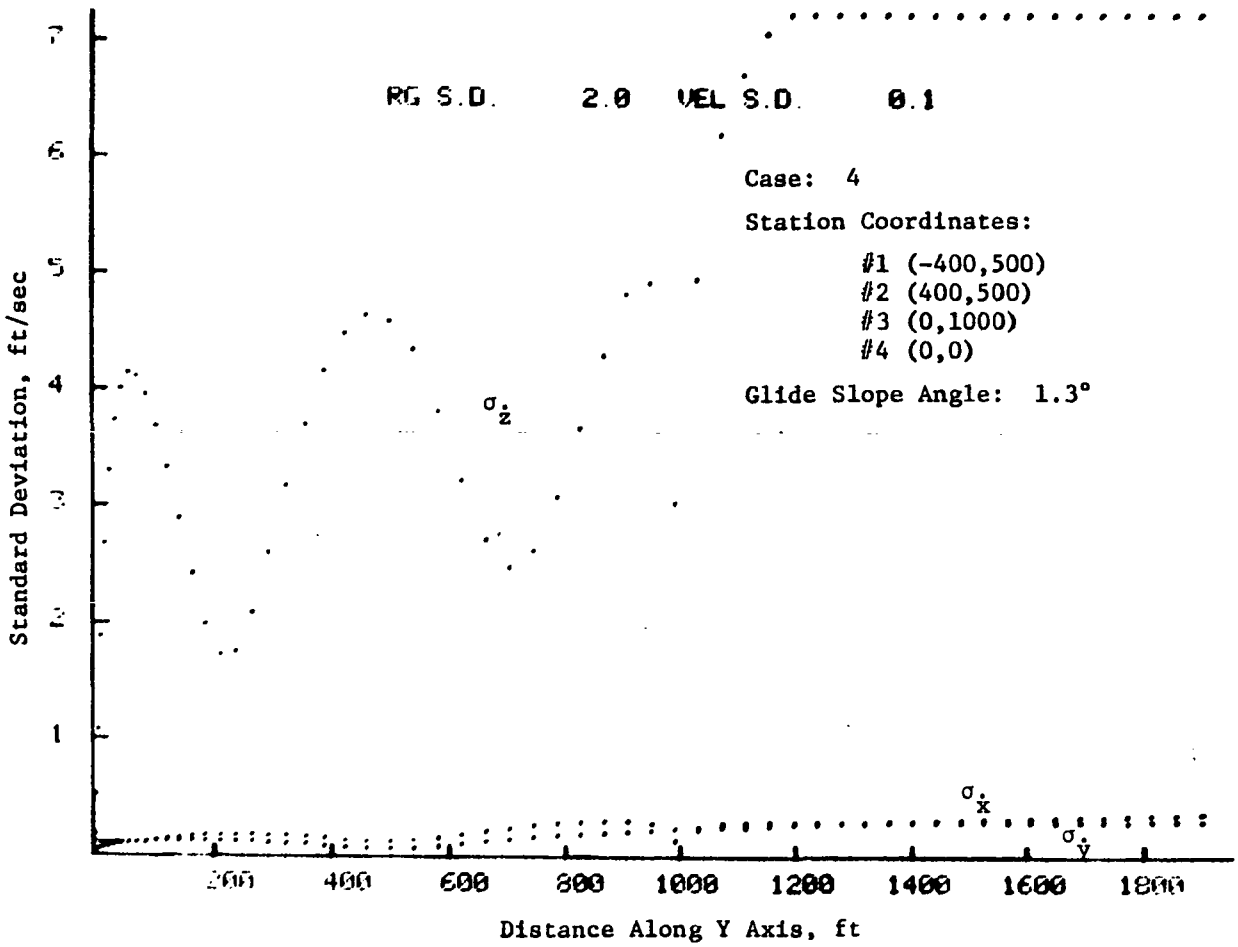

Fig. 4-24. Standard deviation of errors in coordinate rates plotted vs. ground projection of slant range for the specified trajectory. Dots are .5 sec apart. Measurement errors are 2 ft rms in range and .1 fps rms in range rate.

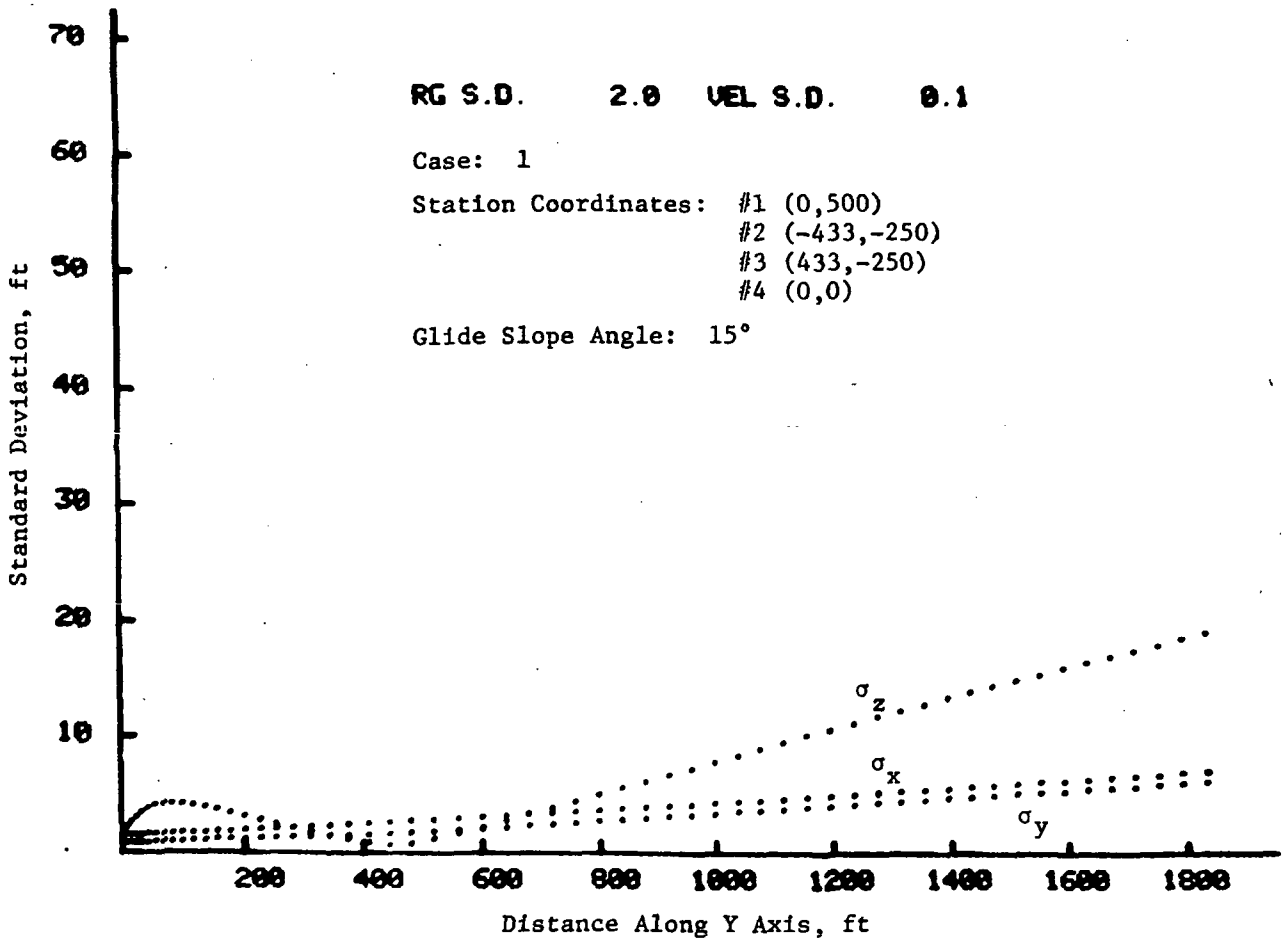

Fig. 4-25. Standard deviation of errors in coordinate positions plotted vs. ground projection of slant range for the specified trajectory. Dots are .5 sec apart. Measurement errors are 2 ft rms in range and .1 fps in range rate.

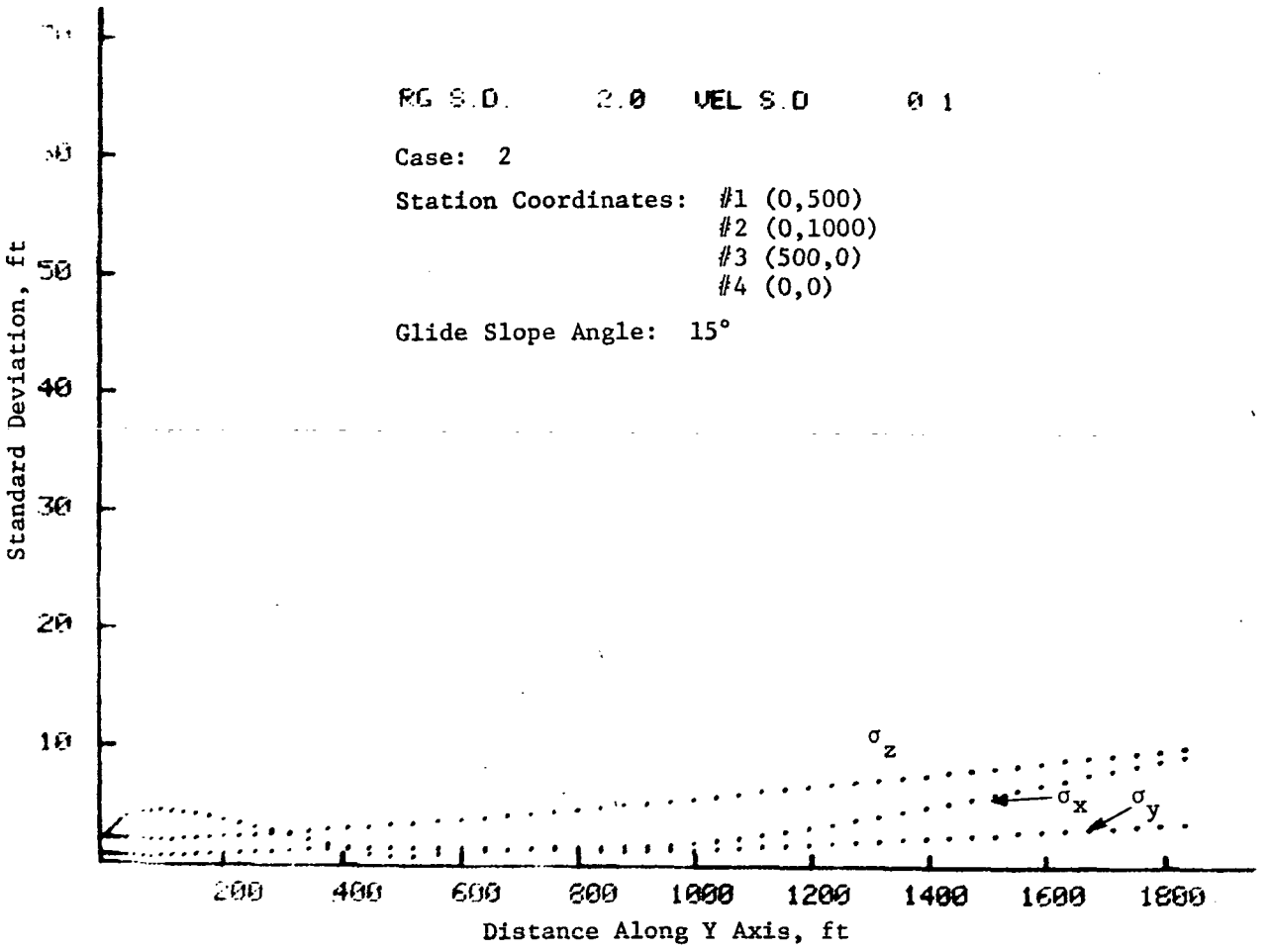

Fig. 4-26. Standard deviation of errors in coordinate positions plotted vs. ground projection of slant range for the specified trajectory. Dots are .5 sec apart. Measurement errors are 2 ft rms in range and .1 fps rms in range rate.

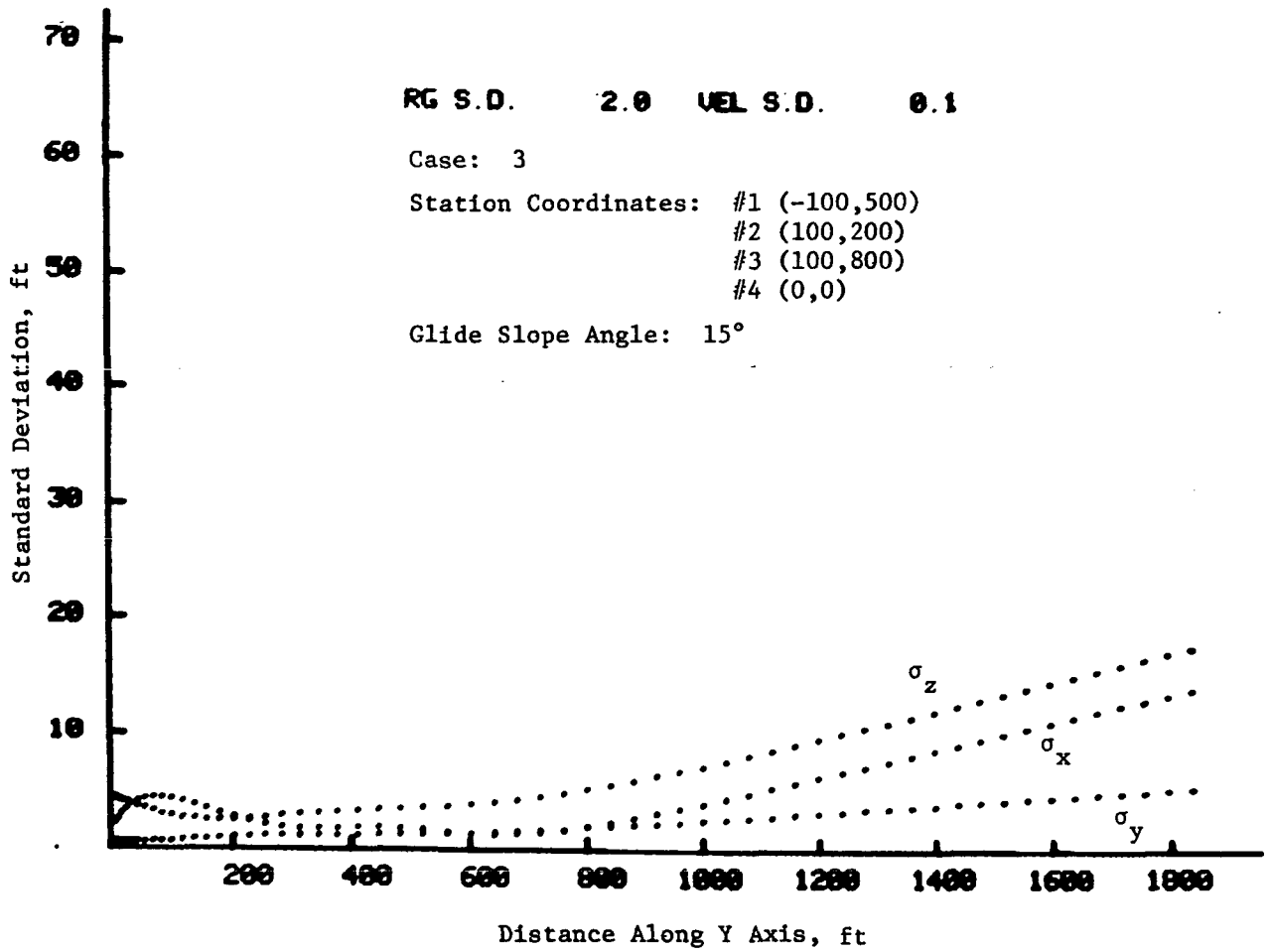

Fig. 4-27. Standard deviation of errors in coordinate positions plotted vs. ground projection of slant range for the specified trajectory. Dots are .5 sec apart. Measurement errors are 2 ft rms in range and .1 fps rms in range rate.

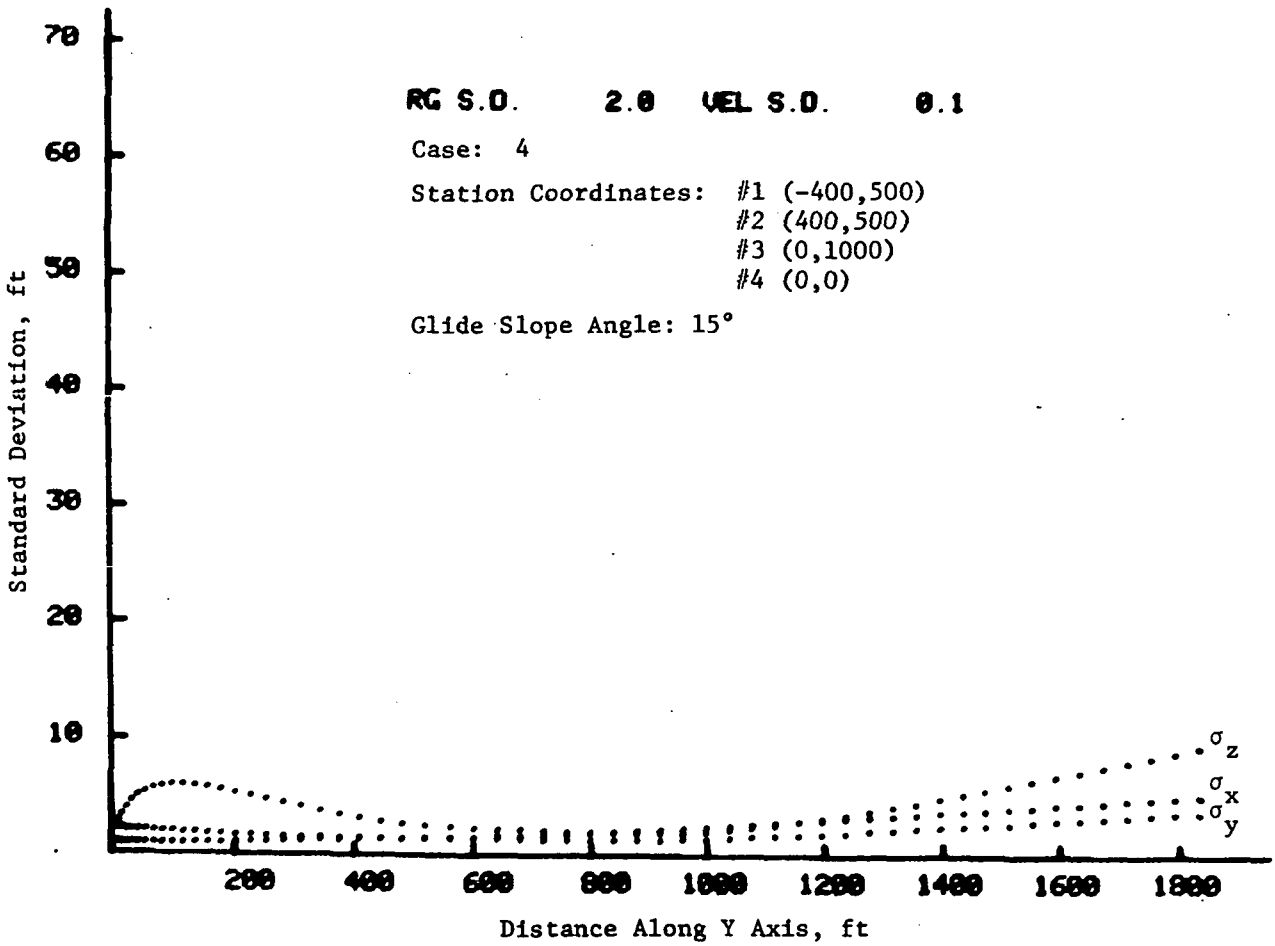

Fig. 4-28. Standard deviation of errors in coordinate positions plotted vs. ground projection of slant range for the specified trajectory. Dots are .5 sec apart. Measurement errors are 2 ft rms in range and .1 fps rms in range rate.

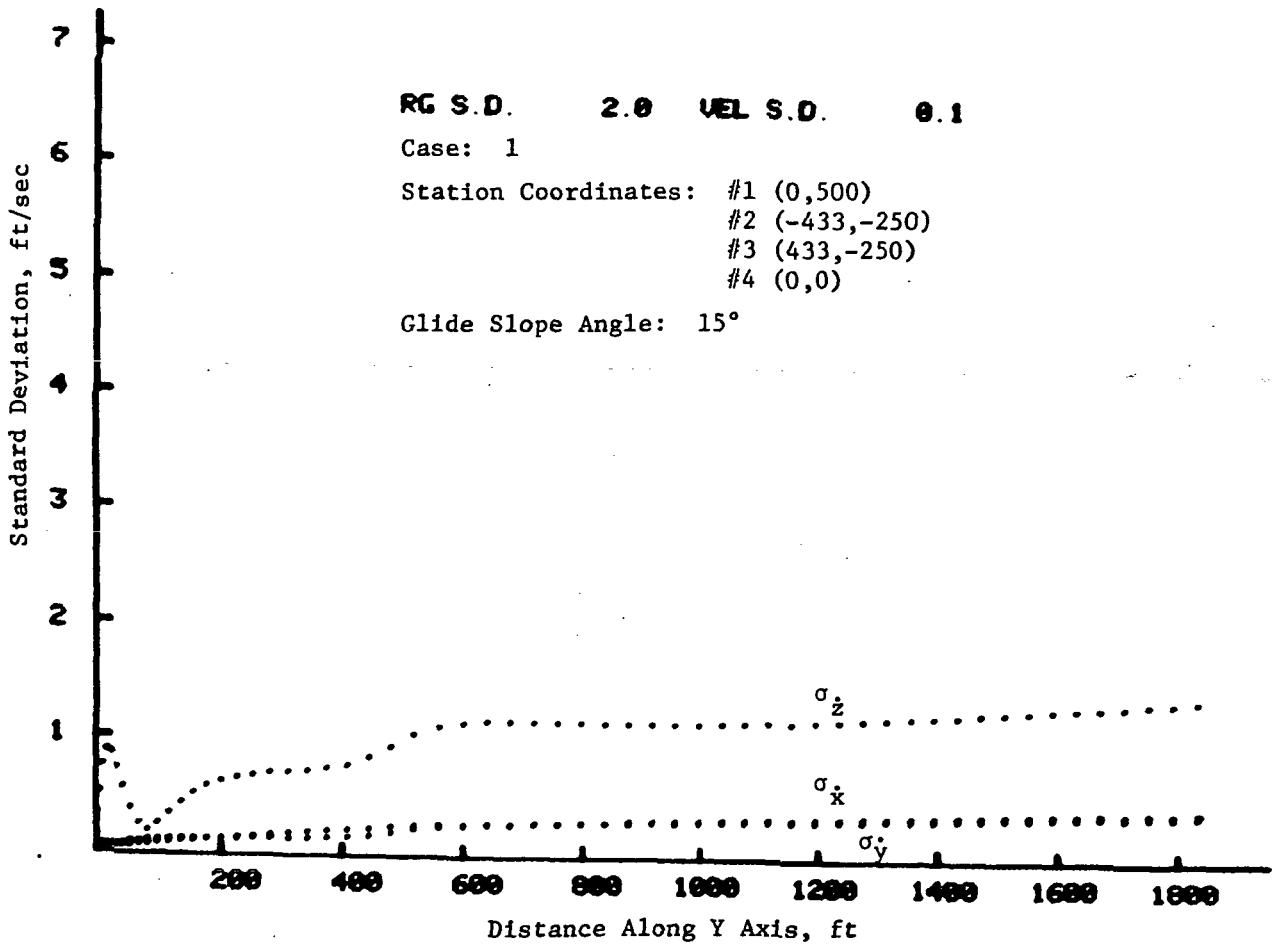

Fig. 4-29. Standard deviation of errors in coordinate rates plotted vs. ground projection of slant range for the specified trajectory. Dots are .5 sec apart. Measurement errors are 2 ft rms in range and .1 fps rms in range rate.

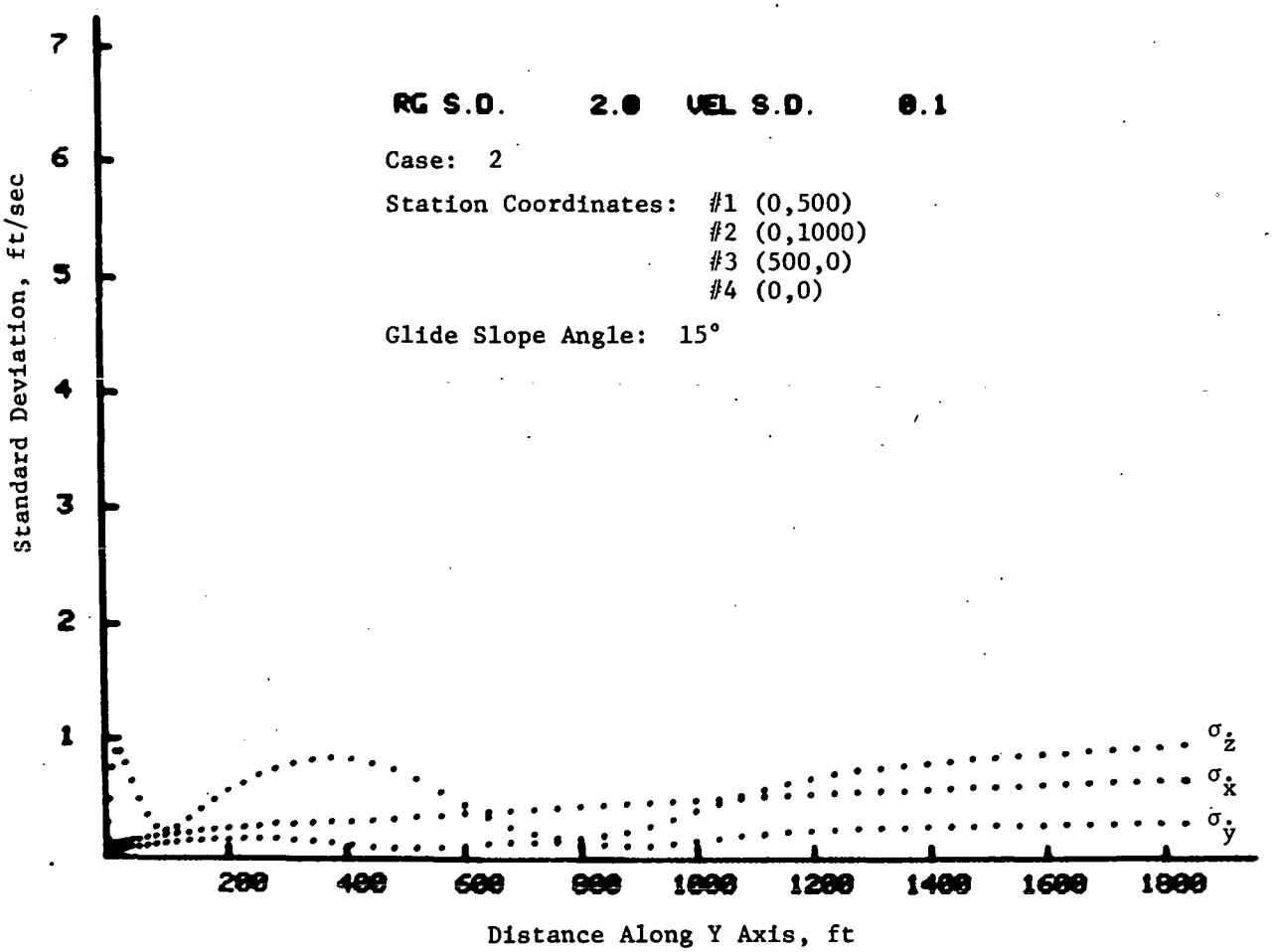

Fig. 4-30. Standard deviation of errors in coordinate rates plotted vs. ground projection of slant range for the specified trajectory. Dots are .5 sec apart. Measurement errors are 2 ft rms in range and .1 fps rms in range rate.

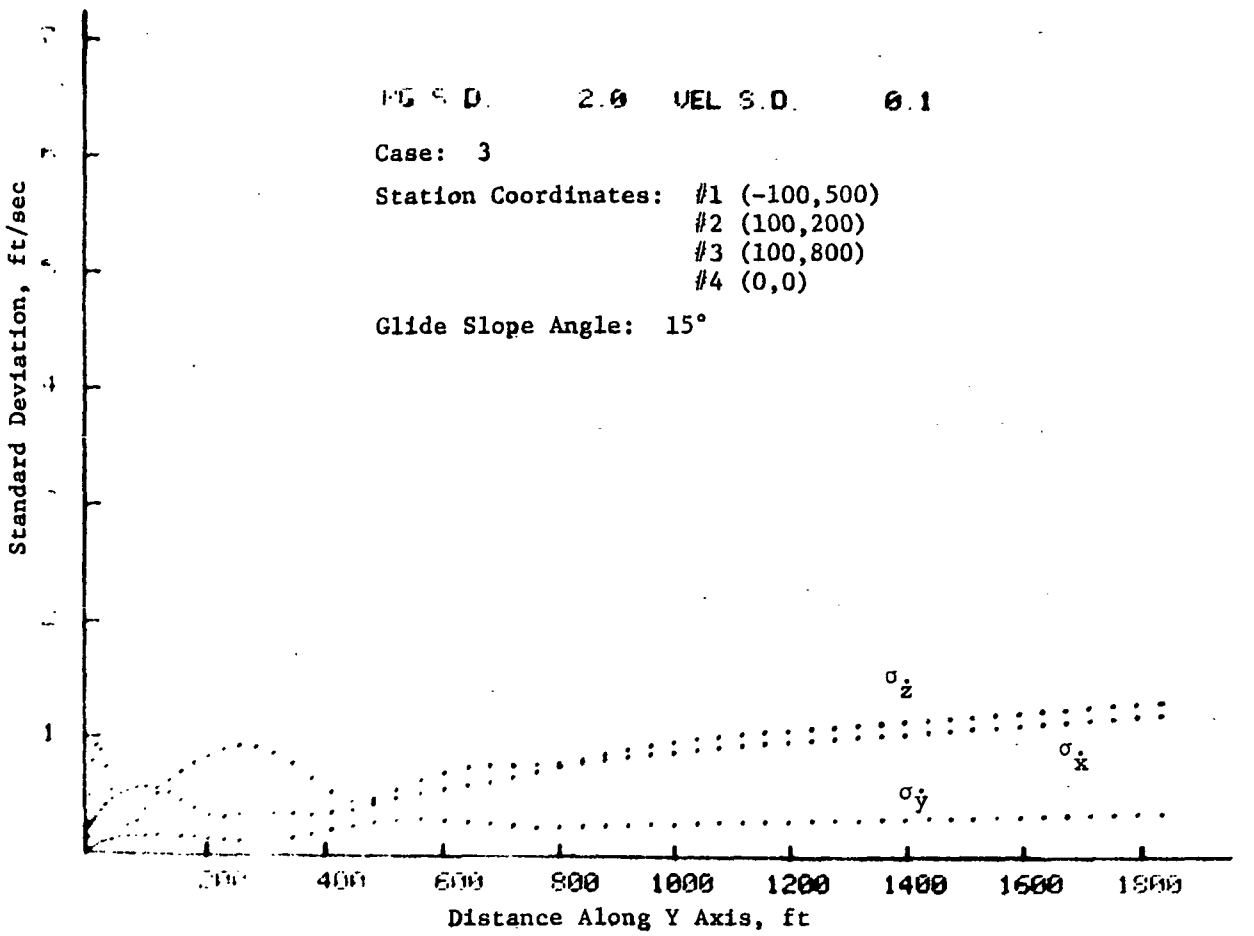

Fig. 4-31. Standard deviation of errors in coordinate rates plotted vs. ground projection of slant range for the specified trajectory. Dots are .5 sec apart. Measurement errors are 2 ft rms in range and .1 fps rms in range rate.

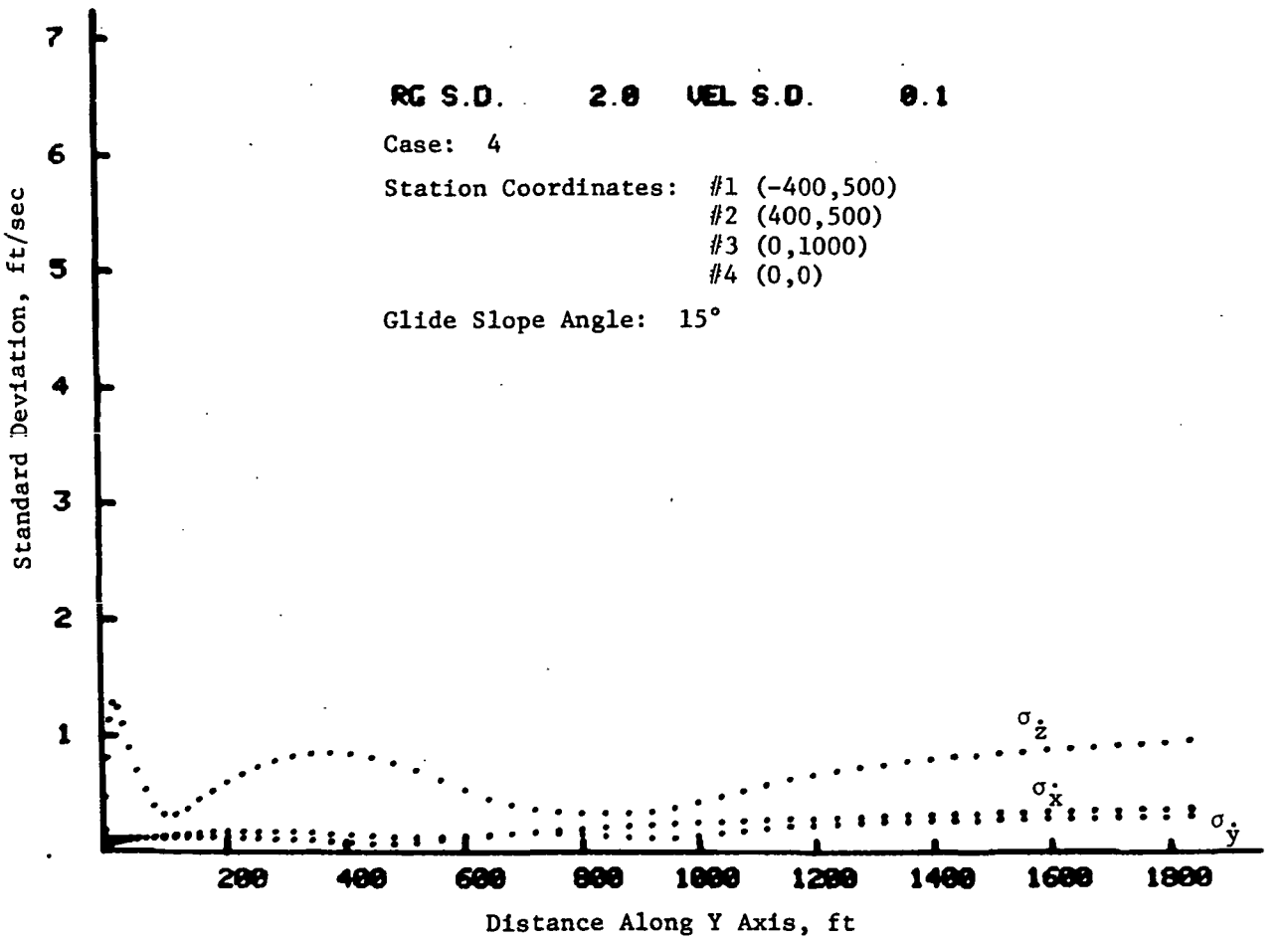

Fig. 4-32. Standard deviation of errors in coordinate rates plotted vs. ground projection of slant range for the specified trajectory. Dots are .5 sec apart. Measurement errors are 2 ft rms in range and .1 fps rms in range rate.

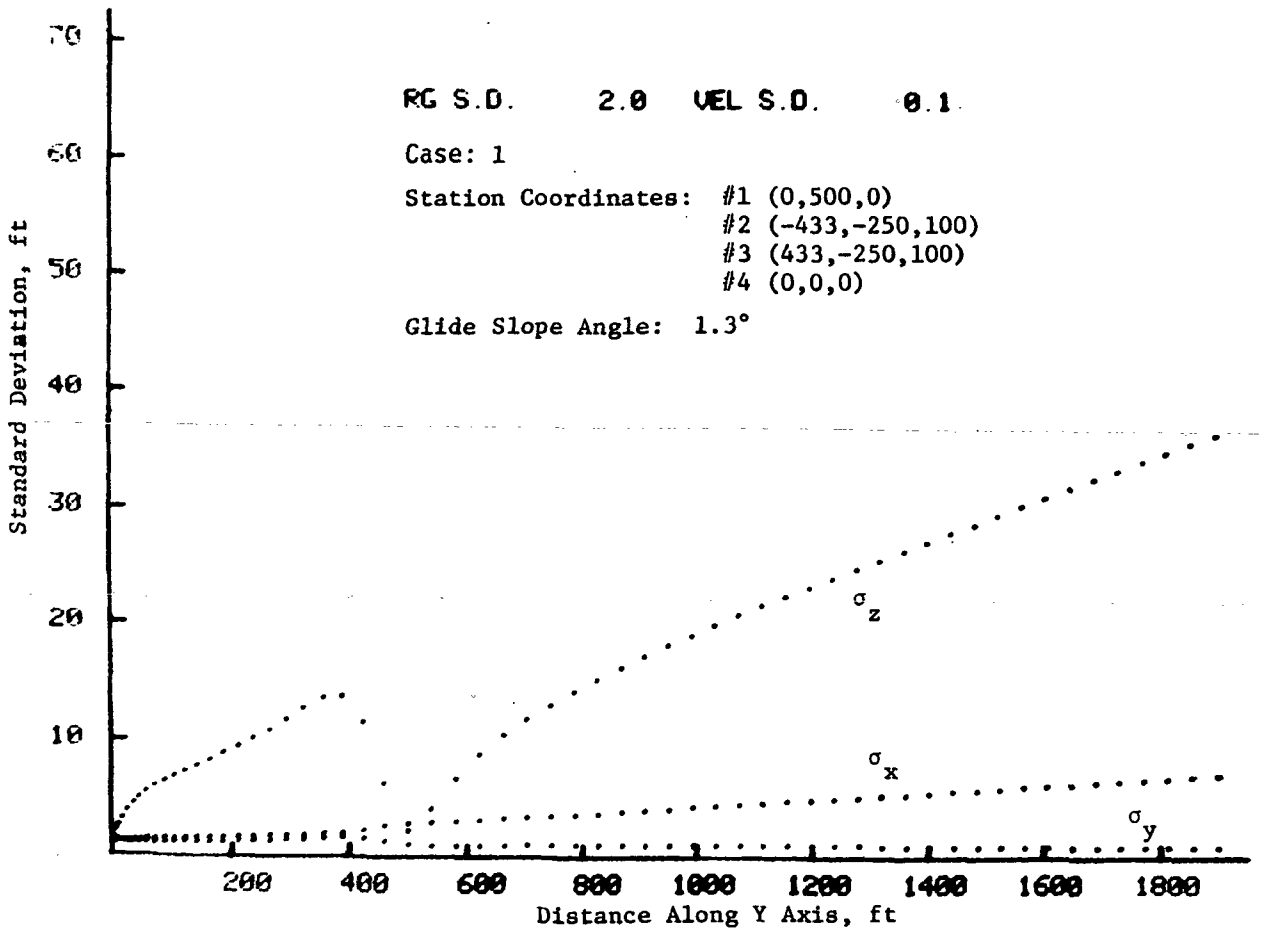

Fig. 4-33. Standard deviation of errors in coordinate positions plotted vs. ground projection of slant range for the specified trajectory. Dots are .5 sec apart. Measurement errors are 2 ft rms in range and .1 fps rms in range rate.

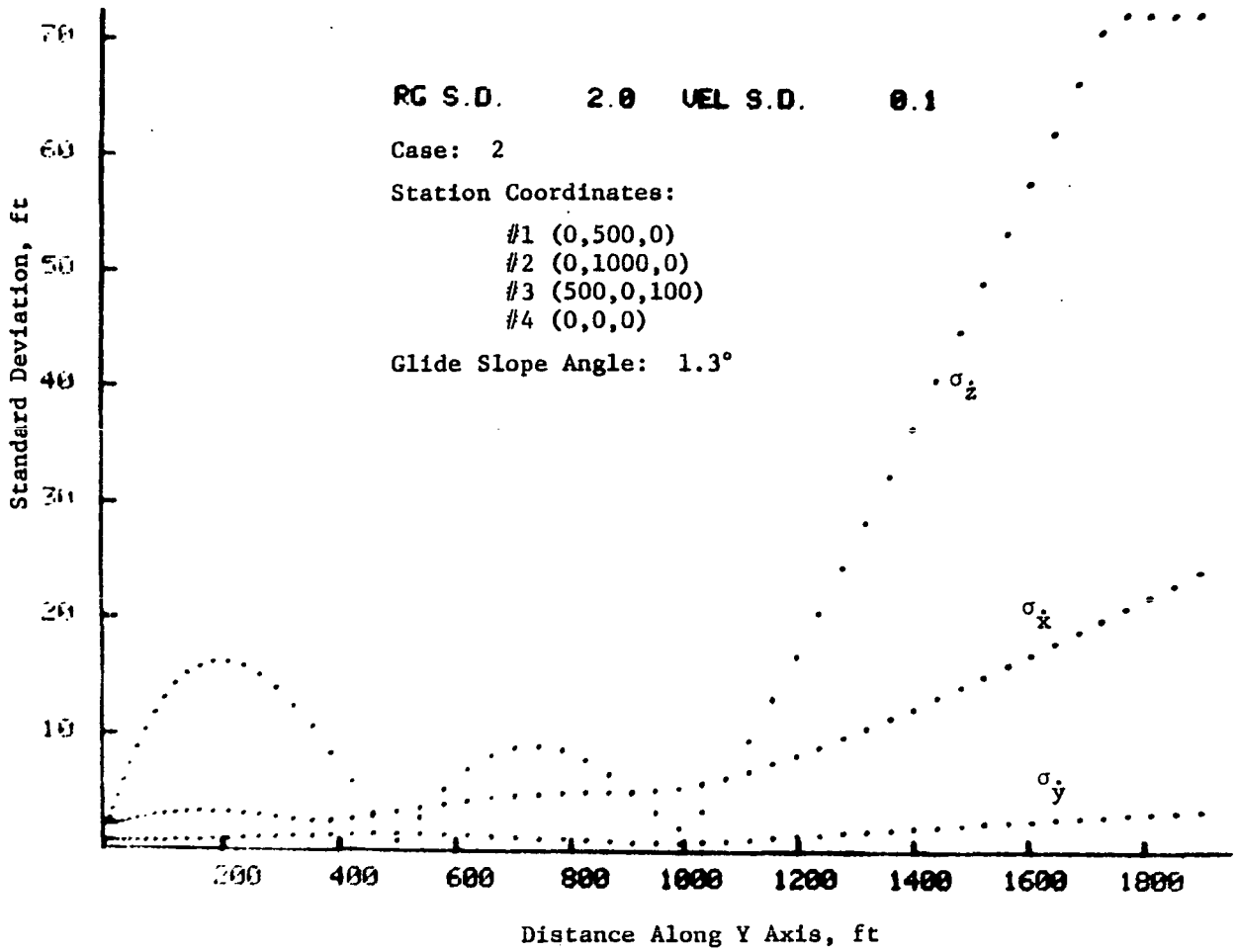

Fig. 4-34. Standard deviation of errors in coordinate positions plotted vs. ground projection of slant range for the specified trajectory. Dots are .5 sec apart. Measurement errors are 2 ft rms in range and .1 fps rms in range rate.

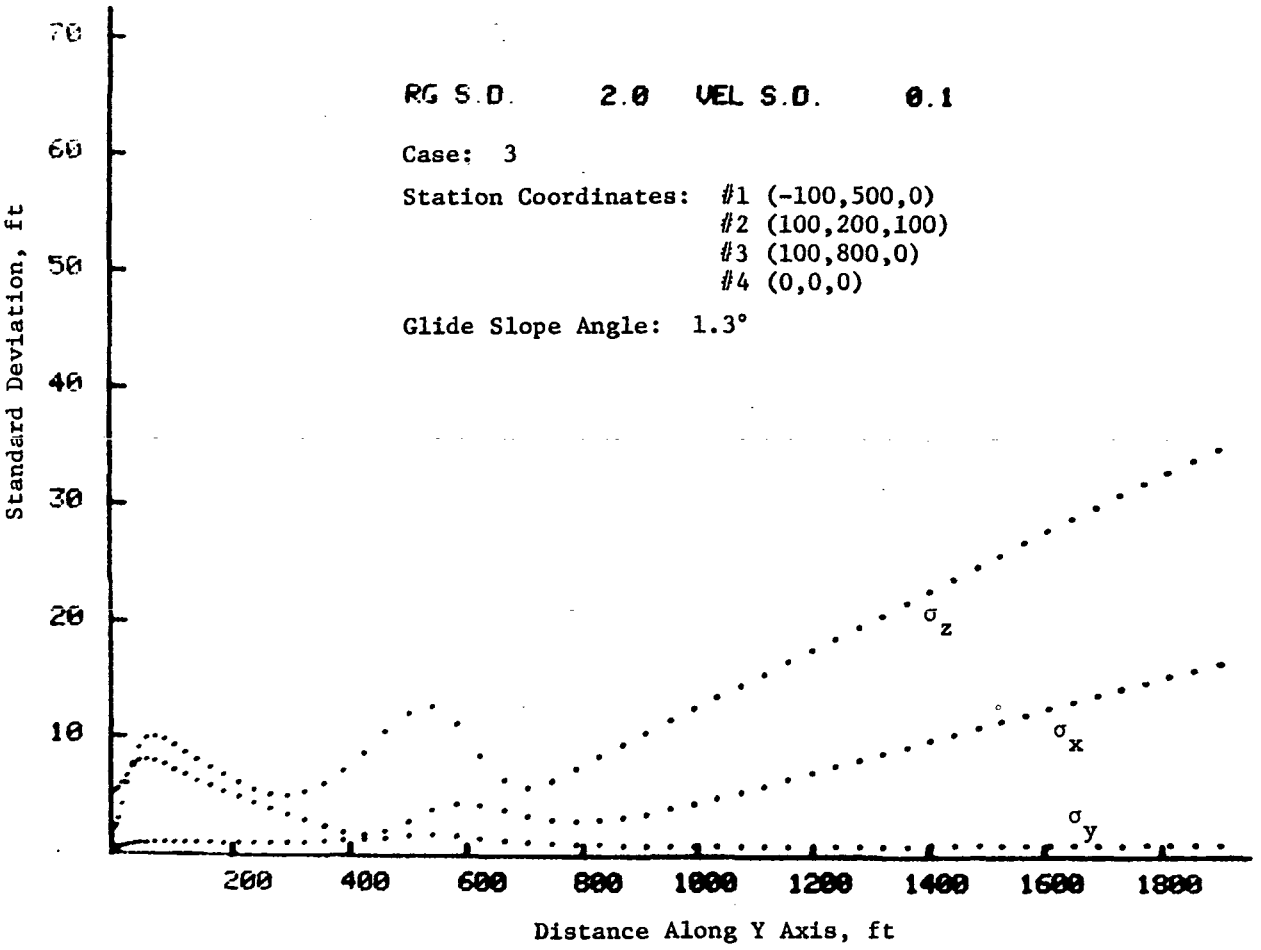

Fig. 4-35. Standard deviation of errors in coordinate positions plotted vs. ground projection of slant range for the specified trajectory. Dots are .5 sec apart. Measurement errors are 2 ft rms in range and .1 fps rms in range rate.

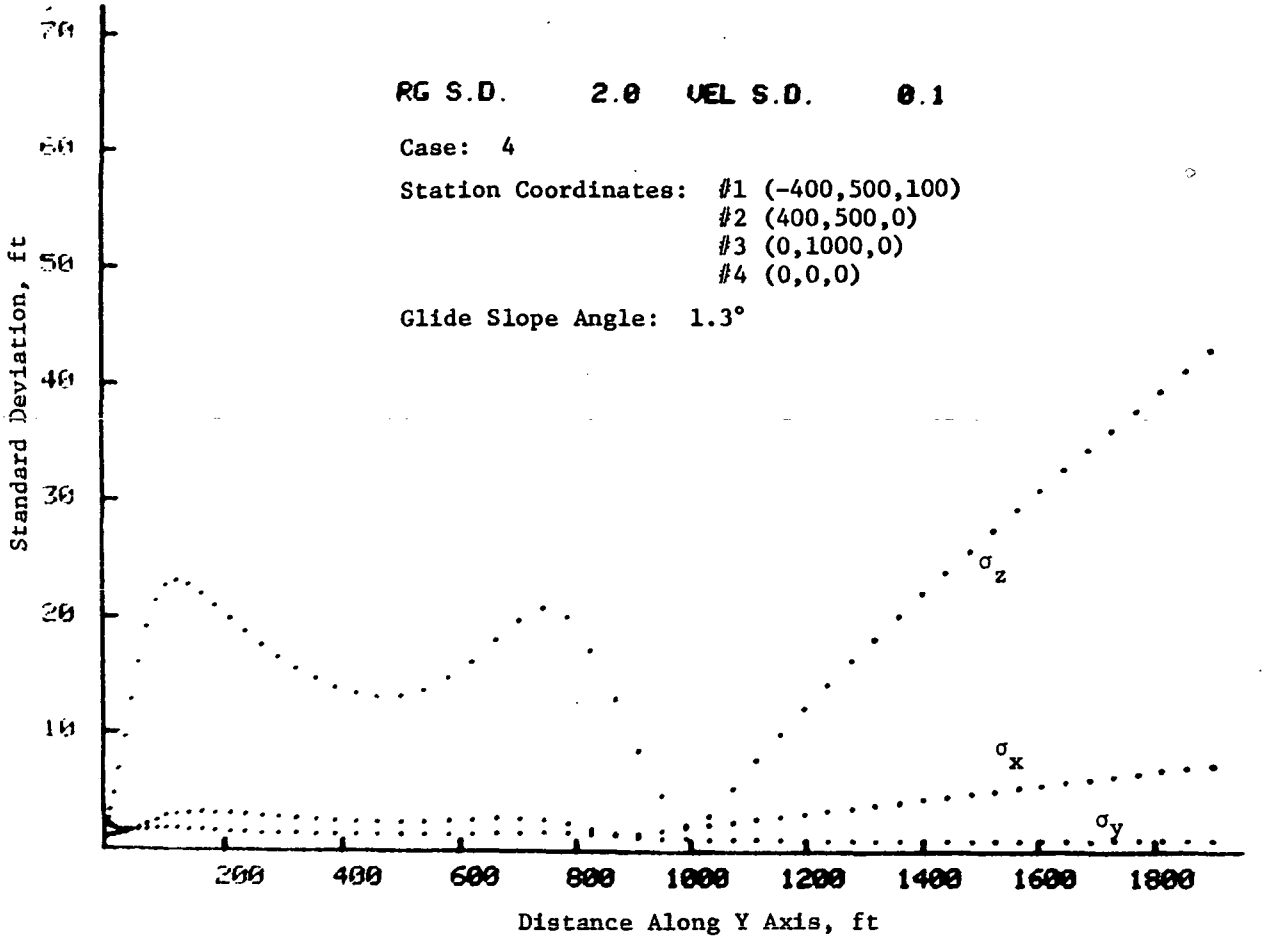

Fig. 4-36. Standard deviation of errors in coordinate positions plotted vs. ground projection of slant range for the specified trajectory. Dots are .5 sec apart. Measurement errors are 2 ft rms in range and .1 fps rms in range rate.

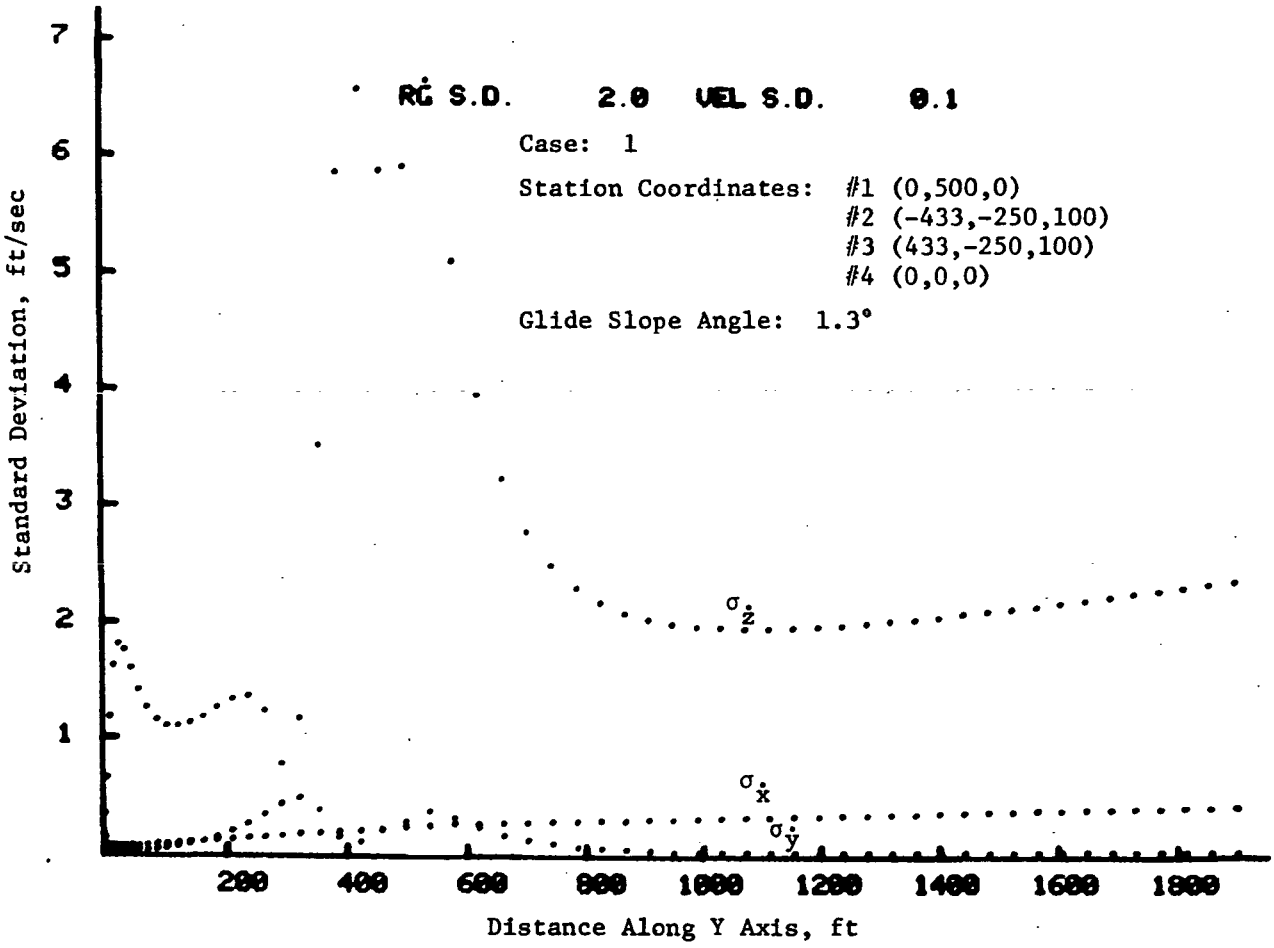

Fig. 4-37. Standard deviation of errors in coordinate rates plotted vs. ground projection of slant range for the specified trajectory. Dots are .5 sec apart. Measurement errors are 2 ft rms in range and .1 fps rms in range rate.

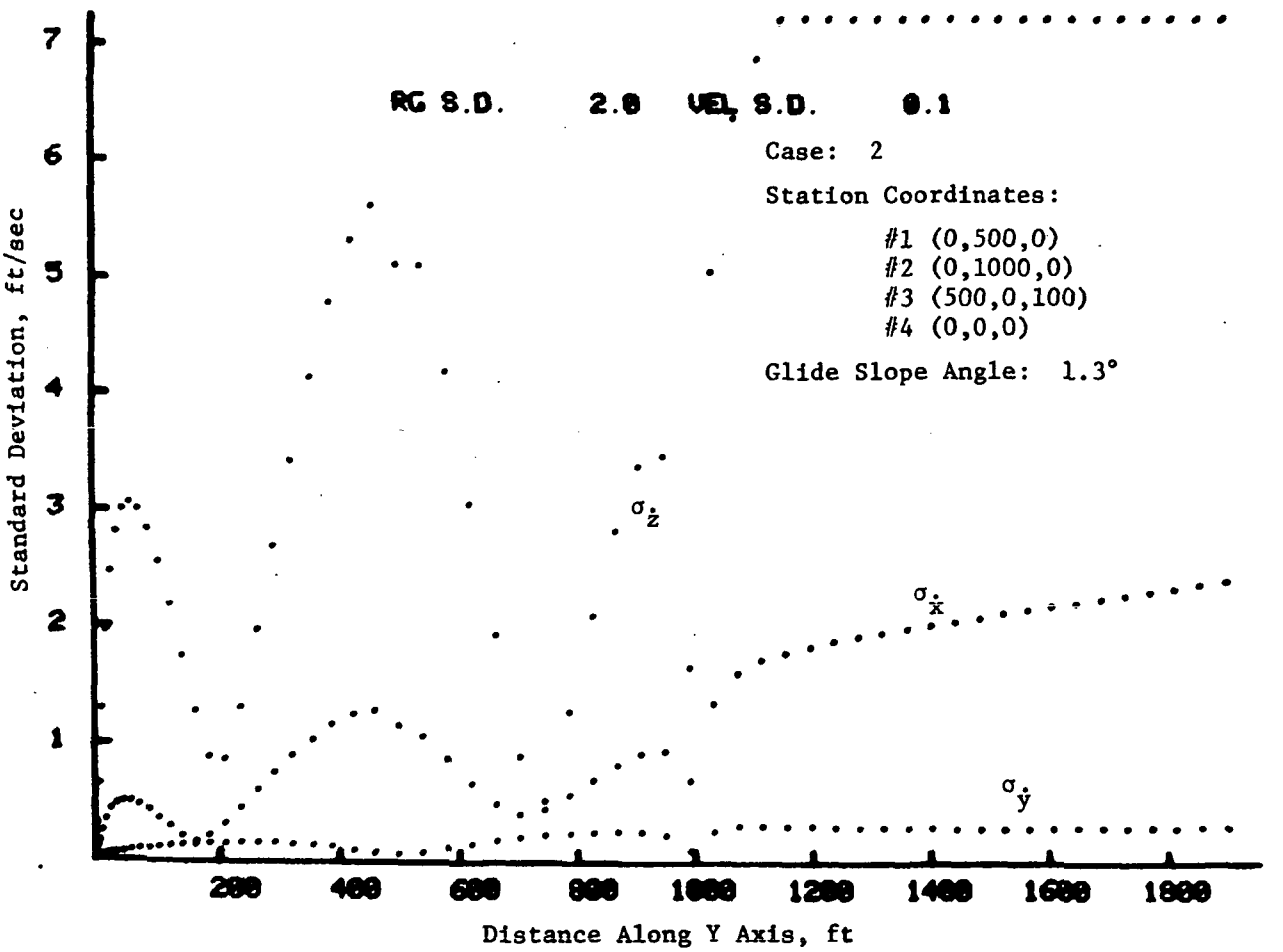

Fig. 4-38. Standard deviation of errors in coordinate rates plotted vs. ground projection of slant range for the specified trajectory. Dots are .5 sec apart. Measurement errors are 2 ft rms in range and .1 fps rms in range rate.

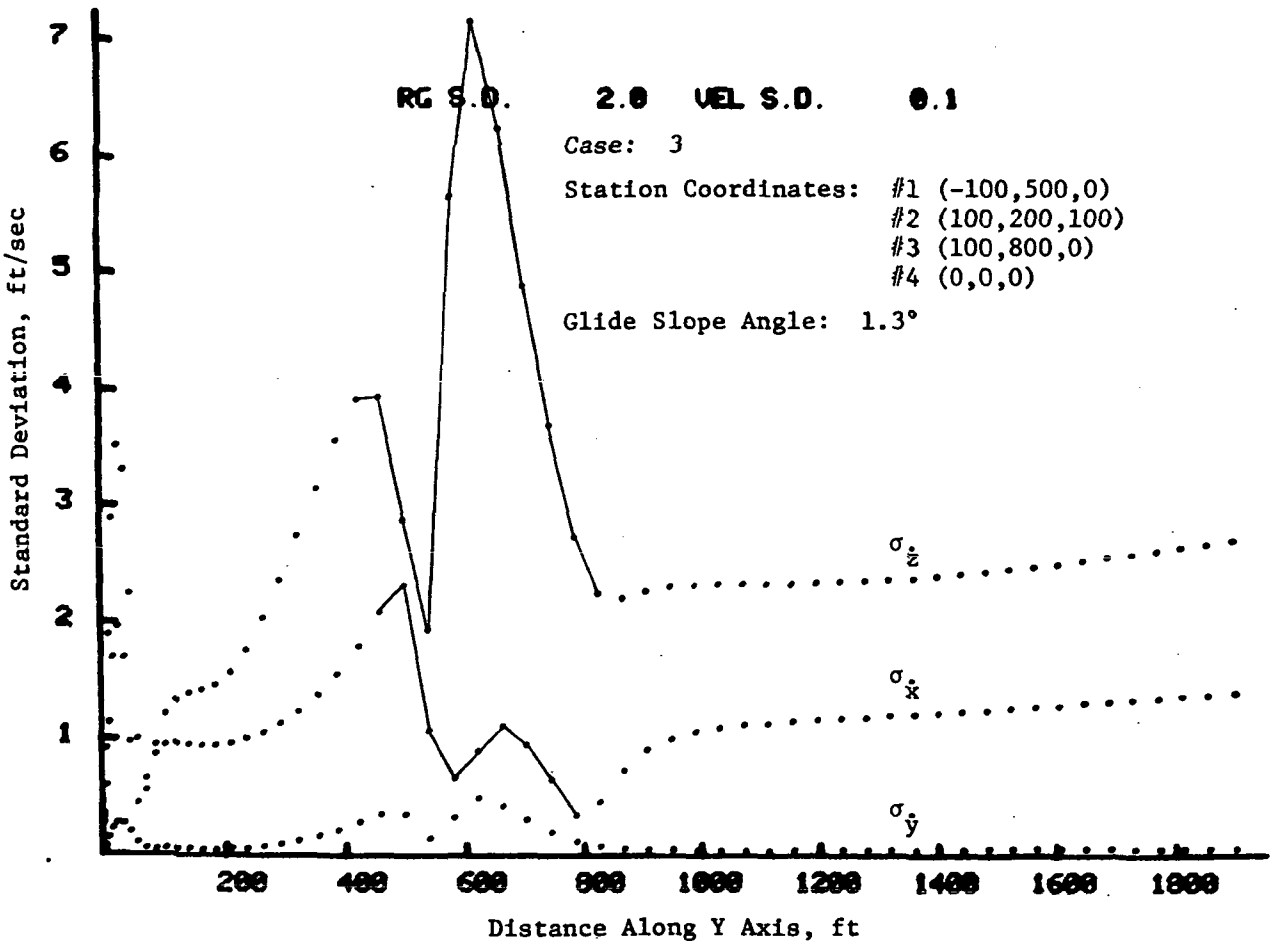

Fig. 4-39. Standard deviation of errors in coordinate rates plotted vs. ground projection of slant range for the specified trajectory. Dots are .5 sec apart. Measurement errors are 2 ft rms in range and .1 fps rms in range rate.

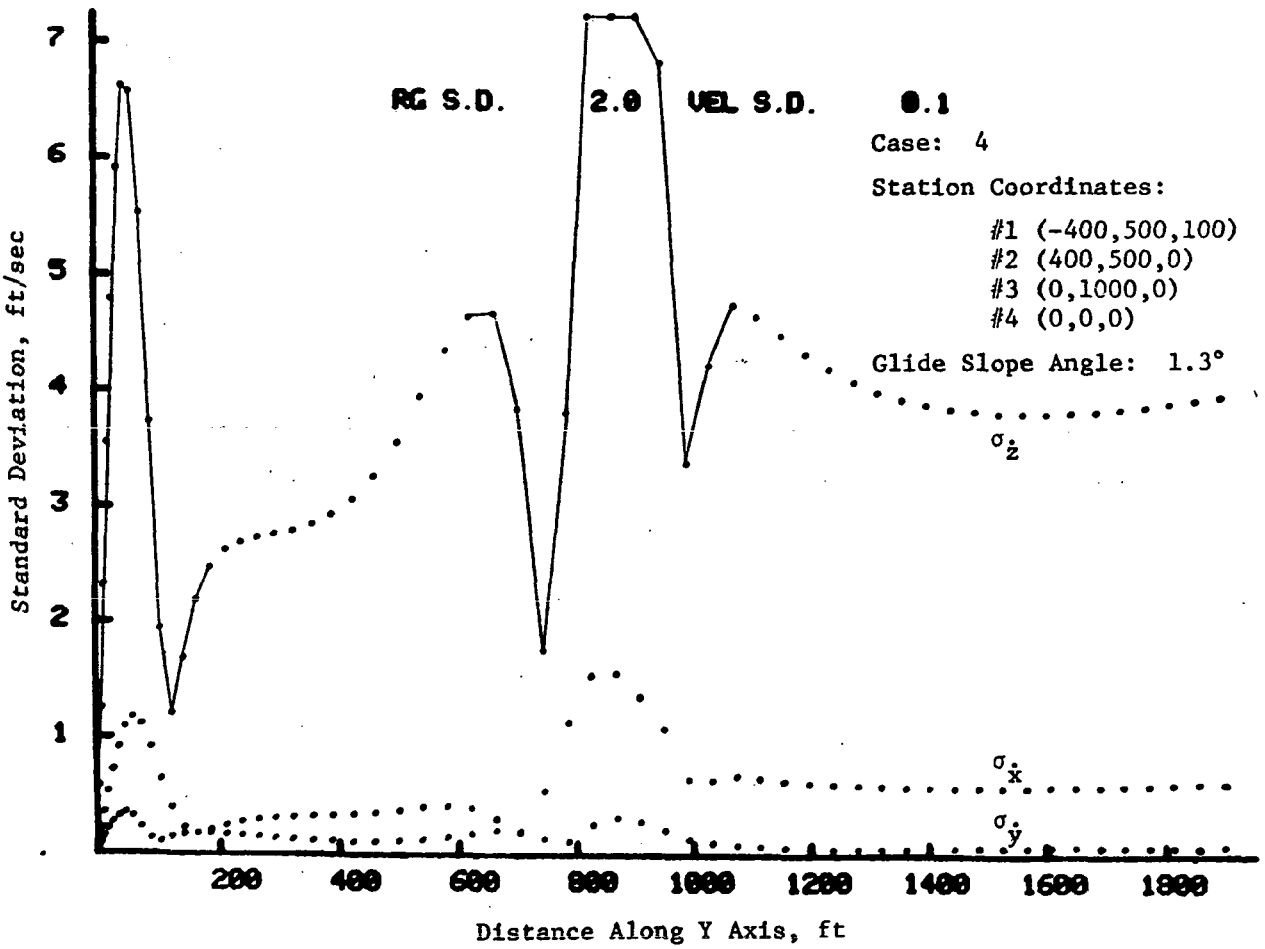

Fig. 4-40. Standard deviation of errors in coordinate rates plotted vs. ground projection of slant range for the specified trajectory. Dots are .5 sec apart. Measurement errors are 2 ft rms in range and .1 fps rms in range rate.

4.4.4 Summary.— It should be kept in mind that the curves presented are for a specific trajectory as given in Fig. 4-15, and that the error characteristics are a strong function of the trajectory. It may be concluded, however, that within the ranges considered (up to 1800 ft), and with glide slopes on the order of 15°, the error characteristics are not strongly dependent on specific receiver locations on the ground. For glide slope angles of 1-2°, the ground receiver location can be used to improve accuracy in the z coordinate. The best ground station configuration for the flat trajectory of this type appears to be Case 3, in which the ground receivers are staggered along the path of the trajectory. Using this configuration, it was possible to maintain the standard deviation in the z coordinate near 10 ft for the last 700 ft of the trajectory. It is possible that other ground station configurations (or more ground receivers) will improve the z measurement accuracy for flat trajectories, and this will be investigated in future work.

4.5 Errors in Estimation of Uncompensated Time Delay Bias

The technique for removal of unknown time delays in the two-way path is described in Section 3.7. Numerical calculations have been made of the estimation errors to be expected, assuming initial acquisition of the aircraft at various points. The results of these calculations are shown in Table 4-7, which gives the initial standard deviation of the time delay bias estimation error at four coordinate points. Table 4-8 provides the same information except that two of the stations (no. 2 and no. 3) have been elevated 100 ft.

As may be seen, the numerical values of the standard deviation of the errors in the bias removal change considerably depending on the coordinate point at which initial acquisition takes place. However, the values are generally under 3 ft rms on a single calculation basis. Using optimal low-pass filtering with a minimum equivalent time constant of 10 sec will reduce these initial standard deviations to 1/10 of the values shown in the table. If a longer equivalent time constant proves feasible, additional reduction in the standard deviation may be achieved. Figure 4-41 is a plot of the reduction in standard deviation of the time delay bias estimation error plotted vs. time, assuming a 10 sample/sec data rate.

Table 4-7. Initial standard deviation of time delay bias estimation error at various coordinate points (all stations in z = 0 plane).

Point (ft)	Initial Standard Deviation of Error in Paths Specified (ft)			
	$2R_1$	$R_1 + R_2$	$R_1 + R_3$	$R_1 + R_4$
(1000,1000,100)	.18	.59	.31	2.93
(1000,1000,500)	.19	.56	.31	2.94
(500,500,100)	.07	.86	.34	2.73
(100,100,50)	.08	1.89	1.09	.94
Station Locations: (ft)	#1 (0,500,0)			
	#2 (-433,-250,0)			
	#3 (433,-250,0)			
	#4 (0, 0, 0)			

Table 4-8. Initial standard deviation of time delay bias estimation error at various coordinate points (two elevated stations).

Point (ft)	Initial Standard Deviation of Error in Paths Specified (ft)			
	$2R_1$	$R_1 + R_2$	$R_1 + R_3$	$R_1 + R_4$
(1000,1000,100)	1.08	.24	.78	1.91
(1000,1000,500)	.49	.12	.49	2.90
(500,500,100)	.59	.02	1.24	2.16
(100,100,50)	.17	.73	3.09	.006
Station Locations: (ft)	#1 (0,500,0)			
	#2 (-433,-250,100)			
	#3 (433,-250,100)			
	#4 (0, 0, 0)			

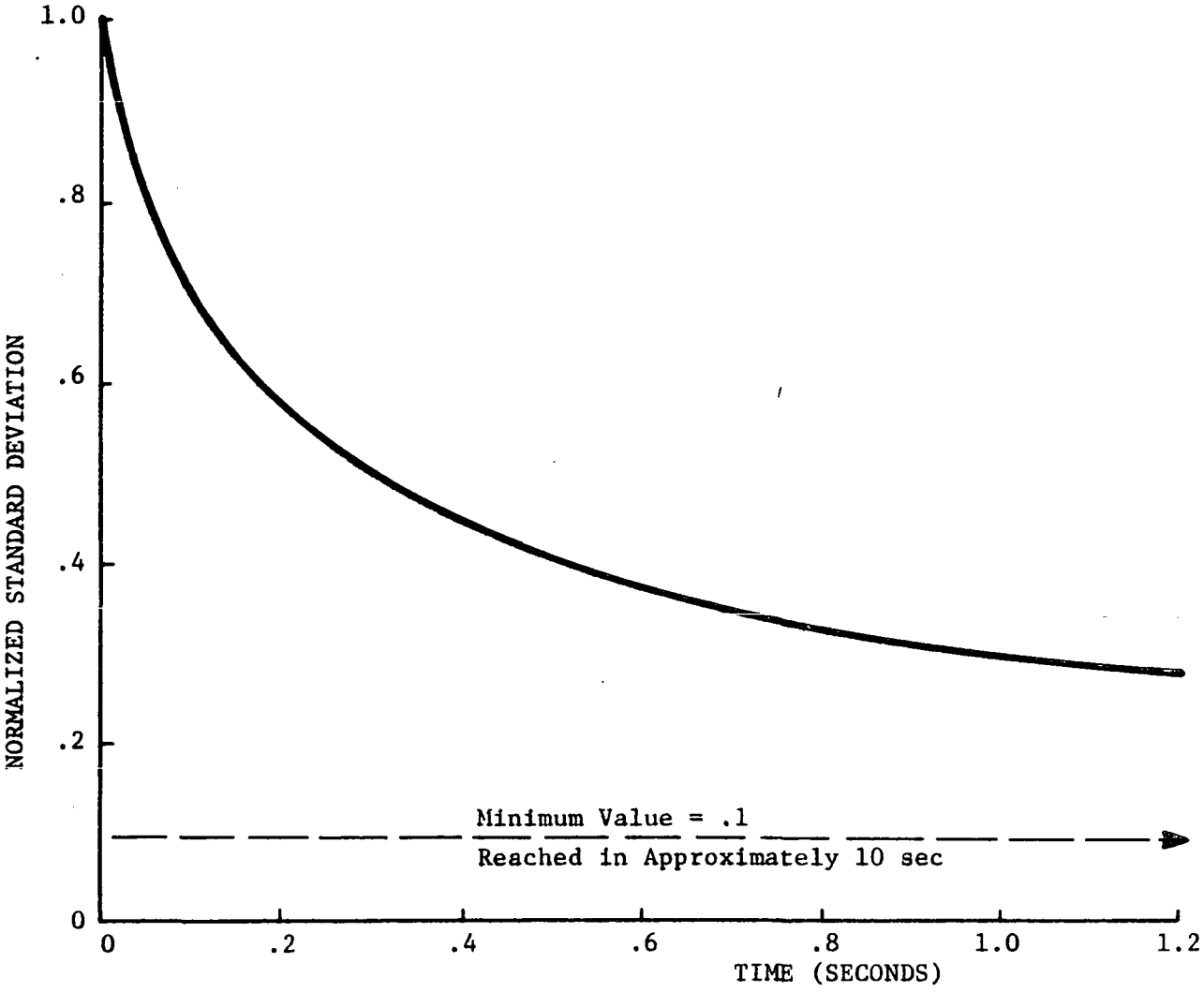

Fig. 4-41. Reduction in standard deviation of time delay bias estimation error plotted vs. time (10 samples/second data rate) for an optimal filter.

The initial standard deviation drops quite fast during the first second and then slowly approaches an asymptotic value of .1 in approximately 10 sec.

From the above calculations, we may conclude that with four or more ground stations, it is feasible to determine the two-way uncompensated time delay bias to an accuracy of .3 ft using an optimal filter with an equivalent time constant of 10 sec. This conclusion is based upon an assumed measurement error in the two-way path of 2 ft rms.

Page Intentionally Left Blank

5.0 COMPUTATIONAL REQUIREMENTS FOR THE MULTILATERATION SYSTEM

5.1 General Requirements

This section describes an investigation into the computer hardware and software requirements for the multilateration system. The basic goal is to solve for position and rate ten times per second, using data from four or more stations. This should be done on a minicomputer system costing approximately $10,000. Use of the weighted least squares algorithms described in Section 3.0 is assumed. These require floating point arithmetic.

The input to the minicomputer will consist of 16-bit digital data from the four ground receivers. It is anticipated that the ground receiver data will be multiplexed so that the received data will consist of 8 16-bit words for each measurement cycle. These words will consist of the four range measurement words and four range rate measurement words (or counts) to be transmitted as fast as possible during each measurement cycle (.1 sec). Output from the computer system will consist of a 16-bit digital line plus a data ready line for providing output to the navigation computer via a data link. In addition to the digital I/O channel, it is necessary to provide analog outputs to drive x-y plotters and strip chart recorders. Eight channels should be sufficient for monitoring the operation of the system. The eight analog output channels could be utilized as follows:

Output Analog Channels and Function

1. x coordinate output
2. y coordinate output
3. z coordinate output
4. $\dot{x}$ coordinate output
5. $\dot{y}$ coordinate output
6. $\dot{z}$ coordinate output
7. ground projection of slant range
8. slant range.

For convenience in programming the minicomputer, a teletype system and high-speed paper tape reader are desirable as input devices. Computer timing requirements are considered in the following section.

5.2 Timing Tests on a Representative Minicomputer (PDP-8/E)

To determine rough estimates of computation time, timing measurements were made on the weighted least squares computation of position only, using the following equation:

$$\bar{x} = (P^T \psi_{\Delta Q}^{-1} P)^{-1} P^T \psi_{\Delta Q}^{-1} Q \tag{5-1}$$

where P is a 4 x 3 constant matrix, $\bar{Q}$ is a 4 x 1 vector of modified measurements and

$$\psi_{\Delta Q} = T \psi_{\Delta A} T^T. \tag{5-2}$$

Here,
$$T = \begin{bmatrix} A_1 & 0 & 0 & 0 \\ 0 & A_2 & 0 & 0 \\ 0 & 0 & A_3 & 0 \\ 0 & 0 & 0 & A_4 \end{bmatrix} \tag{5-3}$$

and

$$\psi_{\Delta A} = \frac{\sigma_A^2}{4} \begin{bmatrix} 1 & -1 & -1 & -1 \\ -1 & 5 & 1 & 1 \\ -1 & 1 & 5 & 1 \\ -1 & 1 & 1 & 5 \end{bmatrix} . \tag{5-4}$$

Some initial simplifications in this algorithm were made to reduce the required computation. Note that

$$\psi_{\Delta Q}^{-1} = T^{-1} \psi_{\Delta A}^{-1} T^{-1} \tag{5-5}$$

where

$$T^{-1} = \begin{bmatrix} \frac{1}{A_1} & 0 & 0 & 0 \\ 0 & \frac{1}{A_2} & 0 & 0 \\ 0 & 0 & \frac{1}{A_3} & 0 \\ 0 & 0 & 0 & \frac{1}{A_4} \end{bmatrix} . \tag{5-6}$$

$\psi_{\Delta A}^{-1}$ was also found to have a relatively simple closed form:

$$\psi_{\Delta A}^{-1} = \frac{1}{\sigma_A^2} \begin{bmatrix} 7 & 1 & 1 & 1 \\ 1 & 1 & 0 & 0 \\ 1 & 0 & 1 & 0 \\ 1 & 0 & 0 & 1 \end{bmatrix} . \tag{5-7}$$

Thus

$$\psi_{\Delta Q}^{-1} = \frac{1}{\sigma_A^2} \begin{bmatrix} \frac{7}{A_1^2} & \frac{1}{A_1 A_2} & \frac{1}{A_1 A_3} & \frac{1}{A_1 A_4} \\ \frac{1}{A_1 A_2} & \frac{1}{A_2^2} & 0 & 0 \\ \frac{1}{A_1 A_3} & 0 & \frac{1}{A_3^2} & 0 \\ \frac{1}{A_1 A_4} & 0 & 0 & \frac{1}{A_4^2} \end{bmatrix} . \tag{5-8}$$

Note also that the variance σ_A^2 cancels out in (5-1), so it need not be included in the calculation.

A Fortran program was written to solve for $\bar{x}$ with the following steps repeated a specified number of times in a DO loop to allow timing with the sweep second hand of a clock.

1) Using precomputed values of A_1 through A_4, compute the non-zero entries in the $\psi_{\Delta Q}^{-1}$ matrix, equation (5-8).

2) Call the matrix multiplication subroutine GMPRD* to form $P^T \psi_{\Delta Q}^{-1}$.

3) Call GMPRD*to form $P^T \psi_{\Delta Q}^{-1} P$.

4) Call GMPRD*to form $P^T \psi_{\Delta Q}^{-1} Q$. (Computation of the q_i's from the A_i's was not included in the timing test.)

5) Call the matrix inversion routine MINV to invert $P^T \psi_{\Delta Q}^{-1} P$.

6) Call GMPRD*to compute $\bar{x}$.

7) Compute $\hat{z}$ from the equation

$$\hat{z} = (2\hat{\mu} - \hat{x}^2 - \hat{y}^2)^{1/2} \quad . \tag{5-9}$$

When this program was run under the Fortran II system on the PDP-8/E, the time per position computation was found to be approximately 0.9 seconds, clearly an unacceptable figure and somewhat greater than expected. An investigation of the Fortran II software revealed that it was not making use of the Extended Arithmetic Element (EAE), and thus required approximately 900 μs to perform a floating point multiplication. A call to the manufacturer revealed that no version of Fortran II is available which does employ the EAE.

Next, the program was run under the new Fortran IV system, which does employ the EAE. Quite surprisingly, the time per position computation was still almost 0.9 seconds. This was traced to the fact that all variables, including integers, are represented and operated upon as floating point numbers in PDP-8/E Fortran IV. The gain in speed for each floating point operation was offset by the many additional floating point operations for array indexing, etc.

To overcome these difficulties, a third version of this program was written in PAL-8 assembly language. The required subroutines GMPRD and MINV (matrix inverse) were also manually translated to assembly language. Floating point operations were performed by calls to the EAE Floating Point Package subroutines described in Chapter 8 of ref. 3. Time per position calculation with this software was improved by a factor of ten to approximately 90 ms. This is still not acceptable, since both position and rate must be computed in 100 ms. However, this time is within a factor of two of being acceptable, so that use of the PDP-8/E might be possible with further algorithm simplification (see next section). (During the course of using the EAE Floating Point Package, which is distinct from the floating point routines used by the Fortran systems, a "bug" was discovered: If a number less than one in

*Matrix product subroutine.

magnitude and a zero are added or subtracted, unnecessary roundoff error results. A patch to the Floating Point Package was written to correct this, and a letter sent to the manufacturer informing him of this problem and the suggested solution.)

5.3 Increasing Algorithm Efficiency

Reference 3 quotes the following "typical times" for floating point operations on the PDP-8/E with the EAE Floating Point Package:

Add	160 μs
Subtract	180 μs
Multiply	200 μs
Divide	160 μs or 190 μs .

Since these are almost two orders of magnitude greater than the average single instruction time, it is reasonable to compare algorithms on the basis of the number of floating point operations they entail.

A count of floating point operations for the position computation algorithm described in the previous section is given below:

	Multiplications and Divisions	Additions and Subtractions
Direct computation of $\psi_{\Delta Q}^{-1}$ from A_i's	12	0
$P^T \psi_{\Delta Q}^{-1}$ via GMPRD	48	48
$(P^T \psi_{\Delta Q}^{-1})$ P via GMPRD	36	36
$(P^T \psi_{\Delta Q}^{-1})$ Q via GMPRD	12	12
Inversion of $P^T \psi_{\Delta Q}^{-1} P$	30	26
$(P^T \psi^{-1} P)^{-1} P^T \psi_{\Delta Q}^{-1} Q$ via GMPRD	9	9
Computation of $\hat{z}$ from eq. (5-9) (Square root counted as 7 multiplications based on times given in ref. 2)	10	2
TOTALS	157	133

If one assumes an average time of 180 μs per floating point operation, then the total of the 290 operations in this algorithm takes approximately 52 ms. The remainder of the 90 ms is taken up by various other operations. Note that the inversion of the 3 x 3 matrix takes only about 20% of the total time, with matrix multiplications accounting for the bulk of the time.

The efficiency of this algorithm could be improved in several ways. Note first of all that the matrix $\psi_{\Delta Q}^{-1}$, equation (5-8), has several zero entries, and that the matrix P (see Section 3.0) has one column of 1's. Taking advantage of these facts reduces the number of multiplications and additions required in forming the various matrix products. Also the matrix $P^T \psi_{\Delta Q}^{-1} P$ is symmetric, so that only six of its elements, rather than all nine, need be computed. Finally, it is more efficient to solve a system of linear equations by a method such as Gaussian elimination than by inverting the matrix and then multiplying by the right hand side vector. The Gaussian elimination algorithm is also simpler when the matrix is symmetric, as in the case here.

An algorithm employing the above ideas is described below and the number of required floating point operations tabulated. It involves direct computation of the elements of the matrix

$$\sigma_A^2 \, P^T \, \psi_{\Delta Q}^{-1} =$$

$$\begin{bmatrix}
-\frac{1}{A_1}\left[7\frac{x_1}{A_1}+\frac{x_2}{A_2}+\frac{x_3}{A_3}+\frac{x_4}{A_4}\right] & -\frac{1}{A_2}\left[\frac{x_1}{A_1}+\frac{x_2}{A_2}\right] & -\frac{1}{A_3}\left[\frac{x_1}{A_1}+\frac{x_3}{A_3}\right] & -\frac{1}{A_4}\left[\frac{x_1}{A_1}+\frac{x_4}{A_4}\right] \\
-\frac{1}{A_1}\left[7\frac{y_1}{A_1}+\frac{y_2}{A_2}+\frac{y_3}{A_3}+\frac{y_4}{A_4}\right] & -\frac{1}{A_2}\left[\frac{y_1}{A_1}+\frac{y_2}{A_2}\right] & -\frac{1}{A_3}\left[\frac{y_1}{A_1}+\frac{y_3}{A_3}\right] & -\frac{1}{A_4}\left[\frac{y_1}{A_1}+\frac{y_4}{A_4}\right] \\
\frac{1}{A_1}\left[7\frac{1}{A_1}+\frac{1}{A_2}+\frac{1}{A_3}+\frac{1}{A_4}\right] & \frac{1}{A_2}\left[\frac{1}{A_1}+\frac{1}{A_2}\right] & \frac{1}{A_3}\left[\frac{1}{A_1}+\frac{1}{A_3}\right] & \frac{1}{A_4}\left[\frac{1}{A_1}+\frac{1}{A_4}\right]
\end{bmatrix} \quad (5\text{-}10)$$

As before, it is assumed that both the q_i's and the A_i's are available.

	Multiplications and Divisions	Additions and Subtractions
Compute $\frac{1}{A_i}$, $\frac{x_i}{A_i}$, $\frac{y_i}{A_i}$, $i = 1, 4$	12	0
Compute directly each element of $\sigma_A^2 P^T \psi_{\Delta Q}^{-1}$, equation (5-10)	15	18
Compute $\sigma_A^2 P^T \psi_{\Delta Q}^{-1} Q$ via conventional matrix multiplication	12	9
Compute the six distinct elements of the symmetric matrix $\sigma_A^2 P^T \psi_{\Delta Q}^{-1} P$, taking advantage of the column of 1's in P to reduce the number of multiplications	12	18
Solve for $\bar{x}$ via symmetrical Gaussian elimination algorithm	17	12
Compute $\hat{z}$ from (5-9) (Square root counted as 7 multiplications)	10	2
TOTALS	78	59

Note that the number of floating point operations required, 137, is approximately one-half of that in the algorithm used for timing tests. A quick look at the weighted least squares algorithm for calculation of rates indicated that it would require approximately the same number of operations as the above position algorithm. It appears, then, that it is probably possible to meet the required 100 ms. time limit for both position and rate calculations, with careful assembly language programming. However, there would be very little margin for any future program changes or additions.

Some additional time could be saved by not updating the weighting matrix for the position calculation at each measurement, but rather, say, at every other measurement. However, it does not appear that this is possible for the rate calculations. The use of an iterative algorithm is another possibility.

5.4 Conclusions and Recommendations

It appears that weighted least squares calculation of position and rate ten times per second is just marginally possible on the PDP-8/E with the Extended Arithmetic Element with careful algorithm pruning and assembly language programming. However, this would place a limitation on future algorithm expansion, and would require a significant amount of programming time to make program modifications.

Barring the discovery of a significantly faster iterative algorithm, it appears that the best solution would be to purchase a minicomputer with a floating point processor. Although it is believed that this option for the PDP-8 costs approximately $7,000, the cost for a floating point processor for the Data General Nova series of computers is only $4000. With this option, a floating point arithmetic operation can be performed in roughly 10 μs. This would allow an ample time margin with the existing algorithms, and might even permit the operational program to be written in Fortran. A complete system (Nova computer with 8K of memory, teletype, floating point processor, and necessary interfaces) should not cost significantly more than $14,000.

Floating point operation times for other minicomputers without a floating point processor are hard to obtain. However, it is believed that neither the Data General Nova 800 with hardware fixed-point multiplication nor the Honeywell 716 can improve upon the PDP-8/E times.

6.0 RECOMMENDATIONS AND CONCLUSIONS

6.1 Recommended Solution Techniques

The accuracy studies of the solution techniques indicate that while the iterative solution described in Section 3.4 provides the minimum variances in the coordinate errors for all cases, it has the disadvantage of requiring several iterations within a computational cycle. Possibilities of convergence problems also exist if the initial solution is considerably in error. For these reasons, it is recommended that a slight amount of accuracy be sacrificed in order to use the completely general explicit solution described in Section 3.5. Advantages of the explicit solution are as follows:

1. Completely general station locations can be used. The station survey positions are entered into the solution as constants, without consideration of whether the stations are in a plane or not. Elevated stations are handled with ease.
2. The solution is straightforward and requires no iterations.
3. The accuracy of the solution differs only slightly from the minimum variance obtained from the iterative solution.
4. Computation times should be reasonable, since a number of the matrices and matrix multiplications do not need to be recalculated in real time.

For range rate calculations, the minimum variance solution outlined in Section 3.6 is straightforward and is recommended for use. For the time-delay bias removal, the technique described in Section 3.7 is recommended with an optimal low-pass filter as described in Section 3.7.3. This technique provides for calculation of the time-delay in each separate two-way path, but does not separate transponder delays from transmitter and receiver delays. To date, no way of separating the delay into transponder, receiver, and transmitter delay has been determined, except by using a separate calibrated transponder at a ground location.

The solution will have the capability of providing coordinate and coordinate rate outputs for three stations in case one station is not receiving data. Also, provision can be made for utilization of more than four ground stations if desired.

A flow chart indicating the recommended calculation scheme is shown in Figure 6-1.

6.2 Recommended Computer Specifications

In Section 5.0, the general considerations for the system minicomputer were discussed. Based on these considerations and known operational requirements, it is recommended that a minicomputer with the following characteristics be purchased:

1. A minicomputer with 16,384 words of memory, a memory cycle time of about 1.0 μs, and a preferred word length of at least 16 bits;
2. A floating point processor to perform floating point arithmetic operations in 10 to 20 μs each;
3. A digital I/O channel providing 16 digital lines plus an interrupt line for input, and 16 digital lines plus a data ready line for output;
4. Eight (8) analog outputs for plotter drive;
5. A teletype interface;
6. A high speed paper tape reader; and
7. FORTRAN IV software capability.

Surveys of various manufacturers were made to determine which minicomputer system would provide the above characteristics for a minimum price. Based on this survey, it appears that a Data General Nova II/10 system will meet the specifications at a minimum price. The total cost (GSA) of the Data General System meeting the above specifications is approximately $14,060.

6.3 Recommended Future Work

During this study, geometrical errors were determined for trajectories consisting of straight-line segments. In future work, more complex trajectories should be considered, including spiral descents and curved, decelerating approaches. In addition to the study of more general trajectories, additional study should be made of the effect of station location on the system accuracy. Using existing programs, additional error contours can be generated for a large number of hypothetical station locations.

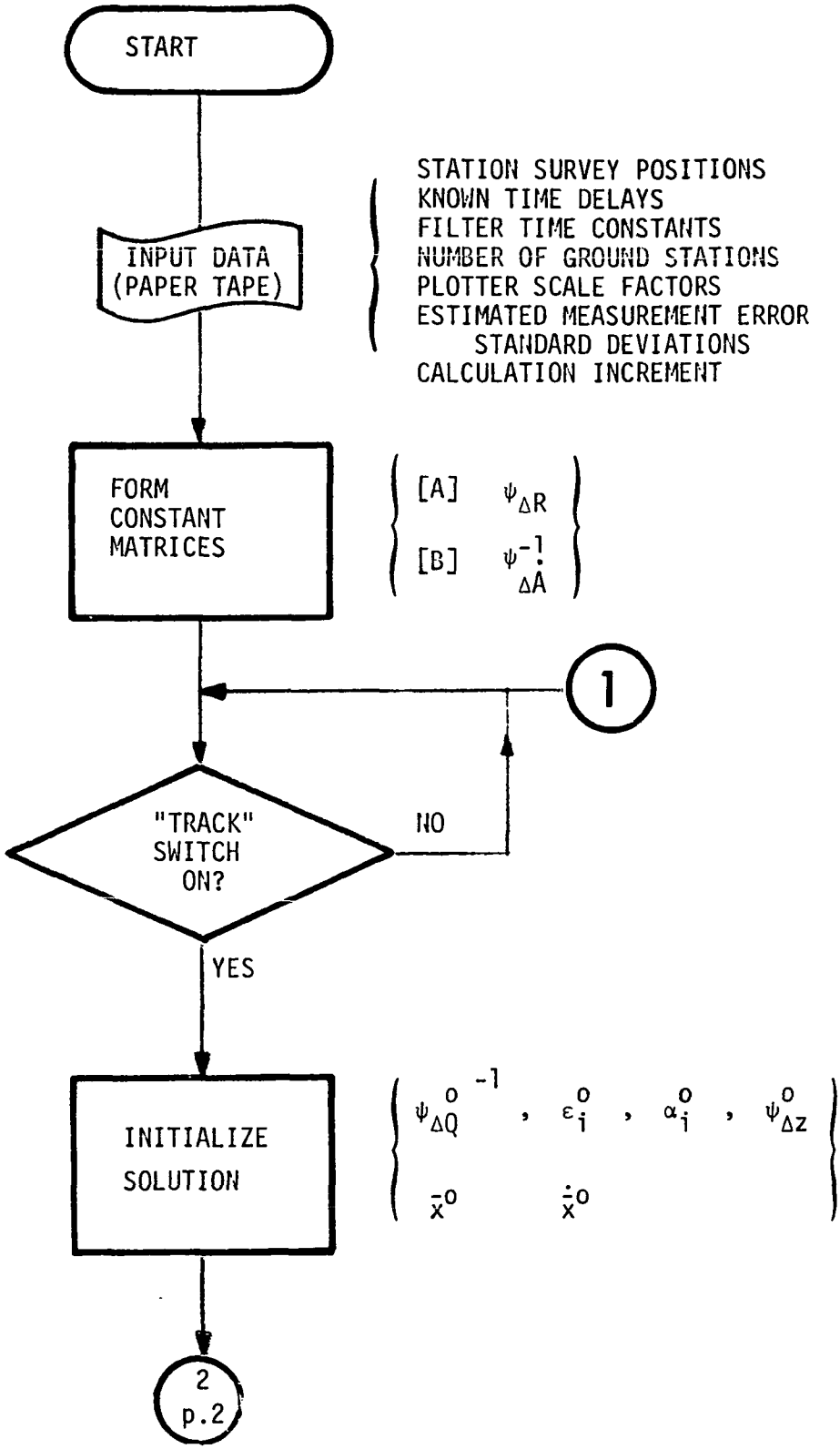

Fig. 6-1. General flow chart for recommended solution techniques--Operational System.

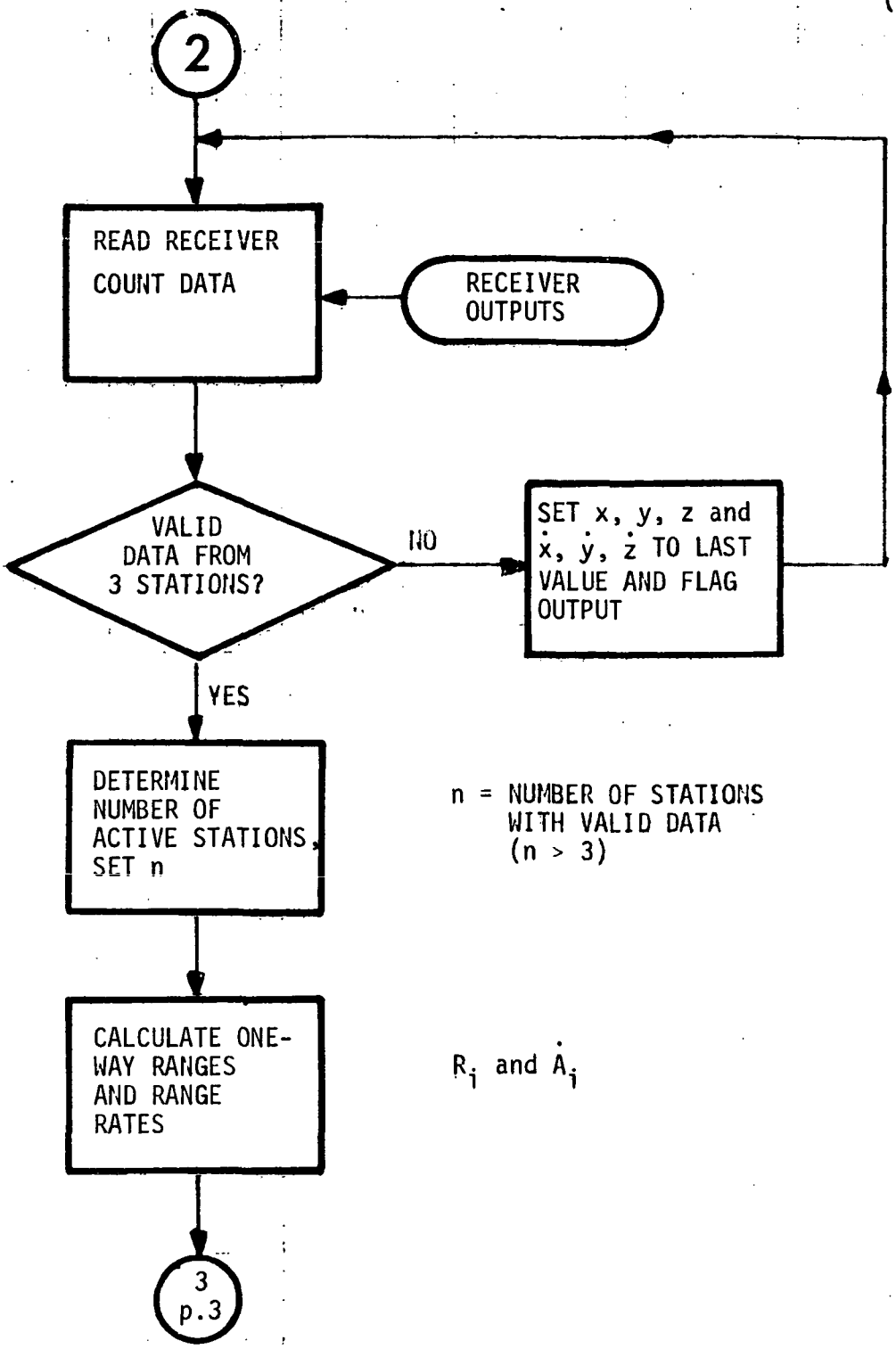

Fig. 6-1. Continued.

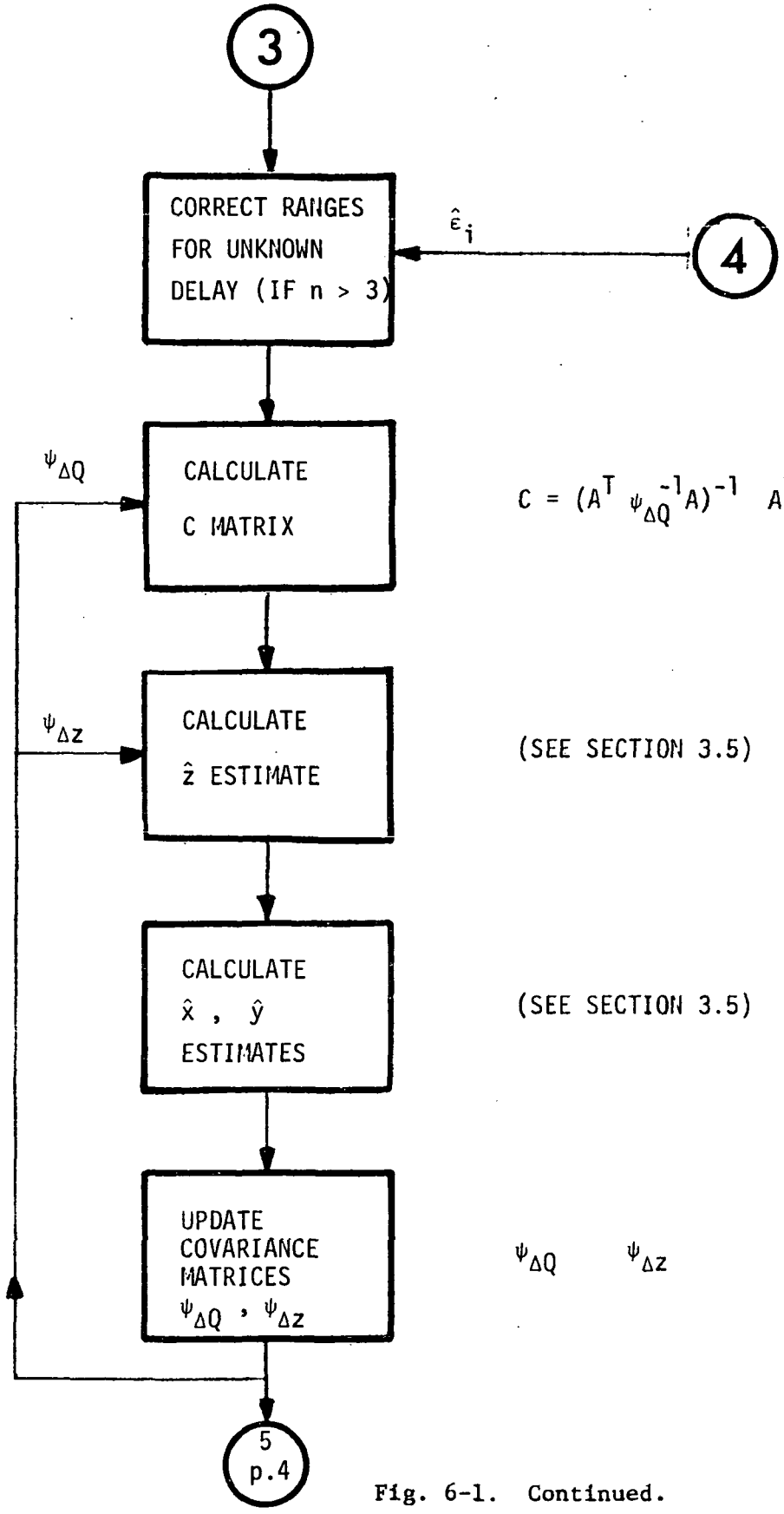

Fig. 6-1. Continued.

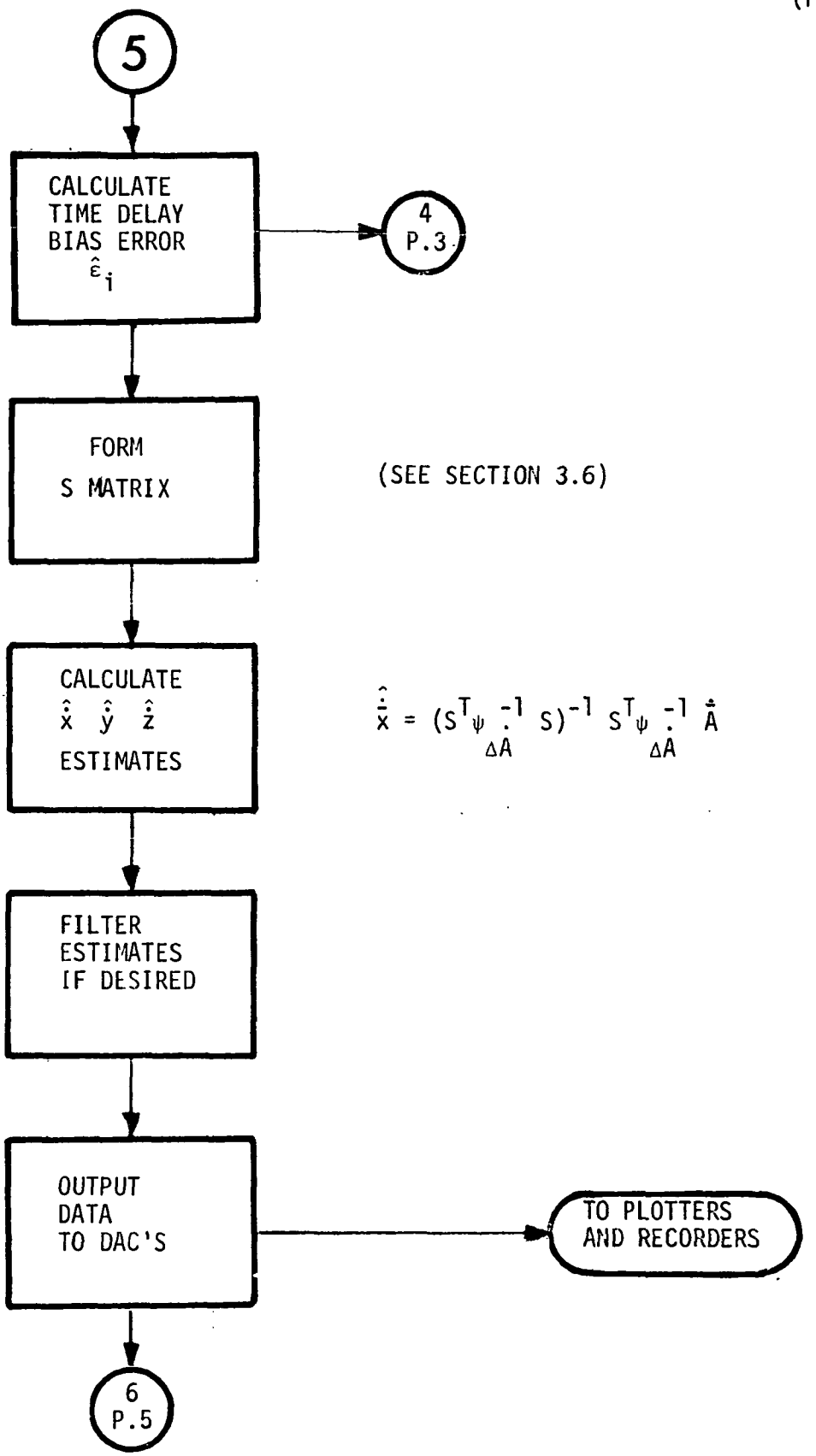

Fig. 6-1. Continued.

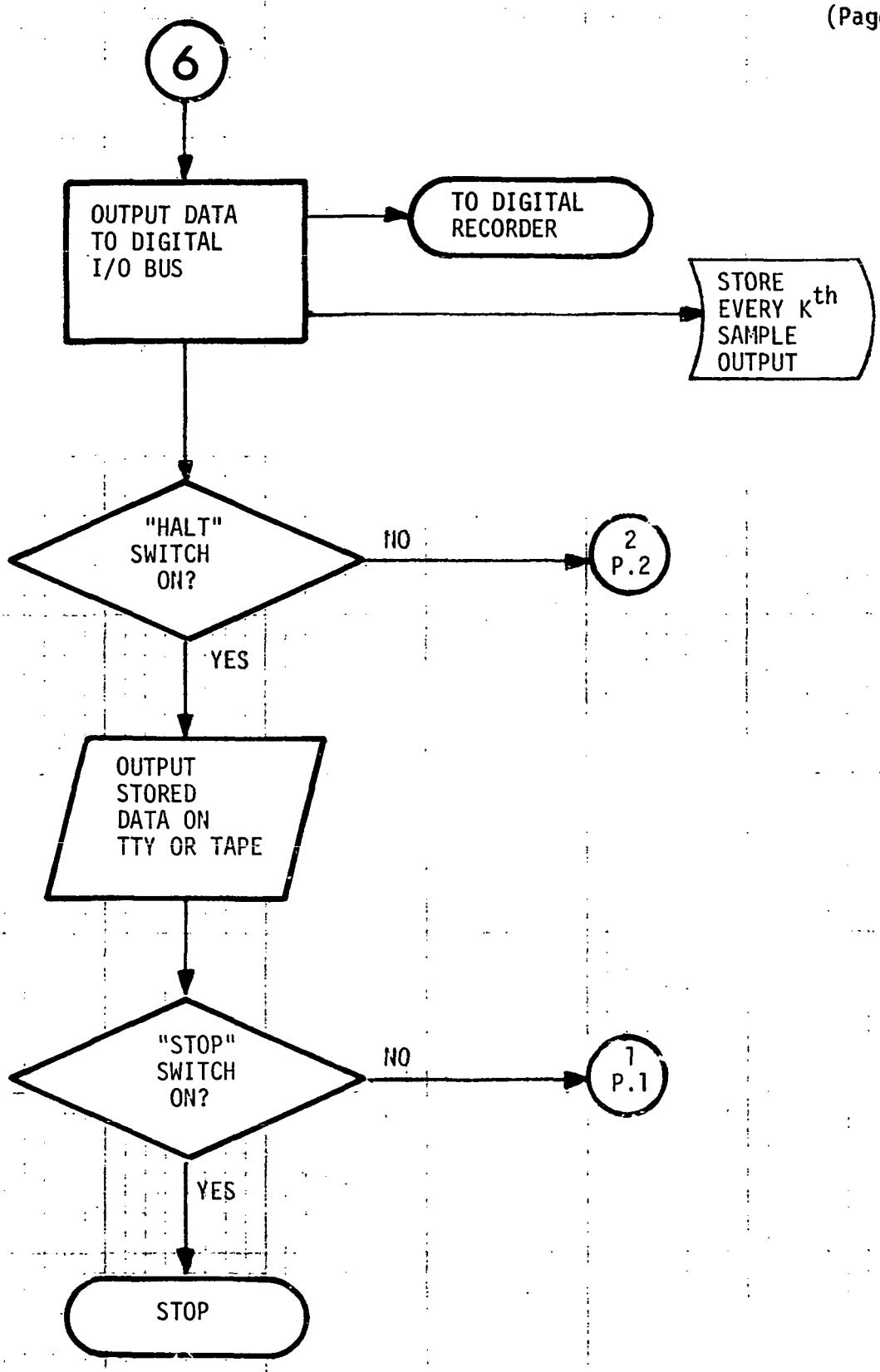

Fig. 6-1. Concluded.

The benefits to be achieved by using more than four ground stations should also be investigated. Since ground stations are anticipated to be low cost, and the added computational burden is not great, it is felt that additional stations may prove worthwhile in cases where the geometrical accuracy requires improvement.

In the studies discussed in this report, a basic measurement error has been assumed. This assumption has been based on analyses accomplished by LRC personnel, slanted toward the determination of hardware-associated errors. Additional analytical work is required to complete some of the hardware error studies. In addition, results from field checks of the equipment should be incorporated in the error studies to provide firm numbers for the basic two-way path measurement errors.

Additional consideration should be given to the integration of the multilateration system into the VALT navigation system. The solutions discussed in this report are all point estimation techniques; that is, smoothing of data based on the sequential measurements has not been recommended. This has been done to prevent time lags in the output data that may detrimentally affect the operation of the navigation and guidance systems on board the aircraft. It is felt, however, that in some cases, smoothing of the output data may be feasible and that the associated time lags could be made compatible with the navigation system. For this reason, navigation system personnel should define the transient characteristics that are necessary in the basic measurement data for compatibility with the navigation and guidance algorithms.

In future work, extensive simulations of the solution technique recommended in Section 5.0 should be conducted to assure that there are no points in the coverage volume where the solution fails. In addition, considerable work is necessary to determine the most efficient algorithms for providing the necessary computations in real time. The associated software must be developed and checked out for the minicomputer selected for use in the system.

7.0 APPENDICES

Page Intentionally Left Blank

APPENDIX A

An Explicit General Solution to the Trilateration Position Location Problem in an Arbitrary Coordinate System

The general solution outlined in this appendix is similar to a solution given in algorithmic form in ref. 4, except that matrix techniques are used to permit extension to the case of redundant ground stations.

For three ground stations, three equations are obtained:

$$R_1^2 = R^2 + p_1^2 - 2\bar{R} \cdot \bar{p}_1 \tag{A-1}$$

$$R_2^2 = R^2 + p_2^2 - 2\bar{R} \cdot \bar{p}_2 \tag{A-2}$$

$$R_3^2 = R^2 + p_3^2 - 2\bar{R} \cdot \bar{p}_3 \tag{A-3}$$

where the nomenclature is defined in Fig. 3-1, page 14.

The solution is started by subtracting (A-1) from both (A-2) and (A-3) to obtain:

$$\frac{R_2^2 - R_1^2 - p_2^2 + p_1^2}{2} = + \bar{R} \cdot (\bar{p}_1 - \bar{p}_2) \tag{A-4}$$

$$\frac{R_3^2 - R_1^2 - p_3^2 + p_1^2}{2} = + \bar{R} \cdot (\bar{p}_1 - \bar{p}_3) \quad . \tag{A-5}$$

Now let the left-hand side, which contains the measurements and surveyed values, be designated as q_1 and q_2 so that the equations become

$$q_1 = + \bar{R} \cdot (\bar{p}_1 - \bar{p}_2) \tag{A-6}$$

$$q_2 = + \bar{R} \cdot (\bar{p}_1 - \bar{p}_3) \quad . \tag{A-7}$$

These equations can be written in matrix form as:

$$\bar{Q} = [P]\, \bar{x} \tag{A-8}$$

where

$$\bar{Q} = \begin{Bmatrix} q_1 \\ q_2 \end{Bmatrix} \qquad \bar{x} = \begin{Bmatrix} x \\ y \\ z \end{Bmatrix}$$

$$[P] = \begin{bmatrix} x_1 - x_2 & y_1 - y_2 & z_1 - z_2 \\ x_1 - x_3 & y_1 - y_3 & z_1 - z_3 \end{bmatrix} .$$

Now partition the matrix [P] and $\bar{x}$ as follows:

$$\bar{Q} = [A \; B] \begin{Bmatrix} \bar{\rho} \\ z \end{Bmatrix} \tag{A-9}$$

where

$$\bar{\rho} = \begin{Bmatrix} x \\ y \end{Bmatrix}$$

$$[A] = \begin{bmatrix} x_1 - x_2 & y_1 - y_2 \\ x_1 - x_3 & y_1 - y_3 \end{bmatrix}$$

and

$$[B] = \begin{Bmatrix} z_1 - z_2 \\ z_1 - z_3 \end{Bmatrix} .$$

With this partitioning, we have

$$\bar{Q} = A\,\bar{\rho} + Bz \tag{A-10}$$

and for A nonsingular, it is possible to solve for $\bar{\rho}$ as

$$\bar{\rho} = A^{-1}\,\bar{Q} - A^{-1}\,Bz \tag{A-11}$$

or

$$\bar{\rho} = C\bar{Q} - CBz \tag{A-12}$$

where

$$[C] = [A]^{-1} = \frac{1}{D}\begin{bmatrix} y_1 - y_3 & y_2 - y_1 \\ x_3 - x_1 & x_1 - x_2 \end{bmatrix}$$

$$D = (x_1 - x_2)(y_1 - y_3) - (x_1 - x_3)(y_1 - y_2) .$$

From the above equation, x and y are found in terms of z as

$$x = k_1 - d_1 z \tag{A-13}$$

$$y = k_2 - d_2 z \tag{A-14}$$

where $$d_1 = \frac{1}{D}\left[(y_1 - y_3)(z_1 - z_2) + (y_2 - y_1)(z_1 - z_3)\right]$$

$$d_2 = \frac{1}{D}\left[(x_3 - x_1)(z_1 - z_2) + (x_1 - x_2)(z_1 - z_3)\right]$$

$$k_1 = \frac{q_1}{D}(y_1 - y_3) + \frac{q_2}{D}(y_2 - y_1)$$

$$k_2 = \frac{q_1}{D}(x_3 - x_1) + \frac{q_2}{D}(x_1 - x_2) \quad .$$

Now, writing eq. (A-1) in terms of x, y, z,

$$R_1^2 = x^2 + y^2 + z^2 + p_1^2 - 2x_1 x - 2y_1 y - 2z_1 z \tag{A-15}$$

and substituting equations (A-13) and (A-14) gives the equation

$$az^2 + bz + c = 0 \tag{A-16}$$

where $$a = 1 + d_1^2 + d_2^2$$

$$b = -2(z_1 + k_1 d_1 + k_2 d_2 - x_1 d_1 - y_1 d_2)$$

$$c = k_1^2 + k_2^2 + p_1^2 - R_1^2 - 2x_1 k_1 - 2y_1 k_2 \quad .$$

Thus, it is possible to solve for z as

$$z = \frac{-b \pm \sqrt{b^2 - 4ac}}{2a} \tag{A-17}$$

and x and y are given by

$$x = k_1 - d_1 z \tag{A-18}$$

$$y = k_2 - d_2 z \quad . \tag{A-19}$$

The sign of z in (A-17) is chosen to make z positive.

Page Intentionally Left Blank

APPENDIX B

MATRIX FORMULATION OF COORDINATE ERRORS

The Taylor Series expansion for the errors in coordinates can be written as a function of the measurement errors ΔR as

$$\overline{\Delta x} = [D]\ \overline{\Delta R} \tag{B-1}$$

where for four stations,

$$\overline{\Delta x} = \begin{Bmatrix} \Delta x \\ \Delta y \\ \Delta z \end{Bmatrix} \qquad \text{and} \qquad \overline{\Delta R} = \begin{Bmatrix} \Delta R_1 \\ \Delta R_2 \\ \Delta R_3 \\ \Delta R_4 \end{Bmatrix} \tag{B-2}$$

and [D] is the matrix of partial derivatives:

$$[D] = \begin{bmatrix} \frac{\partial x}{\partial R_1} & \frac{\partial x}{\partial R_2} & \frac{\partial x}{\partial R_3} & \frac{\partial x}{\partial R_4} \\ \frac{\partial y}{\partial R_1} & \frac{\partial y}{\partial R_2} & \frac{\partial y}{\partial R_3} & \frac{\partial y}{\partial R_4} \\ \frac{\partial z}{\partial R_1} & \frac{\partial z}{\partial R_2} & \frac{\partial z}{\partial R_3} & \frac{\partial z}{\partial R_4} \end{bmatrix} . \tag{B-3}$$

To obtain the variance-covariance matrix, multiply Δx by its transpose and take expected values.

$$\overline{\Delta x}\ \overline{\Delta x}^T = [D]\ \overline{\Delta R}\ \overline{\Delta R}^T [D]^T$$

$$\psi_{\overline{\Delta x}} = E\{\overline{\Delta x}\ \overline{\Delta x}^T\} = [D]\ \psi_{\overline{\Delta R}} [D]^T \tag{B-4}$$

where $\psi_{\overline{\Delta R}}$ is the variance-covariance matrix of the range errors (see Appendix C) and $\psi_{\overline{\Delta x}}$ is the variance-covariance matrix of the coordinate errors. In cases where a coordinate transformation is used of the form

$$X = [K]x$$

then the covariance matrix in the new coordinate system is related to the covariance matrix in the old system as

$$\psi_{\overline{\Delta X}} = K \, \psi_{\overline{\Delta x}} \, K^T \tag{B-5}$$

APPENDIX C

DERIVATION OF THE COVARIANCE MATRIX OF THE RANGE MEASUREMENT ERRORS FOR THE PLANNED MULTILATERATION SYSTEM

The planned system uses two-way range measurements from a single transmitter to four or more ground receivers. Thus the measurements are of the form, for four ground receivers,

$$\begin{aligned} M_1 &= 2R_1 \\ M_2 &= R_1 + R_2 \\ M_3 &= R_1 + R_3 \\ M_4 &= R_1 + R_4 \end{aligned} \tag{C-1}$$

where the M_i are the measurements assuming the transmitter and receiver #1 are colocated. The one-way ranges are given by

$$\begin{aligned} R_1 &= \frac{M_1}{2} \\ R_2 &= M_2 - \frac{M_1}{2} \\ R_3 &= M_3 - \frac{M_1}{2} \\ R_4 &= M_4 - \frac{M_1}{2} \end{aligned} \tag{C-2}$$

If it is assumed that all two-way range measurement errors have equal variance σ^2, then

$$\langle \Delta R_1 \, \Delta R_1 \rangle = \frac{\sigma^2}{4} \tag{C-3}$$

$$\langle \Delta R_1 \, \Delta R_j \rangle = -\frac{\sigma^2}{4} \quad ; \quad j = 2, 3, 4 \tag{C-4}$$

$$\langle \Delta R_j \; \Delta R_j \rangle = \frac{5\sigma^2}{4} \quad ; \qquad j = 2, 3, 4 \tag{C-5}$$

$$\langle \Delta R_j \; \Delta R_k \rangle = \frac{\sigma^2}{4} \quad ; \qquad j = 2, 3, 4, \quad ; k > j \quad . \tag{C-6}$$

Thus, the covariance matrix for the one-way range errors may be written as (for four ground stations)

$$\psi_{\overline{\Delta R}} = \frac{\sigma^2}{4} \begin{vmatrix} 1 & -1 & -1 & -1 \\ -1 & 5 & 1 & 1 \\ -1 & 1 & 5 & 1 \\ -1 & 1 & 1 & 5 \end{vmatrix} \quad . \tag{C-7}$$

A similar expression is obtained for the range rate errors if it is assumed that all two-way range rate measurements have equal variance.

APPENDIX D

COVARIANCE MATRIX OF COORDINATE ERRORS FOR A LINEARIZED SOLUTION FOR THE SPECIAL CASE OF ALL GROUND STATIONS IN A PLANE

In this solution as given in Section 3.3.2, the solution is given by

$$\bar{x} = (P^T \psi_{\Delta Q}^{-1} P)^{-1} P^T \psi_{\Delta Q} \bar{Q} \tag{D-1}$$

where $\psi_{\Delta Q}$ is the covariance matrix of the range difference measurements. The covariance matrix of errors in the vector $\bar{x}$ is found by taking the expected value of $\overline{\Delta x}\ \overline{\Delta x}^T$ to obtain:

$$\psi_{\overline{\Delta x}} = (P^T \psi_{\Delta Q}^{-1} P)^{-1} \tag{D-2}$$

where

$$\psi_{\Delta Q} = T\ \psi_{\overline{\Delta R}}\ T^T \tag{D-3}$$

and the matrix T is defined in Section 3.3.2.

Since in this case, the vector $\bar{x}$ is

$$\bar{x} = \begin{Bmatrix} x \\ y \\ u \end{Bmatrix}$$

where $u = R^2/2$, the variance of the z coordinate errors must be found from a Taylor Series expansion of the equation for z, This equation is

$$z = [2u - x^2 - y^2]^{1/2} = F(x, y, u) \quad . \tag{D-4}$$

Thus we have

$$\Delta z = [D]\ \Delta\bar{x} \tag{D-5}$$

where D is a matrix of partial derivitives given explicitly by

$$[D] = \left\{ \frac{-x}{z} , \frac{-y}{z} , \frac{1}{z} \right\} \quad . \tag{D-6}$$

This variance of errors in the z coordinate is therefore

$$\sigma_{\Delta z}^{2} = D \, \psi_{\overline{\Delta x}} \, D^{T} \quad . \tag{D-7}$$

APPENDIX E

COVARIANCE MATRIX OF COORDINATE ERRORS FOR A LINEARIZED SOLUTION FOR THE SPECIAL CASE OF ALL GROUND STATIONS NOT IN A PLANE

For this solution, as given in Section 3.3.3, we have for four ground stations:

$$\bar{x} = (P^T P)^{-1} P^T \bar{Q} \quad . \tag{E-1}$$

The covariance matrix for errors in the vector $\bar{x}$ is

$$\psi_{\overline{\Delta x}} = (P^T P)^{-1} P^T \psi_{\overline{\Delta Q}} P (P^T P)^{-1} \tag{E-2}$$

where $\psi_{\Delta Q}$ is found as shown in Appendix D and

$$\bar{x} = \begin{Bmatrix} x \\ y \\ z \end{Bmatrix} \quad .$$

For more than four ground stations, the weighted least squares technique may be used, and the associated covariance matrix is

$$\psi_{\overline{\Delta x}} = (P^T \psi_{\Delta Q}^{-1} P)^{-1} \quad . \tag{E-3}$$

Page Intentionally Left Blank

APPENDIX F

THE OVER-DETERMINED (ITERATIVE) SOLUTION FOR THE DATA OBTAINED FROM THE RF MULTILATERATION SYSTEM

F.1 Over-Determined Solution for Four Ground Stations

The methods for obtaining the following are given below:

(1) The over-determined solution for x, y, z -- as obtained from four direct (basic) measurements, A, B, C, and D.

(2) The variance-covariance matrix for the errors in x, y, z.

Since the errors in A, B, C, and D are assumed to be uncorrelated and to have equal standard deviations (viz 10 ft), it is believed to be advantageous to derive (1) and (2) above from A, B, C, and D directly--and hence from the ellipsoids which they represent.

That is,

$$2\sqrt{(x-x_1)^2 + (y-y_1)^2 + (z-z_1)^2} = A_1 \quad \text{(F-1)}$$

$$\sqrt{(x-x_1)^2 + (y-y_1)^2 + (z-z_1)^2} + \sqrt{(x-x_2)^2 + (y-y_2)^2 + (z-z_2)^2} = A_2 \quad \text{(F-2)}$$

$$\sqrt{(x-x_1)^2 + (y-y_1)^2 + (z-z_1)^2} + \sqrt{(x-x_3)^2 + (y-y_3)^2 + (z-z_3)^2} = A_3 \quad \text{(F-3)}$$

$$\sqrt{(x-x_1)^2 + (y-y_1)^2 + (z-z_1)^2} + \sqrt{(x-x_4)^2 + (y-y_4)^2 + (z-z_4)^2} = A_4 . \quad \text{(F-4)}$$

Note: If the attitudes of the transmitter and receivers are zero, then $z_1 = z_2 = z_3 = z_4 = 0$. For "exactness", the survey positions should be used.

Now expand the left-hand sides of the above equations in a Taylor Series expansion around an initial estimate, e.g., the presently available solution, neglecting all except the first-order terms. The results are as follows:

$$f_1(x,y,z)]_o + \frac{\partial f_1}{\partial x}\Big]_o \Delta x + \frac{\partial f_1}{\partial y}\Big]_o \Delta y + \frac{\partial f_1}{\partial z}\Big]_o \Delta z = A \quad \text{(F-5)}$$

$$f_2(x,y,z)]_o + \frac{\partial f_2}{\partial x}\Big]_o \Delta x + \frac{\partial f_2}{\partial y}\Big]_o \Delta y + \frac{\partial f_2}{\partial z}\Big]_o \Delta z = B \qquad \text{(F-6)}$$

$$f_3(x,y,z)]_o + \frac{\partial f_3}{\partial x}\Big]_o \Delta x + \frac{\partial f_3}{\partial y}\Big]_o \Delta y + \frac{\partial f_3}{\partial z}\Big] \Delta z = C \qquad \text{(F-7)}$$

$$f_4(x,y,z)]_o + \frac{\partial f_4}{\partial x}\Big]_o \Delta x + \frac{\partial f_4}{\partial y}\Big]_o \Delta y + \frac{\partial f_4}{\partial z}\Big]_o \Delta z = D \quad .$$

In the above,

$$f_1(x,y,z)]_o = 2\sqrt{(x-x_1)^2 + (y-y_1)^2 + (z-z_1)^2} \qquad \text{(F-9)}$$

is evaluated at $(x,y,z) = (x_o, y_o, z_o)$, which is the initial (starting) estimate for x,y,z. Similarly, $f_2(x,y,z)]_o$ and the others are so defined.

Now define the following:

$$\begin{aligned} \Delta A_1 &= A_1 - f_1(x,y,z)]_o \\ \Delta A_2 &= A_2 - f_2(x,y,z)]_o \\ \Delta A_3 &= A_3 - f_3(x,y,a)]_o \\ \Delta A_4 &= A_4 - f_4(x,y,z)]_o \ . \end{aligned} \qquad \text{(F-10)}$$

Also, simplify the notation from $\frac{\partial f_1}{\partial x}\Big]_o$ to $\frac{\partial f_1}{\partial x}$ and so on. Thus, $\frac{\partial f_1}{\partial x}$ is to be evaluated at $(x,y,z) = (x_o, y_o, z_o)$ -- or at new (improved) values in subsequent iterations.

The notation can be further simplified to the following:

$$[D]_{4x3} \underset{3x1}{\begin{pmatrix} \Delta x \\ \Delta y \\ \Delta z \end{pmatrix}} = \begin{pmatrix} \Delta A_1 \\ \Delta A_2 \\ \Delta A_3 \\ \Delta A_4 \end{pmatrix}_{4x1} . \qquad \text{(F-11)}$$

where

$$[D]_{4x3} = \left[\begin{array}{c}\text{Matrix}\\ \text{of}\\ \text{Partial}\\ \text{Differentials}\end{array}\right]_{4x3} = \begin{bmatrix} \frac{\partial f_1}{\partial x} & \frac{\partial f_1}{\partial y} & \frac{\partial f_1}{\partial z} \\ \frac{\partial f_2}{\partial x} & \frac{\partial f_2}{\partial y} & \frac{\partial f_2}{\partial z} \\ \frac{\partial f_3}{\partial x} & \frac{\partial f_3}{\partial y} & \frac{\partial f_3}{\partial z} \\ \frac{\partial f_4}{\partial x} & \frac{\partial f_4}{\partial y} & \frac{\partial f_4}{\partial z} \end{bmatrix} . \qquad \text{(F-12)}$$

For further simplification of notation, let

$$\underset{\sim}{\Delta x} \equiv \begin{pmatrix} \Delta x \\ \Delta y \\ \Delta z \end{pmatrix}_{3x1} , \qquad \text{(F-13)}$$

$$\underset{\sim}{\Delta A} \equiv \begin{pmatrix} \Delta A_1 \\ \Delta A_2 \\ \Delta A_3 \\ \Delta A_4 \end{pmatrix}_{4x1} , \qquad \text{(F-14)}$$

$$D \equiv [D]_{4x3} .$$

Consequently,

$$D_{4x3}\ \underset{\sim}{\Delta x}_{3x1} = \underset{\sim}{\Delta A}_{4x1} \qquad \text{(F-15)}$$

Therefore,

$$D^T D\ \Delta x = D^T\ \Delta A , \qquad \text{(F-16)}$$

where

$D^T \equiv$ the transpose of D.

The least-squares solution for $\underset{\sim}{\Delta x}$ is thus obtained from the following:

$$\underset{\sim}{\Delta x} = (D^T D)^{-1} D^T\ \underset{\sim}{\Delta A} ,$$

$$= G^{-1} D^T\ \underset{\sim}{\Delta A} , \qquad \text{(F-17)}$$

where

$$G \equiv D^T D \tag{F-18}$$

and

$G^{-1} \equiv$ the inverse of G.

The value so obtained for Δx provides an improvement over the original estimate of $(x,y,z) = (x_o, y_o, z_o)$ and the above process is repeated until no further change (improvment) in Δx results.

F.2 Variance-Covariance Matrix of Errors in x, y, z

In the above expression for Δx, let us multiply both sides by their respective transposes and then take the expected values. The result is the following:

$$V_{\underset{\sim}{\Delta x}} = G^{-1} D^T V_{\underset{\sim}{\Delta A}} D(G^{-1})^T ,$$

$$= G^{-1} D^T V_{\underset{\sim}{\Delta A}} D G^{-1} \quad \text{(since G is symmetric)}, \tag{F-19}$$

where

$V_{\underset{\sim}{\Delta x}} \equiv$ the variance-covariance matrix of $\underset{\sim}{\Delta x}$

and

$V_{\underset{\sim}{\Delta A}} \equiv$ the variance-covariance matrix of $\underset{\sim}{\Delta A}$

$$= \sigma^2_{\Delta A} = \begin{bmatrix} 1 & 0 & 0 & 0 \\ 0 & 1 & 0 & 0 \\ 0 & 0 & 1 & 0 \\ 0 & 0 & 0 & 1 \end{bmatrix}$$

$$= \sigma^2_{\Delta A} I \tag{F-20}$$

where $I \equiv$ the identity matrix.

Hence,

$$V_{\underset{\sim}{\Delta x}} = \sigma^2_{\Delta A} G^{-1} D^T I D G^{-1}$$

$$= \sigma^2_{\Delta A} G^{-1} D^T D \cdot G^{-1}$$

$$= \sigma_{\Delta A}^2 \, G^{-1} \quad . \tag{F-21}$$

Since

$$G^{-1} \, G = I \quad ,$$

$$\underset{\Delta x}{\psi} = V_{\underset{\sim}{\Delta x}} = \sigma_R^2 \, G^{-1} \quad . \tag{F-22}$$

F.3 Calculation of the Partials

Define

$$R_i = \sqrt{(x-x_i)^2 + (y-y_i)^2 + (z-z_i)^2} \tag{F-23}$$

for i = 1, 2, 3, 4.

Consequently,

$$D = \begin{bmatrix} \frac{2(x-x_1)}{R_1} & \frac{2(y-y_1)}{R_1} & \frac{2(z-z_1)}{R_1} \\ \frac{x-x_1}{R_1} + \frac{x-x_2}{R_2} & \frac{y-y_1}{R_1} + \frac{y-y_2}{R_2} & \frac{z-z_1}{R_1} + \frac{z-z_2}{R_2} \\ \frac{x-x_1}{R_1} + \frac{x-x_3}{R_3} & \frac{y-y_1}{R_1} + \frac{y-y_3}{R_3} & \frac{z-z_1}{R_1} + \frac{z-z_3}{R_3} \\ \frac{x-x_1}{R_1} + \frac{x-x_4}{R_4} & \frac{y-y_1}{R_1} + \frac{y-y_4}{R_4} & \frac{z-z_1}{R_1} + \frac{z-z_4}{R_4} \end{bmatrix} \quad . \tag{F-24}$$

F.4 Advantages of the Over-Determined Solution

The following are advantages of using the over-determined solution:

(1) All of the observational data get used in a valid least-squares solution.

(2) It provides the standard (i.e., the best attainable solution) against which all simplifications and shortcuts can be compared.

(3) It indicates whether a particular computational simplification is warranted, or whether a more nearly exact solution is essential.

(4) The variances and also the covariances of the errors in x, y, and z are readily obtained via matrix algebra in the calculation of the GDOPs associated with the over-determined solution. It is believed that the correlation structure (and hence the variance-covariance "picture") may change significantly throughout the track of the helicopter. This implies that the "uncertainty ellipsoid" associated with x, y, z is changing its orientation throughout the track. In fact, if the variance-covariance matrix at one point cannot be obtained at another point via the multiplication by a single scalar, a case for Kalman filtering can be made. Depending on the speed with which the correlation structure changes, Kalman filtering may produce spectacular improvements in accuracy.

(5) The matrix algebra used in obtaining GDOPs for the over-determined solution can also readily be used to obtain GDOPs for the exactly determined solution.

F.5 Disadvantages of the Over-Determined Solution

(1) The major disadvantage is the necessity of using iterative techniques with associated loss of computational time.

(2) Problems of convergence of the solution may arise if the initial solution is considerably in error.

APPENDIX G

DERIVATION OF ERROR VARIANCES FOR THE EXPLICIT MINIMUM VARIANCE SOLUTION GIVEN IN SECTION 3.5

In this solution, the variance of the z estimate is given by

$$\sigma^2_{\Delta\hat{z}} = (U^T \psi^{-1}_{\Delta z} U)^{-1} \tag{G-1}$$

where U is a n x 1 unit matrix and $\psi_{\Delta z}$ is the covariance matrix of the n z(i) solutions obtained from the equations

$$a\, z^2(i) + b_i\, z(i) + c_i = 0 \ . \tag{G-2}$$

To determine $\psi_{\Delta z}$, the first step is to obtain an expression for the variation in z(i) in terms of variations of the coefficients a, b, and c. Taking differentials in eq. G-2 and solving for $\Delta z(i)$ gives, since $\Delta a = 0$,

$$\Delta z(i) = \left(\frac{-z}{2az + b_i}\right) \Delta b_i - \left(\frac{1}{2az + b_i}\right) \Delta c_i \qquad i = 1,n \ . \tag{G-3}$$

In the terms in parentheses, z is used instead of z(i) as an approximation. In matrix form

$$\overline{\Delta z} = [K]\ [z\overline{\Delta b} + \overline{\Delta c}] \tag{G-4}$$

where

$$[K] = -\begin{bmatrix} \frac{1}{2az + b_1} & 0 & . & . \\ 0 & \frac{1}{2az + b_2} & . & . \\ 0 & . & . & . \\ . & \text{ETC} & . & . \end{bmatrix}_{n \times n} ,$$

$$\overline{\Delta b} = \begin{Bmatrix} \Delta b_1 \\ \Delta b_2 \\ . \\ . \\ \Delta b_n \end{Bmatrix}_{n \times 1}, \qquad \overline{\Delta c} = \begin{Bmatrix} \Delta c_1 \\ \Delta c_2 \\ . \\ . \\ \Delta c_n \end{Bmatrix}_{n \times 1}, \text{ and } \quad \overline{\Delta z} = \begin{Bmatrix} \Delta z(1) \\ \Delta z(2) \\ . \\ . \\ \Delta z(n) \end{Bmatrix}_{n \times 1}.$$

The differentials Δb_i and Δc_i are found from the expressions for a_i and b_i (see Section 3.5)

$$b_i = -2z_i - 2B^T C^T CQ + 2\rho_i{}^T CB \tag{G-5}$$

$$\Delta b_i = -2B^T C^T C\Delta Q \tag{G-6}$$

$$\overline{\Delta b} = -2UB^T C^T C\Delta Q \qquad (U = n \times 1 \text{ unit matrix}) \tag{G-7}$$

$$\overline{\Delta b} = -2UB^T C^T CT\overline{\Delta R} \tag{G-8}$$

$$C_i = -R_i{}^2 + \rho_i{}^T\rho_i - 2\rho_i{}^T CQ + Q^T C^T CQ + z_i{}^2 \tag{G-9}$$

$$\Delta C_i = -2R_i\,\Delta R_i - 2\rho_i{}^T C\Delta Q + 2Q^T C^T C\Delta Q \tag{G-10}$$

$$\overline{\Delta C} = -2R\,\overline{\Delta R} - 2\gamma C\,\Delta Q + 2UQ^T C^T\,\Delta Q \tag{G-11}$$

$$\overline{\Delta C} = 2\{-R + (UQ^T C^T C - \gamma C)\,T\}\,\overline{\Delta R} \tag{G-12}$$

where

$$[R] = \begin{bmatrix} R_1 & 0 & . & . \\ 0 & R_2 & . & . \\ . & . & . & \\ . & . & . & R_n \end{bmatrix}_{n \times n} \qquad [T] = \begin{bmatrix} R_1 & 0 & . & -R_n \\ 0 & R_2 & . & -R_n \\ . & . & R_{n-1} & -R_n \\ . & . & . & -R_n \end{bmatrix}_{(n \times 1) \times n}$$

$$\gamma = \begin{bmatrix} x_1 & y_1 \\ x_2 & y_2 \\ . & . \\ . & . \\ x_n & y_n \end{bmatrix}_{n \times 2}.$$

Now, letting

$$V = -2UB^T C^T C \qquad (n \times n) \qquad \text{(G-13)}$$

and

$$S = 2\ \{-R + (UQ^T C^T C - \gamma C)\ T\} \qquad (n \times n) \qquad \text{(G-14)}$$

we have

$$\overline{\Delta z} = K[z\ V + S]\ \overline{\Delta R} \qquad (n \times 1) \qquad \text{(G-15)}$$

and

$$\psi_{\overline{\Delta z}} = E\ \{\overline{\Delta z}\ \overline{\Delta z}^T\} = K[zV + S]\ \psi_{\overline{\Delta R}}\ [zV + S]^T\ K^T \qquad \text{(G-16)}$$

where $\psi_{\overline{\Delta z}}$ is the covariance matrix of the one-way range measurement errors.

The covariance matrix of $\hat{\rho}$ is found as follows. Since

$$\hat{\rho} = CQ - CB\hat{z} \qquad \text{(G-17)}$$

then

$$\Delta\hat{\rho} = C\ \overline{\Delta Q} - CB\ \Delta\hat{z} \qquad \text{(G-18)}$$

$$\Delta\hat{\rho} = CT\ \overline{\Delta R} - CB\ \Delta\hat{z} \qquad \text{(G-19)}$$

but

$$\Delta\hat{z} = (U^T\ \psi^{-1}_{\overline{\Delta z}}\ U)^{-1}\ U^T\ \psi^{-1}_{\overline{\Delta z}}\ \overline{\Delta z} \qquad \text{(G-20)}$$

$$\Delta\hat{z} = F\ \overline{\Delta z}$$

therefore

$$\Delta\hat{\rho} = CT\ \overline{\Delta R} - CBFK\ [zV + S]\ \overline{\Delta R}$$

$$\Delta\hat{\rho} = \{CT - CBFK\ [zV + S]\}\ \overline{\Delta R}\ . \qquad \text{(G-21)}$$

Let

$$W = CT - CBFK\ [zV + S]$$

then

$$\psi_{\Delta\hat{\rho}} = W\ \psi_{\overline{\Delta R}}\ W^T\ , \qquad \text{(G-22)}$$

where, as previously indicated $\psi_{\overline{\Delta R}}$ is the covariance matrix of the one-way range measurement errors (see Appendix C).

Error Variances when Matrix $\psi_{\overline{\Delta z}}$ cannot be Inverted

In some cases, it may be impossible to invert the matrix $\psi_{\overline{\Delta z}}$ because of high correlation between errors in calculation of the z(i). (i.e., roundoff errors in computation may preclude the inversion.) In this case, a procedure as follows is suggested:

1. Use the average (unweighted) value of the z(i) to calculate $\psi_{\overline{\Delta z}}$.
2. Select the z estimate $\hat{z}$ as the value of z(i) which has the minimum variance. Variances are determined from the diagonal of $\psi_{\overline{\Delta z}}$.
3. Calculate $\hat{x}$ and $\hat{y}$ as before, using the estimate $\hat{z}$ in the equation for $\bar{\rho}$.

When the above procedure is followed, the variance of errors in $\hat{z}$ will be as determined from the selected diagonal term of $\psi_{\overline{\Delta z}}$, and the variance of the x and y estimate is calculated as follows:

Since

$$\Delta\hat{\rho} = C\Delta Q - CB\Delta\hat{z} \qquad \text{(G-23)}$$

and now,

$$\Delta\hat{z} = \frac{1}{2a<z> + b_i} \left(<z>\ \Delta b_i + \Delta C_i\right) , \qquad \text{(G-24)}$$

where the nomenclature has been previously defined. The variations in b_i and C_i are given by (i is index for selected z(i) value)

$$\Delta b_i = -\ 2B^T C^T CT\ \overline{\Delta R} \qquad \text{(G-25)}$$

$$\Delta C_i = \left[-\ 2\ R' - 2\rho_i{}^T CT + 2Q^T C^T CT\right]\ \overline{\Delta R} \ , \qquad \text{(G-26)}$$

where $R' = \{a_1, a_2, a_3, a_4\}$

$$a_j = 1, \quad j = i$$

$$a_j = 0, \quad j \neq i \quad .$$

For simplicity in notation, let

$$k_i = \frac{-1}{2a\langle z \rangle + b_i} \tag{G-27}$$

$$S' = [\, -2R' - 2\rho_i{}^T CT + 2Q^T C^T CT] \tag{G-28}$$

and

$$V = -2BC^T C\ T \quad . \tag{G-29}$$

Then we have,

$$\Delta\hat{z} = k_i\ [\langle z \rangle V + S']\ \overline{\Delta R} \tag{G-30}$$

and

$$\Delta\hat{\rho} = \{CT - CBk_i\ [\langle z \rangle V + S']\}\ \overline{\Delta R} \tag{G-31}$$

or

$$\Delta\hat{\rho} = W'\ \overline{\Delta R} \quad , \tag{G-32}$$

so that we have for the covariance matrix of errors in $\hat{x}$ and $\hat{y}$ estimates,

$$\psi_{\Delta\hat{\rho}} = W'\ \psi_{\overline{\Delta R}}\ W'^T \quad . \tag{G-33}$$

Page Intentionally Left Blank

APPENDIX H

ERROR COVARIANCE MATRIX FOR COORDINATE RATES

In Section 3.6, the solution for coordinate rates in terms of the range and range rate measurements is given as

$$\dot{\bar{x}} = (S^T \psi_{\Delta\dot{A}}^{-1} S)^{-1} S^T \psi_{\Delta\dot{A}}^{-1} \dot{\bar{A}} \tag{H-1}$$

where the $\dot{\bar{A}}$ are the measurements and the remaining matrices are defined in the text. For simplicity, define

$$[H] = (S^T \psi_{\Delta\dot{A}}^{-1} S)^{-1} S^T \psi_{\Delta\dot{A}}^{-1} \tag{H-2}$$

so that

$$\dot{\bar{x}} = H \dot{\bar{A}} \quad . \tag{H-3}$$

Now, recalling that [H] is a function of the position (x, y, z) estimate, small error in $\dot{\bar{x}}$ is given by

$$\Delta\dot{\bar{x}} = H\Delta\dot{\bar{A}} + \Delta H \dot{\bar{A}} \quad . \tag{H-4}$$

Since $\dot{\bar{A}} = S\dot{x}$, eq. (H-4) may be written as

$$\Delta\dot{\bar{x}} = H \overline{\Delta\dot{A}} + \Delta H S\dot{x} \quad . \tag{H-5}$$

Also, postmultiplying eq. (H-2) by S gives

$$HS = I \tag{H-6}$$

where I is an identity matrix. Thus

$$\Delta H S + H \Delta S = 0 \tag{H-7}$$

or

$$\Delta HS = - H\Delta S \quad . \tag{H-8}$$

Therefore,

$$\Delta\dot{\bar{x}} = H\,\overline{\dot{\Delta A}} - H\Delta S\,\dot{\bar{x}} \tag{H-9}$$

and since $\dot{\bar{x}} \approx \Delta\dot{\bar{x}}/\Delta t$ we can also write

$$\Delta\dot{\bar{x}} = H\,\overline{\dot{\Delta A}} - H\dot{S}\,\Delta\bar{x} \quad . \tag{H-10}$$

The covariance matrix of the errors is found by taking the expected value of $\dot{\Delta\bar{x}}\,\dot{\Delta\bar{x}}^T$ as follows:

$$\psi_{\Delta\dot{\bar{x}}} = E\left\{\dot{\Delta\bar{x}}\,\dot{\Delta\bar{x}}^T\right\} = H\,\psi_{\Delta\dot{A}}\,H^T + H\dot{S}\,\psi_{\overline{\Delta x}}\,\dot{S}^T\,H^T \tag{H-11}$$

where it is assumed that the covariance terms $E\{\dot{\Delta A}\,\Delta\bar{x}^T\}$ are zero (i.e., no correlation between range rate measurements and position estimates).

The first term in eq. (H-11) can be reduced to obtain for the coordinate rate error covariance matrix,

$$\psi_{\dot{\Delta\bar{x}}} = (S^T\,\psi_{\Delta\dot{A}}^{-1}\,S)^{-1} + H\dot{S}\,\psi_{\Delta\bar{x}}\,\dot{S}^T\,H^T \tag{H-12}$$

where $\psi_{\Delta\bar{x}}$ is the covariance matrix of the coordinate position errors and the remaining matrices are defined above.

8.0 REFERENCES

Page Intentionally Left Blank

8.0 REFERENCES

1. Deutsch, R.: Estimation Theory. Prentice-Hall, Inc., 1965.

2. Hoffman, W. C., et al.: Navigation and Guidance Requirements for Commercial VTOL Operations. NASA CR-132423, Interim Technical Report Contract NAS1-12199, Aerospace Systems, Inc., January, 1974.

3. Digital Equipment Corporation: Introduction to Programming. PDP-8 Handbook Series, Digital Equipment Corporation, Maynard, Massachusetts.

4. Eschal, P. R., et al.: 3D Multilateration: A Precision Geodetic Measurement System. NASA TM 33-605, JPL, California Institute of Technology, Pasadena, California, March 15, 1973.